Observational Evidence of relativity in and around compact stars

Dipankar Bhattacharya
IUCAA, Pune

Object Types

Object Types

* Neutron stars
  * Non-accreting
  * Accreting

Object Types

* Neutron stars
  * Non-accreting
  * Accreting
* Black Holes
  * Accreting

Object Types

* Neutron stars
  * Non-accreting
    - radio
    - x-ray
  * Accreting
* Black Holes
  * Accreting

Object Types

* Neutron stars
  * Non-accreting - radio - x-ray
  * Accreting - x-ray
* Black Holes
  * Accreting - x-ray

Object Types

* Neutron stars
  * Non-accreting - radio
    - x-ray
  * Accreting - x-ray
* Black Holes
  * Accreting - x-ray

Timing, Spectroscopy

Radio pulsars

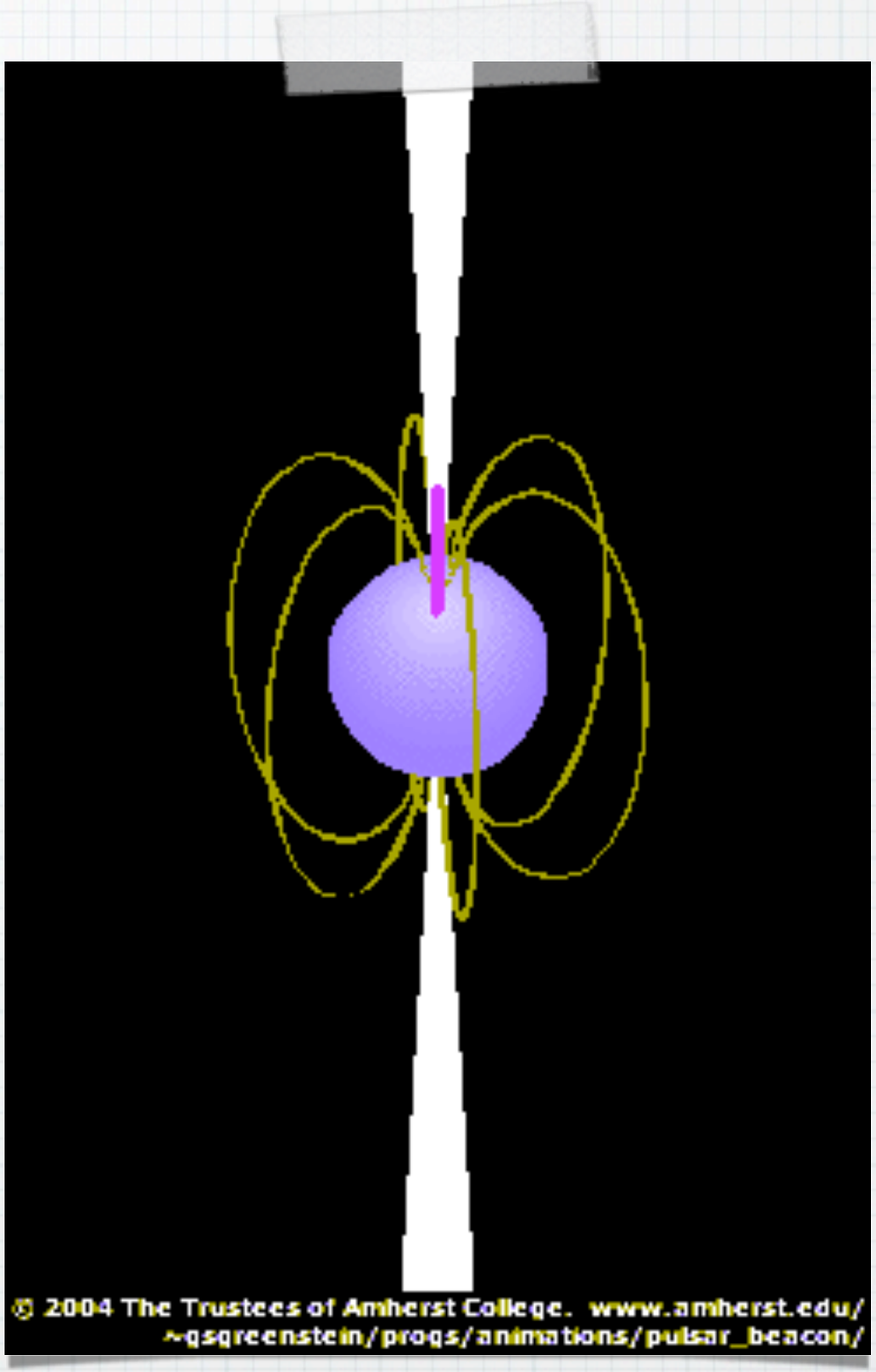

Radio pulsars

- strongly magnetized NS

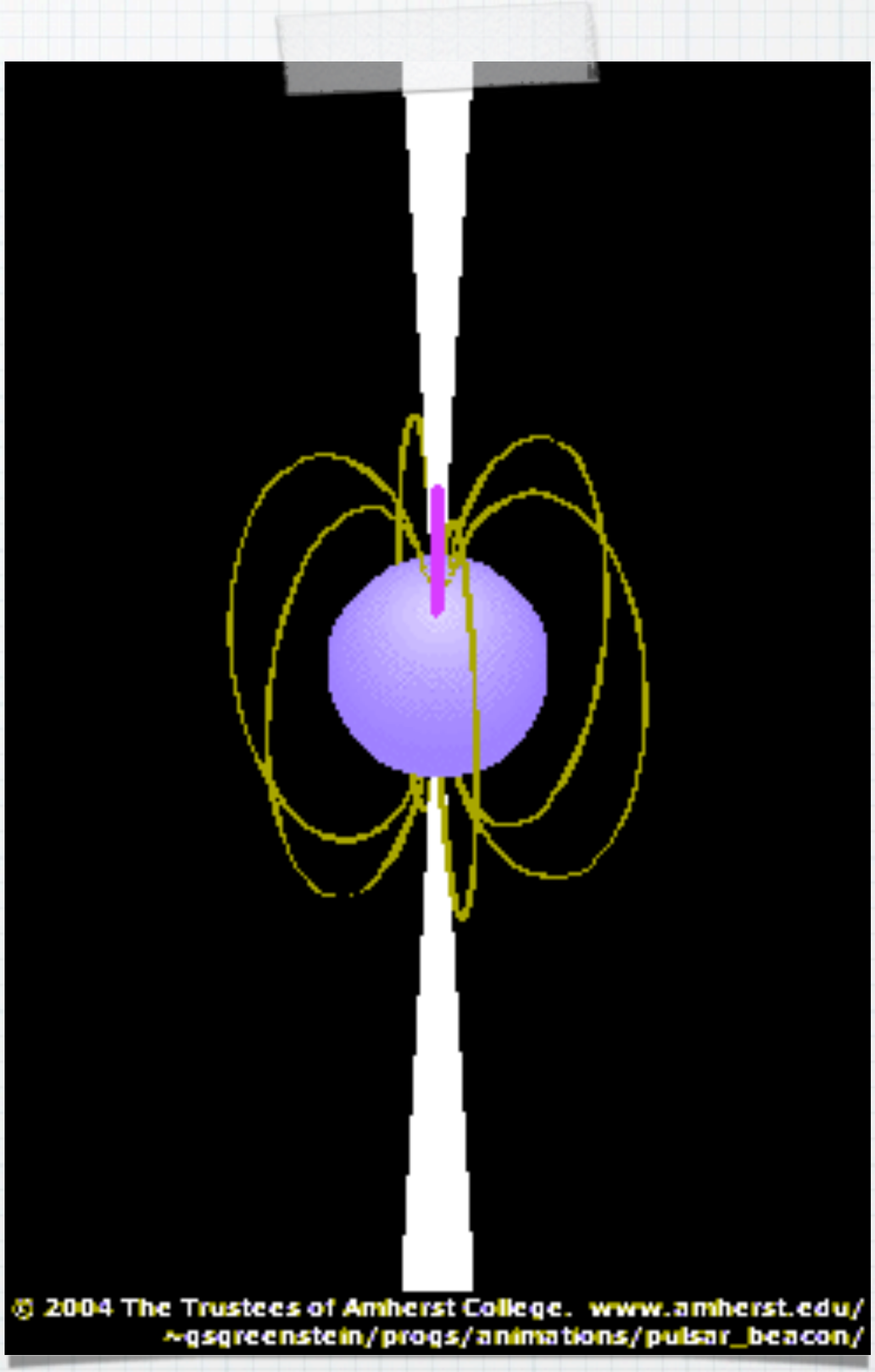

Radio pulsars

- strongly magnetized NS
- fast and stable rotation

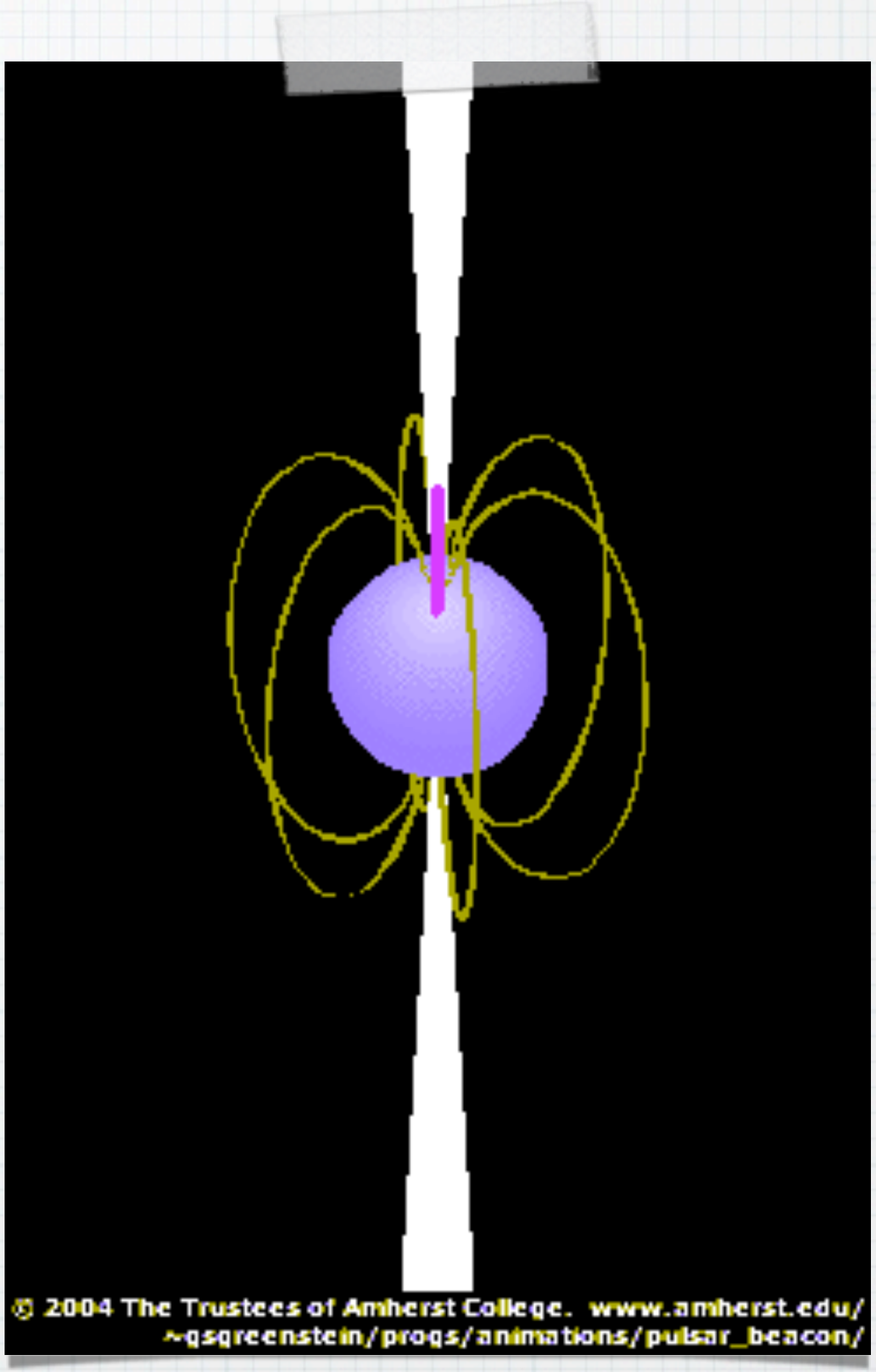

Radio pulsars

- strongly magnetized NS
- fast and stable rotation
- relativistic beams

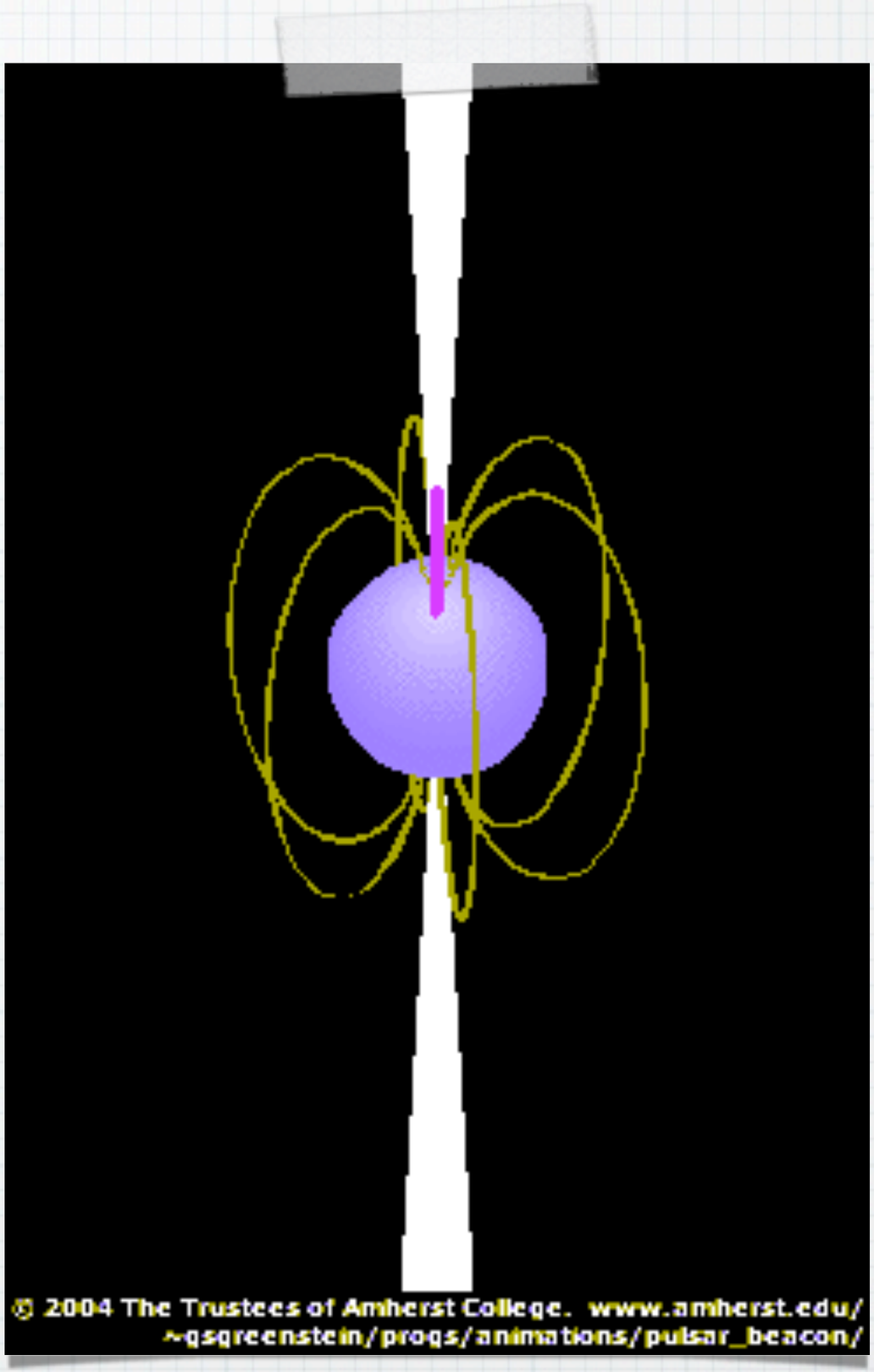

Radio pulsars

- strongly magnetized NS
- fast and stable rotation
- relativistic beams
- sharp pulse profile

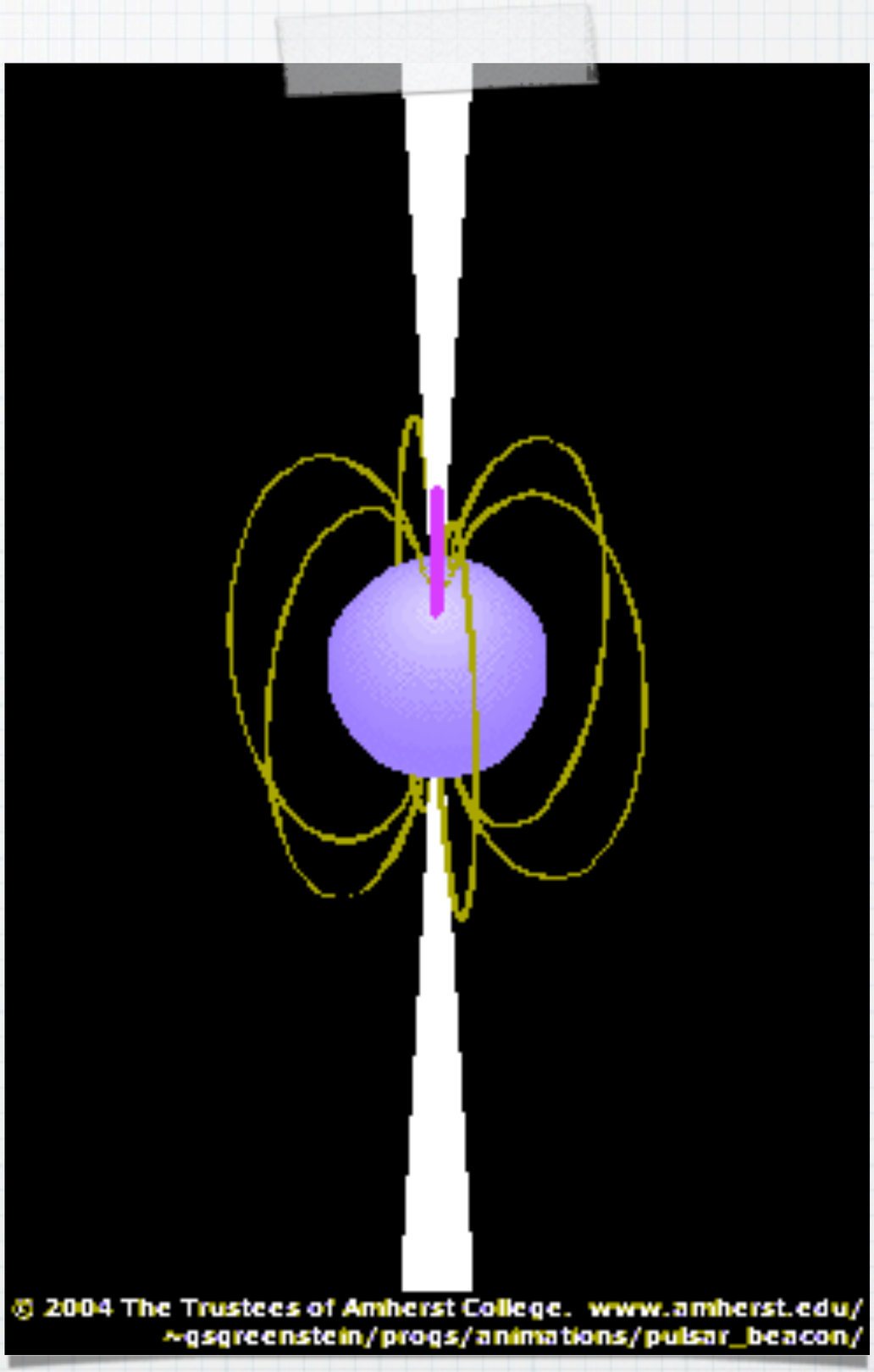

Radio pulsars

- strongly magnetized NS
- fast and stable rotation
- relativistic beams
- sharp pulse profile
- excellent clocks

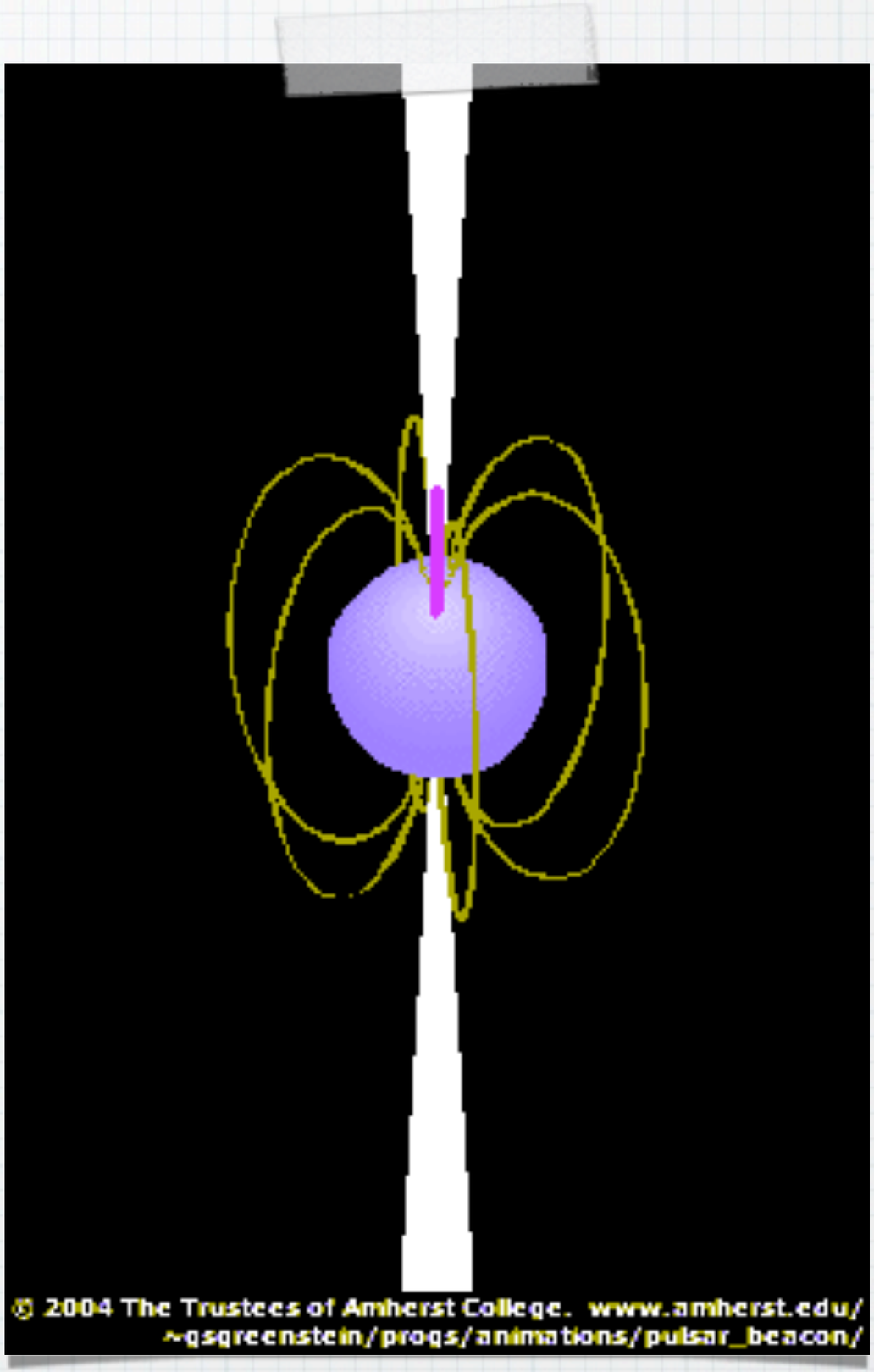

Radio pulsars

- strongly magnetized NS
- fast and stable rotation
- relativistic beams
- sharp pulse profile
- excellent clocks
- in binary systems, great probes of local gravity

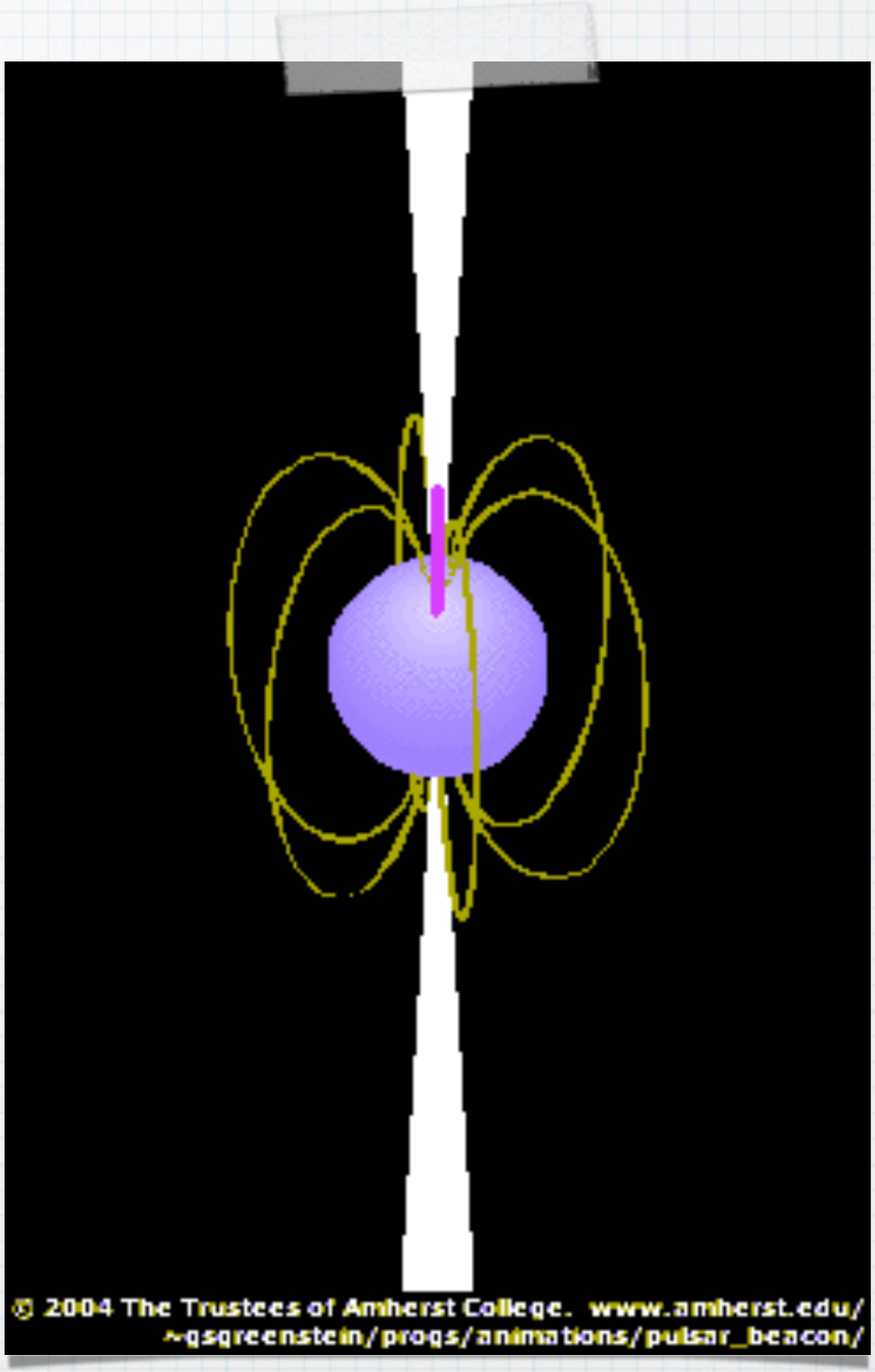

Binary Pulsar Timing

Pulse arrival time

$$t = \tau - D/f^2 + \Delta_{SS} - \Delta_R - \Delta_E - \Delta_S$$

$$u - e\sin u = 2\pi\left[\left(\frac{T-T_0}{P_b}\right) - \frac{\dot{P}_b}{2}\left(\frac{T-T_0}{P_b}\right)^2\right]$$

$$\omega = \omega_0 + \left(\frac{P_b\dot{\omega}}{\pi}\right)\tan^{-1}\left[\sqrt{\frac{1+e}{1-e}}\ \tan\frac{u}{2}\right]$$

$$\begin{aligned}\Delta_R &= x\sin\omega(\cos u - e) \\ &\quad + x\sqrt{1-e^2}\cos\omega\sin u\end{aligned}$$

$$\Delta_E = \gamma\sin u$$

$$\begin{aligned}\Delta_S &= -2r\ln\left\{1 - e\cos u - s\left[\sin\omega(\cos u - e)\right.\right. \\ &\quad \left.\left. + \sqrt{1-e^2}\cos\omega\sin u\right]\right\}\end{aligned}$$

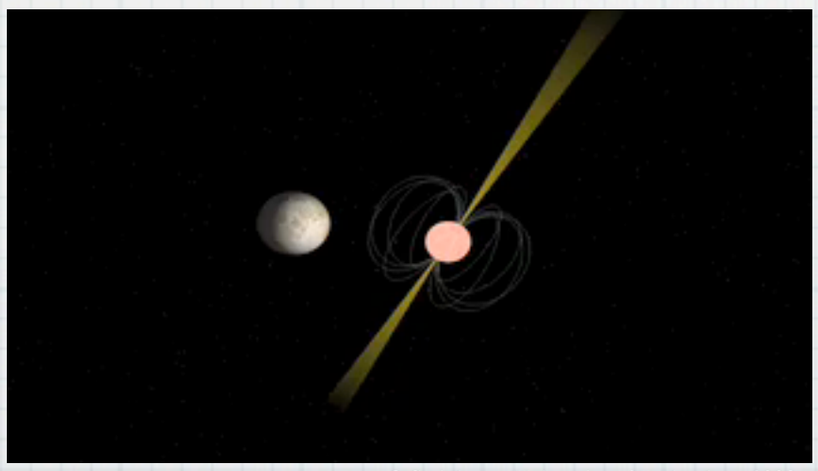

Binary Pulsar Timing

Pulse arrival time

$$t = \tau - D/f^2 + \Delta_{SS} - \Delta_R - \Delta_E - \Delta_S$$

$$u - e\sin u = 2\pi\left[\left(\frac{T-T_0}{P_b}\right) - \frac{\dot{P}_b}{2}\left(\frac{T-T_0}{P_b}\right)^2\right]$$

$$\omega = \omega_0 + \left(\frac{P_b\dot{\omega}}{\pi}\right)\tan^{-1}\left[\sqrt{\frac{1+e}{1-e}}\ \tan\frac{u}{2}\right]$$

$$\begin{aligned}\Delta_R &= x\sin\omega(\cos u - e) \\ &\quad + x\sqrt{1-e^2}\cos\omega\sin u\end{aligned}$$

$$\Delta_E = \gamma\sin u$$

$$\begin{aligned}\Delta_S &= -2r\ln\{1 - e\cos u - s[\sin\omega(\cos u - e) \\ &\quad + \sqrt{1-e^2}\cos\omega\sin u]\}\end{aligned}$$

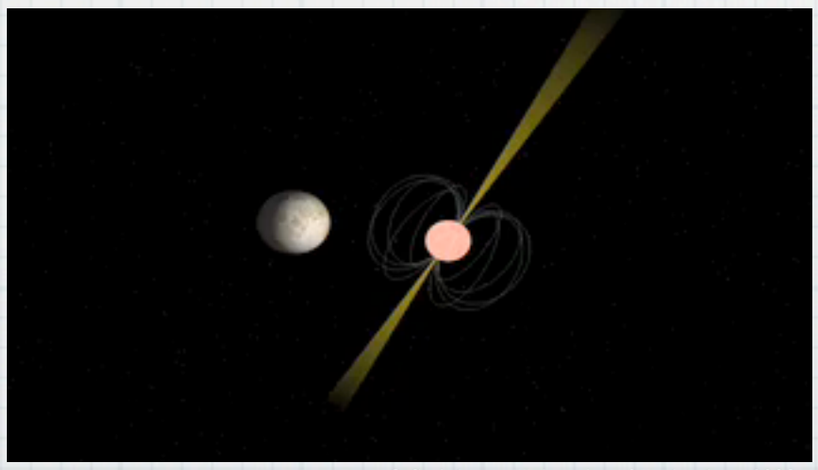

Post Keplerian parameters

Binary Pulsar Timing

PK parameters in relativity

$$\dot{\omega} = 3\left(\frac{P_\mathrm{b}}{2\pi}\right)^{-5/3}(T_\odot M)^{2/3}(1-e^2)^{-1},$$

$$\gamma = e\left(\frac{P_\mathrm{b}}{2\pi}\right)^{1/3} T_\odot^{2/3} M^{-4/3}\, m_2(m_1+2m_2),$$

$$\dot{P}_\mathrm{b} = -\frac{192\pi}{5}\left(\frac{P_\mathrm{b}}{2\pi}\right)^{-5/3}\left(1+\frac{73}{24}e^2+\frac{37}{96}e^4\right)(1-e^2)^{-7/2}\, T_\odot^{5/3}\, m_1 m_2\, M^{-1/3},$$

$$r = T_\odot\, m_2,$$

$$s = x\left(\frac{P_\mathrm{b}}{2\pi}\right)^{-2/3} T_\odot^{-1/3}\, M^{2/3}\, m_2^{-1}.$$

$$\boxed{T_\odot \equiv GM_\odot/c^3}$$

Damour & Deruelle 1986

PSR 1913+16

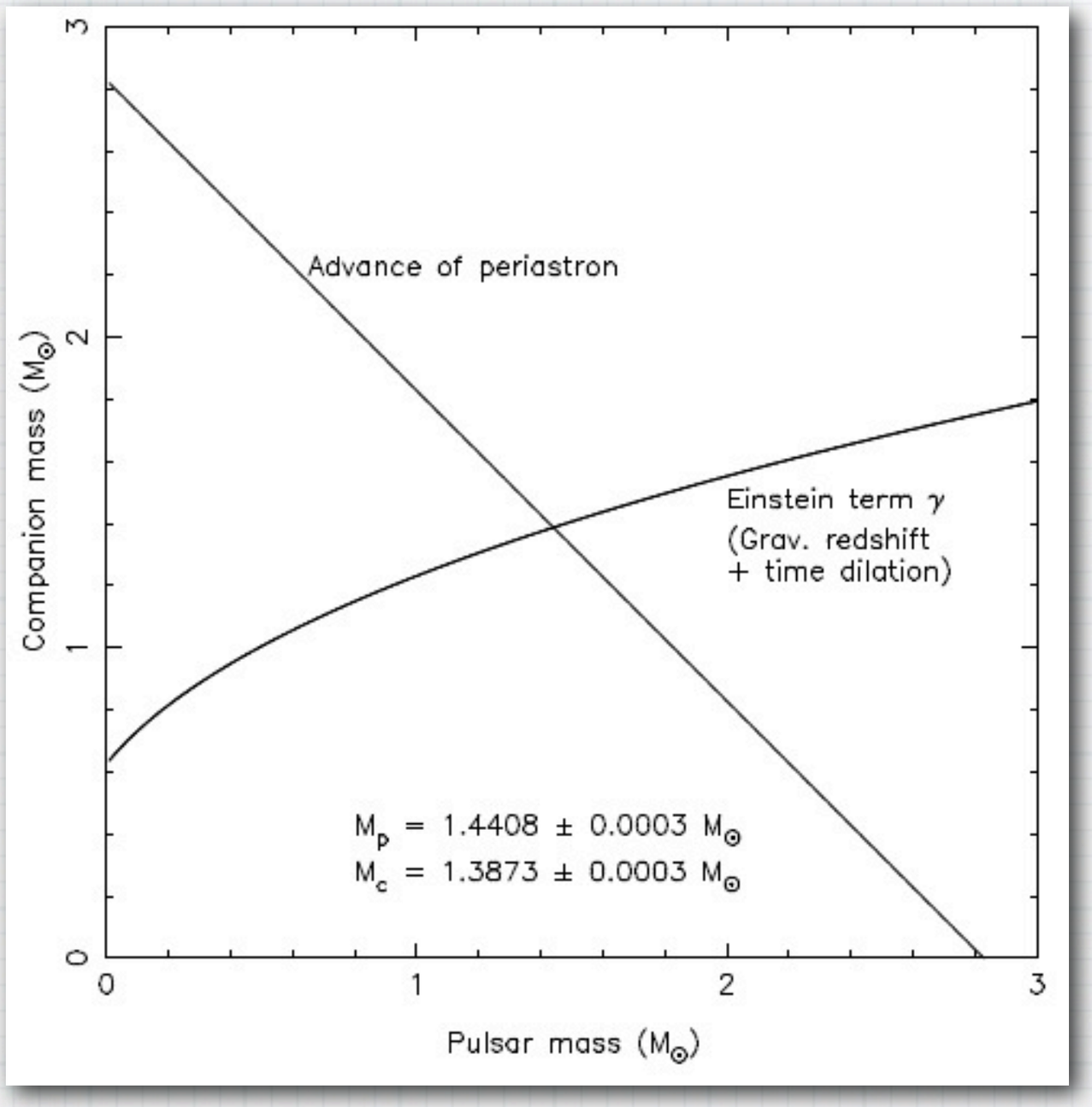

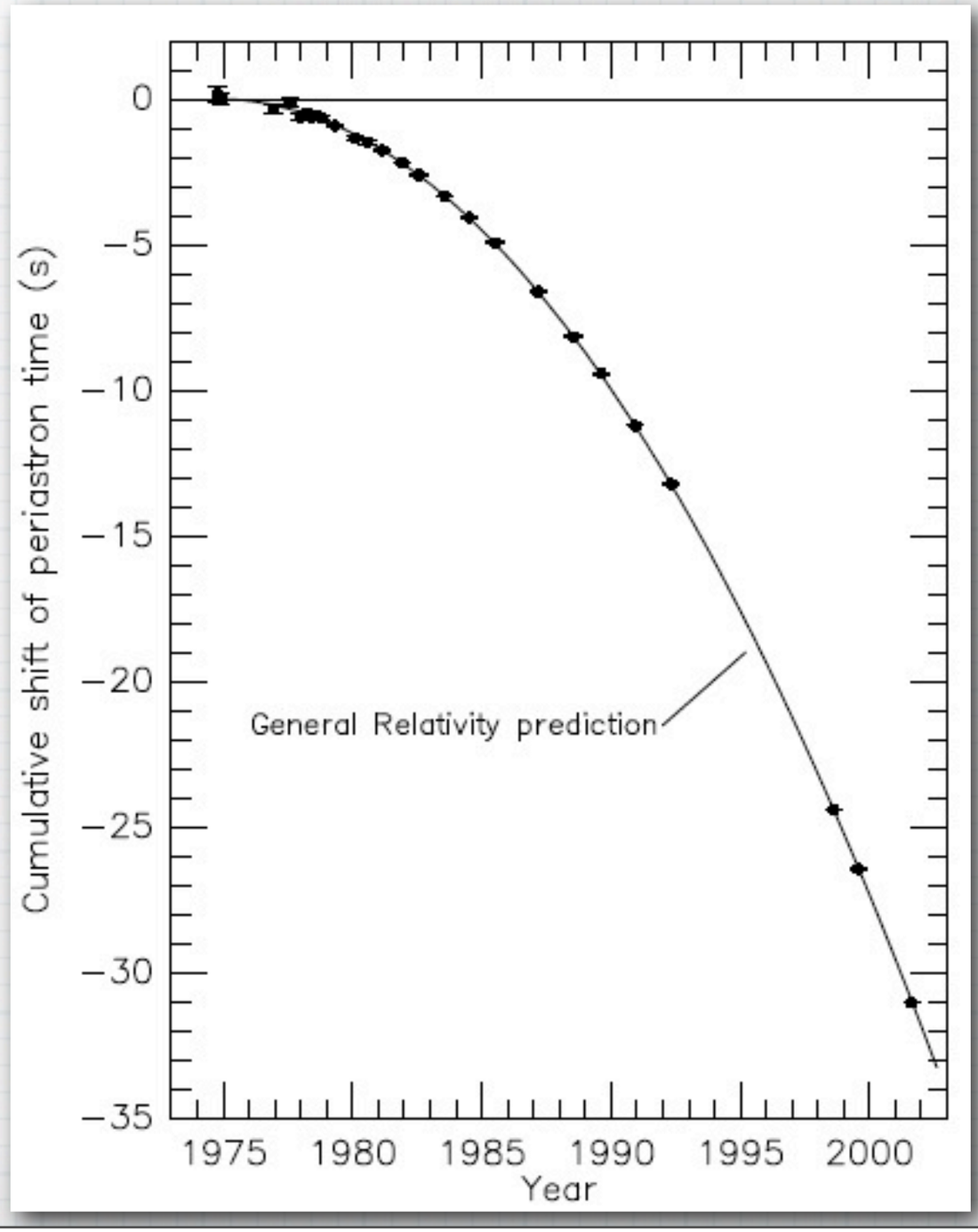

Weisberg & Taylor 2003

Test of GR prediction

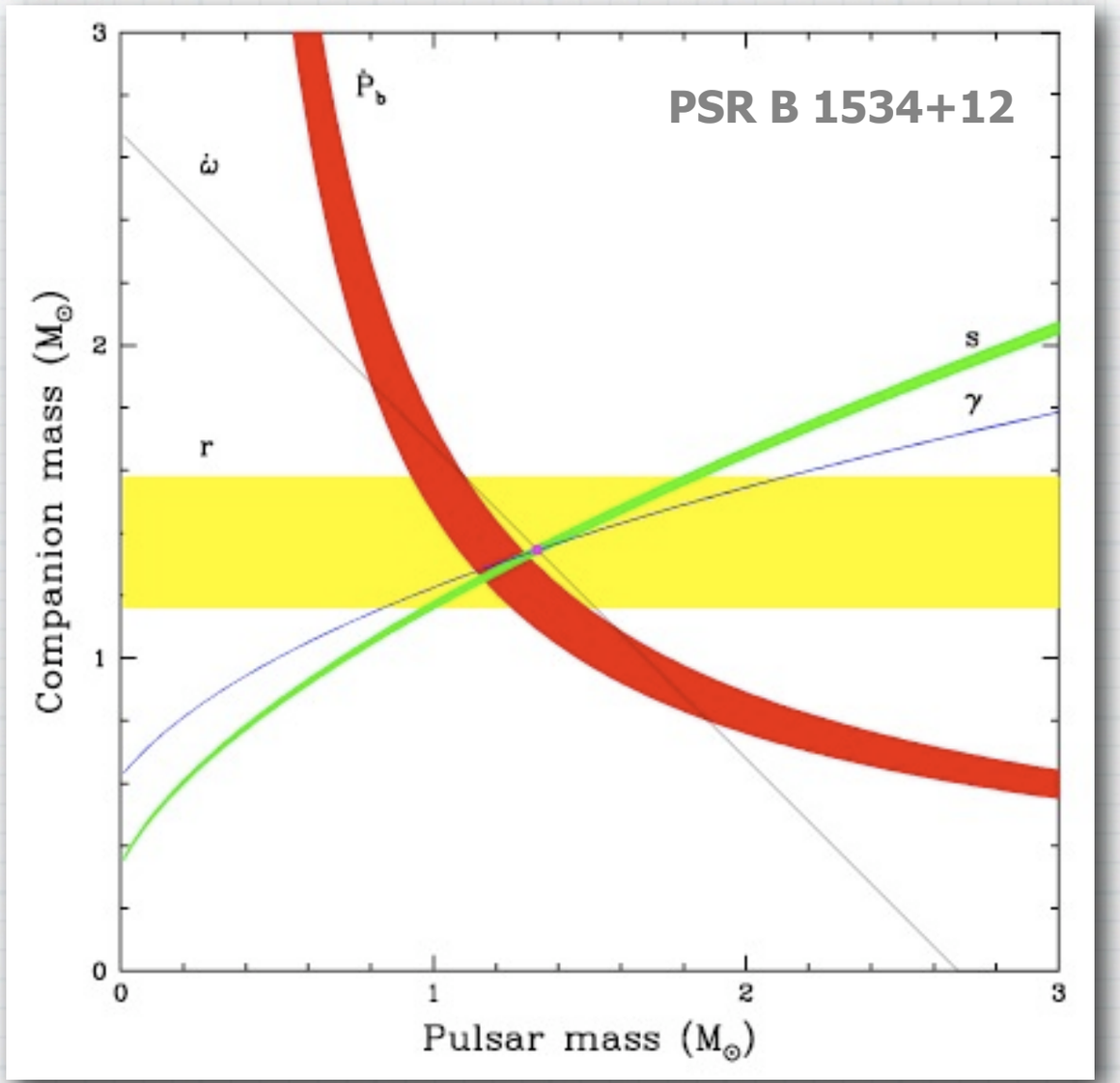

Shklovskii effect

Stairs et al 2002

The Double Pulsar J0737-3039

PSR A:

period: 23 ms

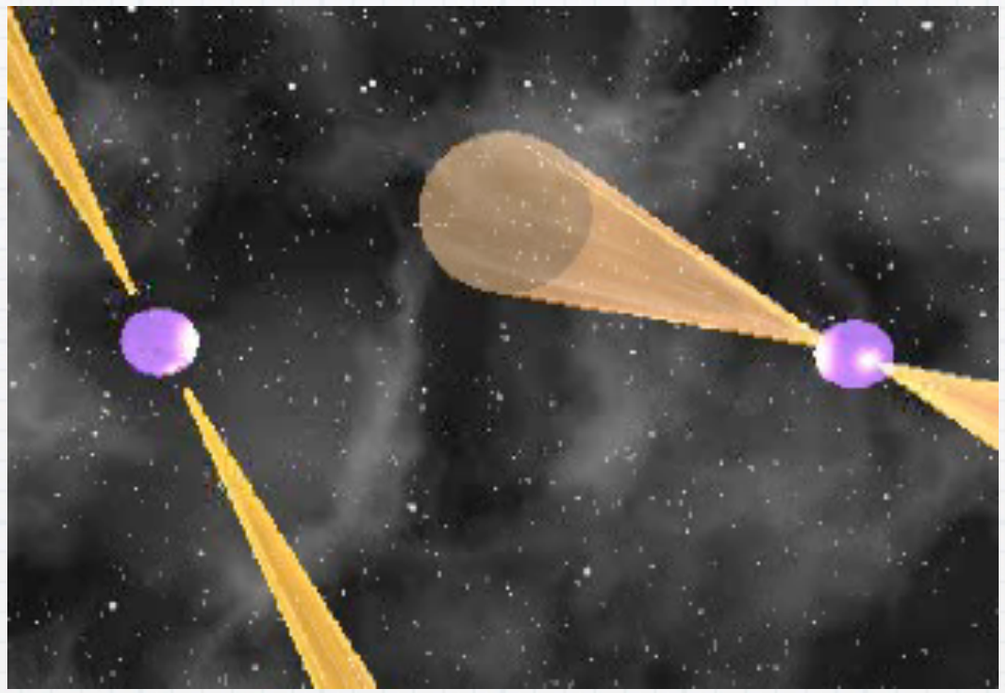

© Michael Kramer

PSR B:

period: 2.8 sec

orbital period P_b: 2.4 hr

e = 0.088

$d\omega/dt$ = 17 deg / y

$dP_b/dt = -1.25 \times 10^{-12}$

The Double Pulsar J0737-3039

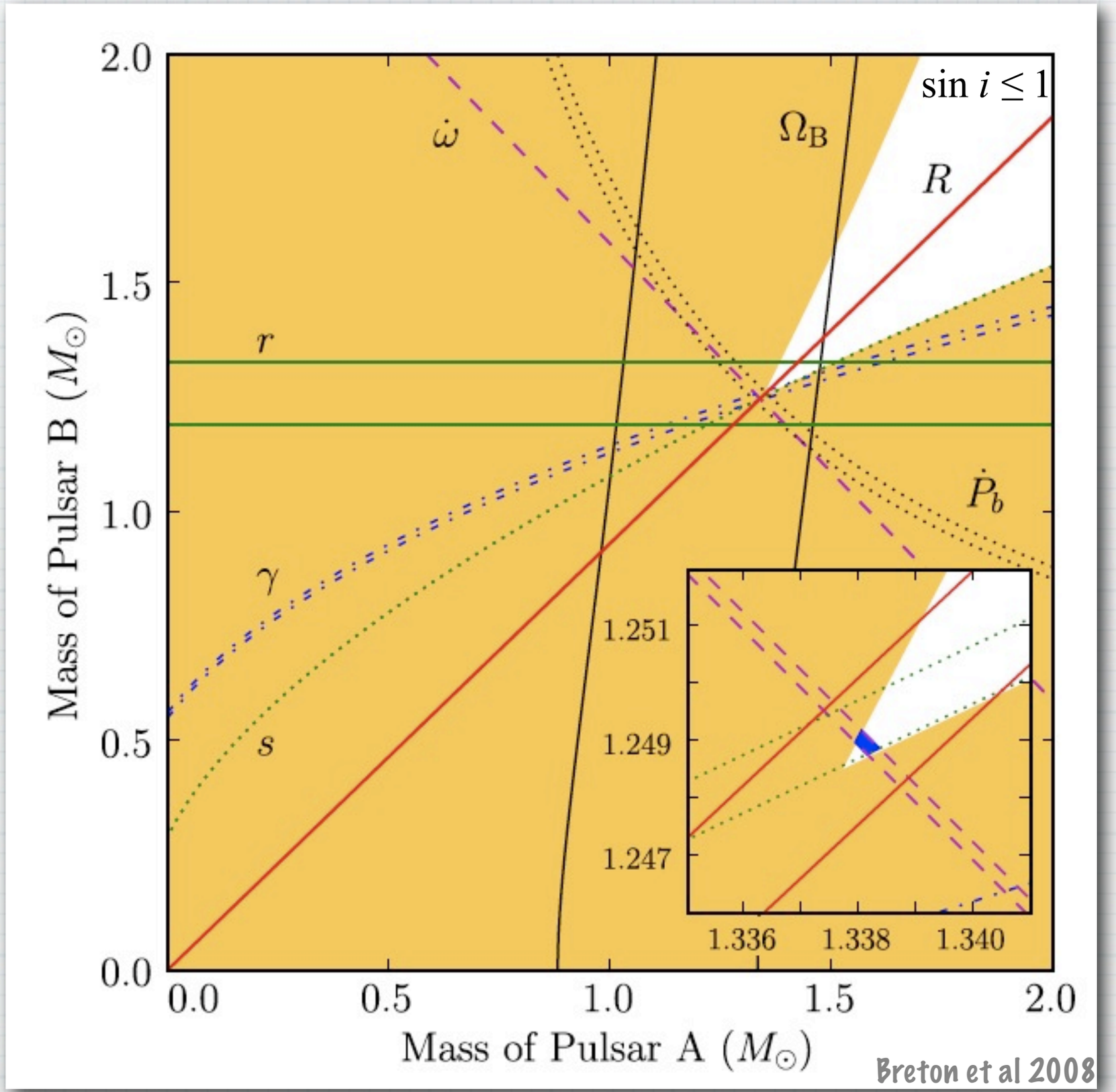

Breton et al 2008

Geodetic Precession

Geodetic Precession

$$\frac{d\mathbf{S}_1}{dt} = \mathbf{\Omega}_1^s \times \mathbf{S}_1$$

$$\Omega_1^s = \frac{1}{2}\left(\frac{P_b}{2\pi}\right)^{-5/3} \frac{m_2(4m_1 + 3m_2)}{(1-e^2)(m_1+m_2)^{4/3}} T_\odot^{2/3}$$

Geodetic Precession

$$\frac{d\mathbf{S}_1}{dt} = \mathbf{\Omega}_1^s \times \mathbf{S}_1$$

J1141-6545: 1.35 deg/y
B1913+16: 1.21 deg/y
B1534+12: 0.52 deg/y

$$\Omega_1^s = \frac{1}{2}\left(\frac{P_b}{2\pi}\right)^{-5/3} \frac{m_2(4m_1 + 3m_2)}{(1-e^2)(m_1+m_2)^{4/3}} T_\odot^{2/3}$$

Geodetic Precession

$$\frac{d\mathbf{S}_1}{dt} = \mathbf{\Omega}_1^s \times \mathbf{S}_1$$

$$\Omega_1^s = \frac{1}{2}\left(\frac{P_b}{2\pi}\right)^{-5/3} \frac{m_2(4m_1 + 3m_2)}{(1-e^2)(m_1+m_2)^{4/3}} T_\odot^{2/3}$$

J1141-6545: 1.35 deg/y
B1913+16: 1.21 deg/y
B1534+12: 0.52 deg/y

B1913+16

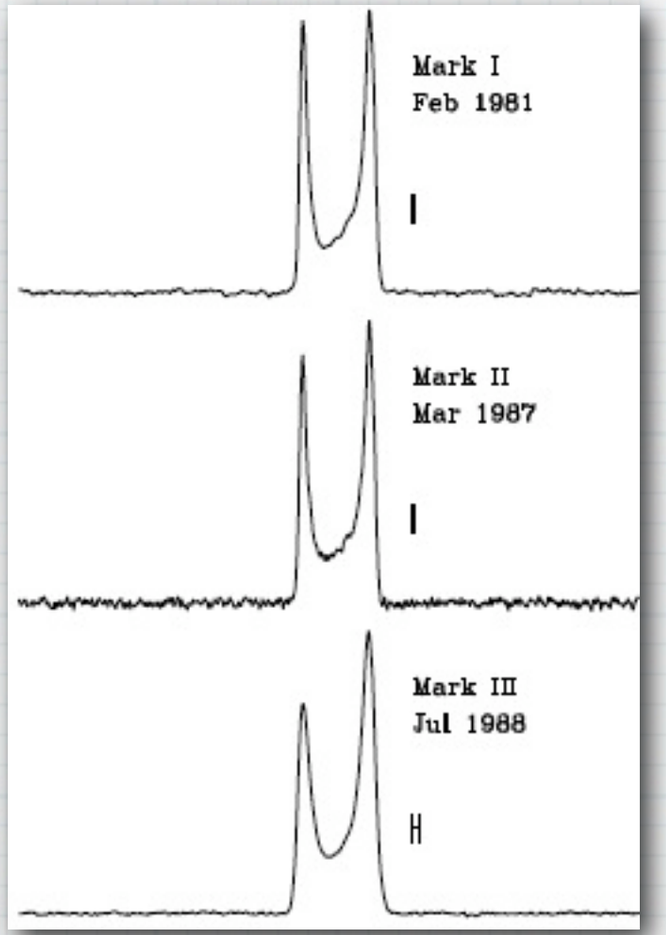

Taylor & Weisberg 1989

Geodetic Precession

$$\frac{d\mathbf{S}_1}{dt} = \mathbf{\Omega}_1^s \times \mathbf{S}_1$$

$$\Omega_1^s = \frac{1}{2}\left(\frac{P_b}{2\pi}\right)^{-5/3} \frac{m_2(4m_1 + 3m_2)}{(1-e^2)(m_1+m_2)^{4/3}} T_\odot^{2/3}$$

J1141-6545: 1.35 deg/y
B1913+16: 1.21 deg/y
B1534+12: 0.52 deg/y
J0737-3039B: 5 deg/y

B1913+16

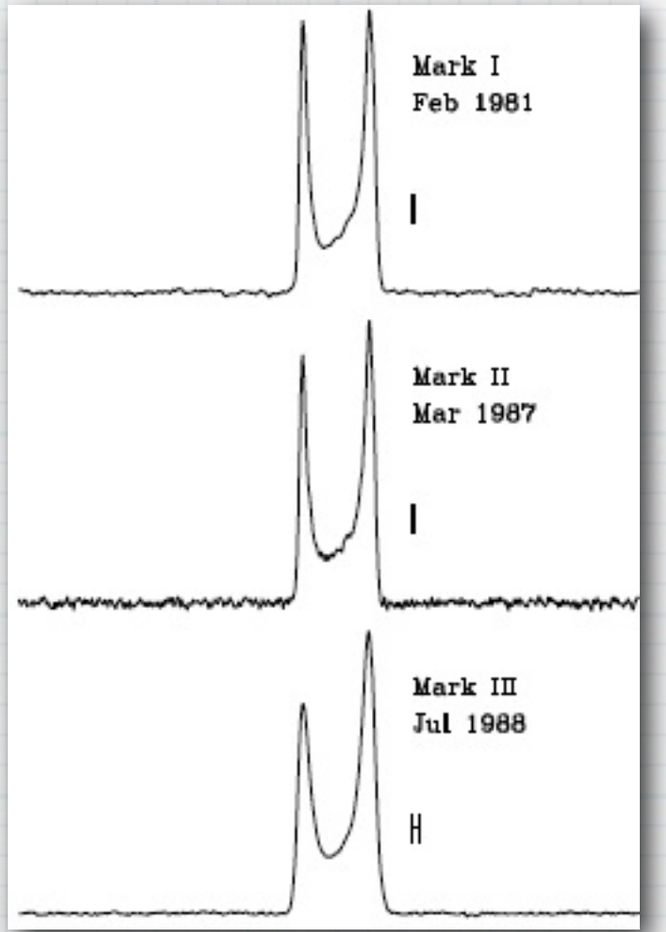

Taylor & Weisberg 1989

Geodetic Precession

$$\frac{d\mathbf{S}_1}{dt} = \mathbf{\Omega}_1^s \times \mathbf{S}_1$$

$$\Omega_1^s = \frac{1}{2}\left(\frac{P_b}{2\pi}\right)^{-5/3} \frac{m_2(4m_1 + 3m_2)}{(1-e^2)(m_1+m_2)^{4/3}} T_\odot^{2/3}$$

J1141-6545: 1.35 deg/y
B1913+16: 1.21 deg/y
B1534+12: 0.52 deg/y
J0737-3039B: 5 deg/y

B1913+16

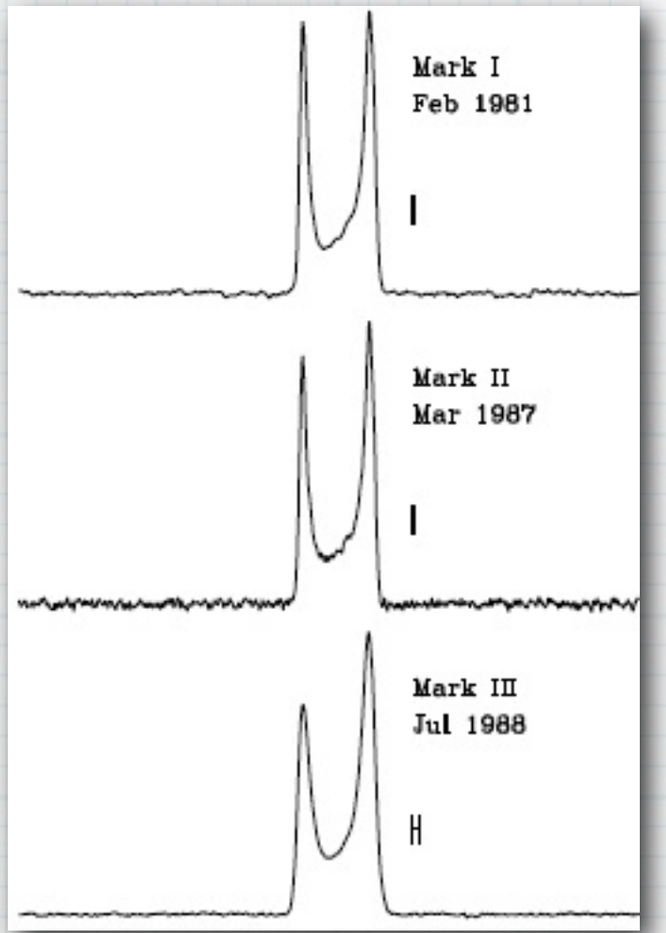

Taylor & Weisberg 1989

J0737-3039 B

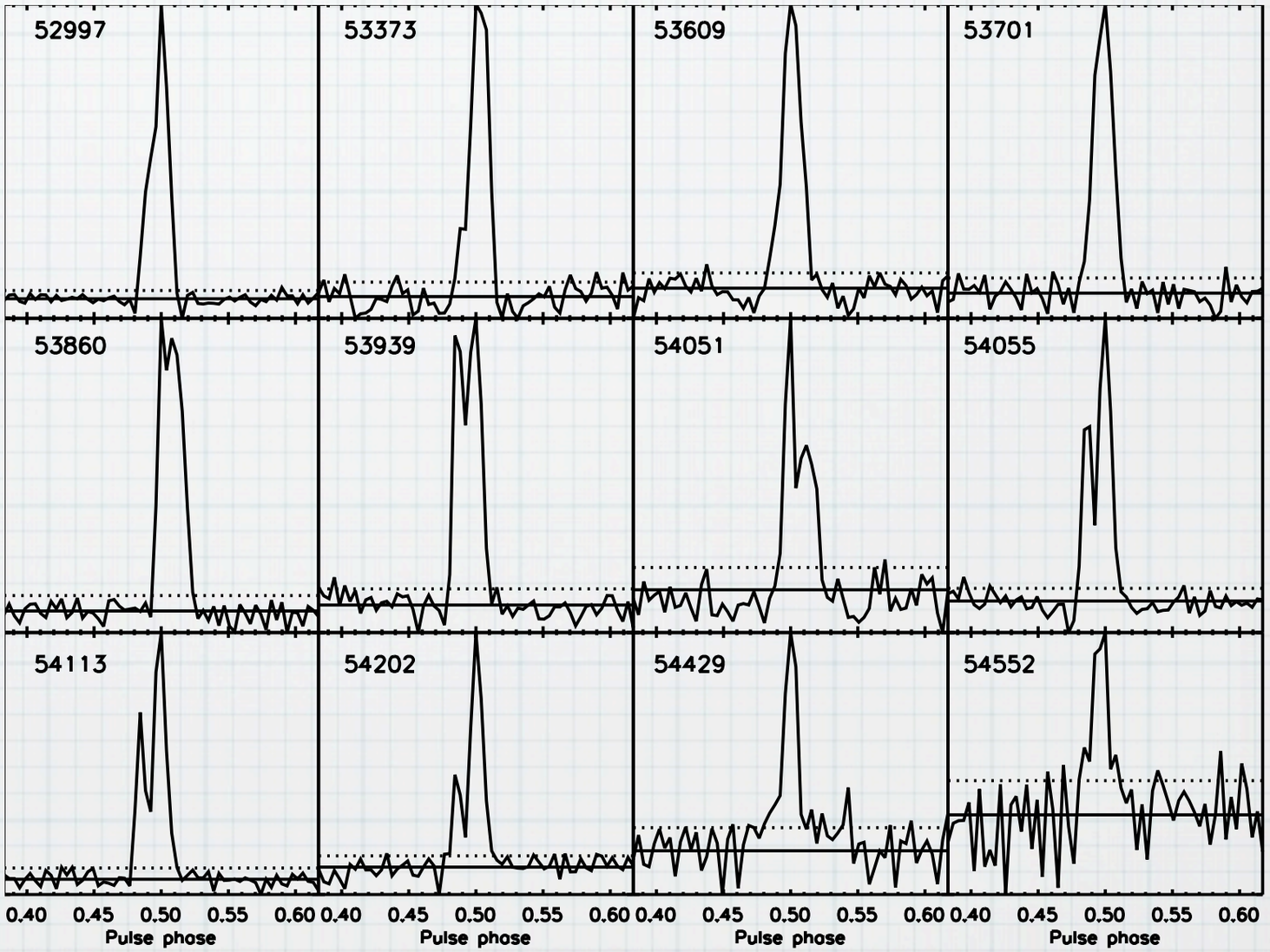

Perera et al 2011

Geodetic Precession of J0737B

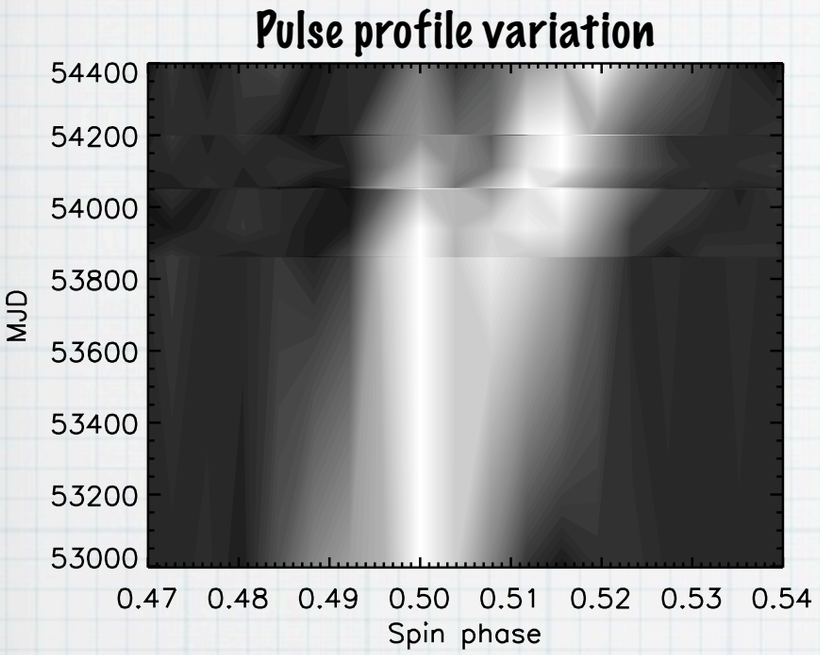

Perera et al 2011

Geodetic Precession of J0737B

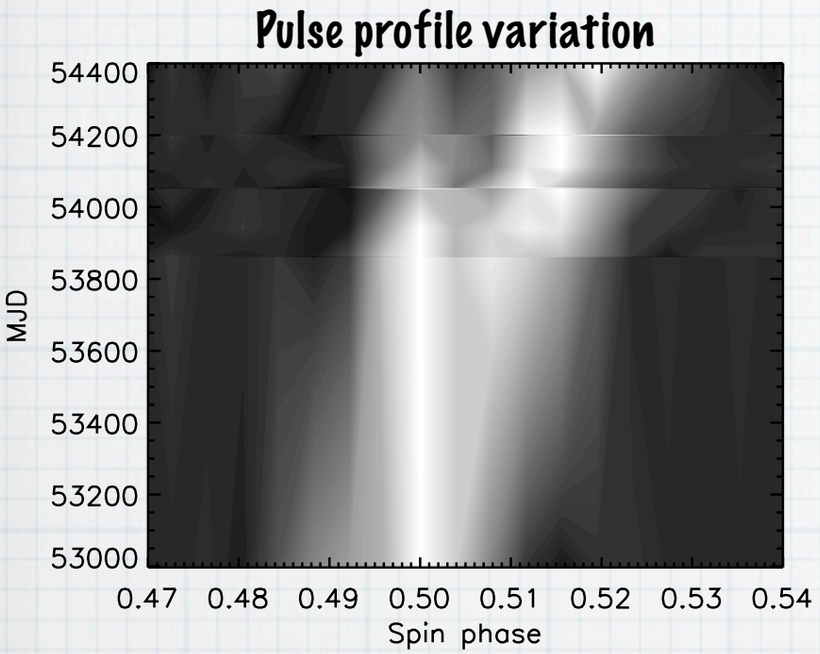

Perera et al 2011

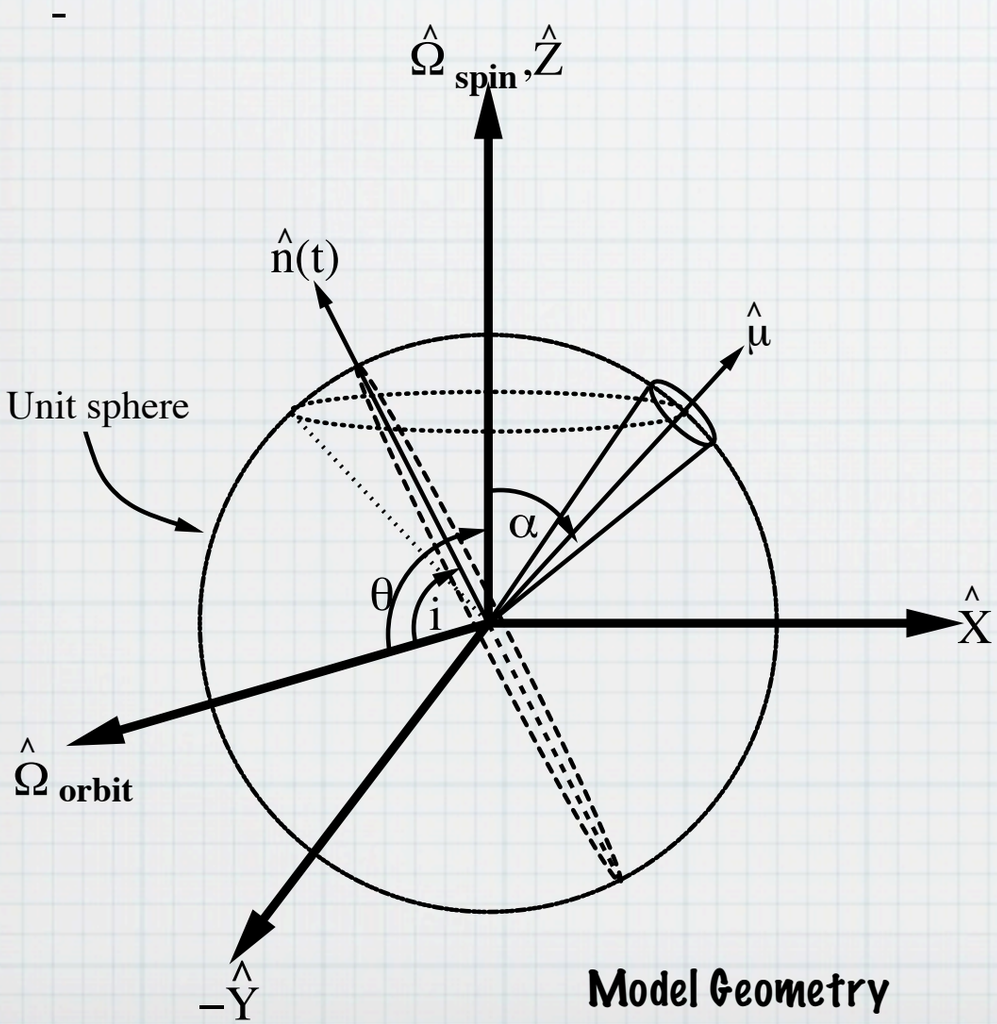

Model Geometry

Geodetic Precession of J0737B

Perera et al 2011

Pulse profile variation

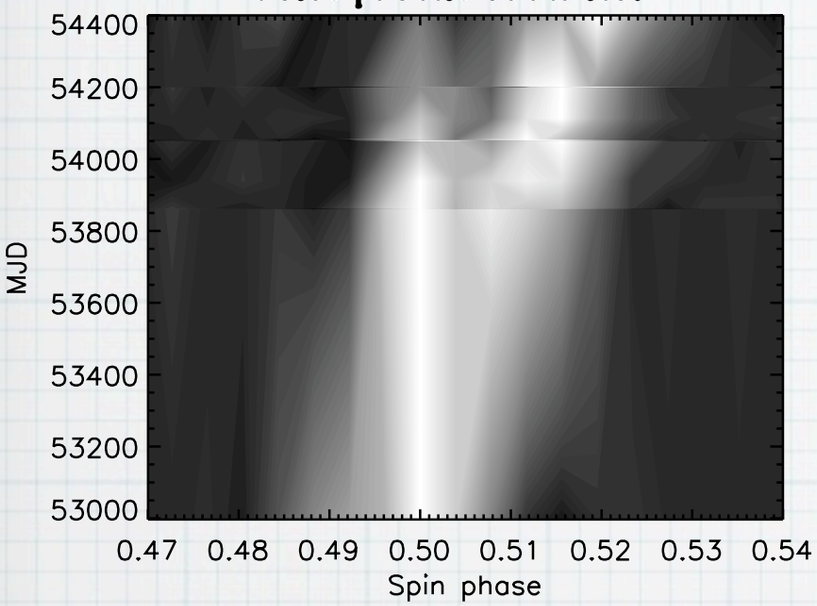

Beam Illumination

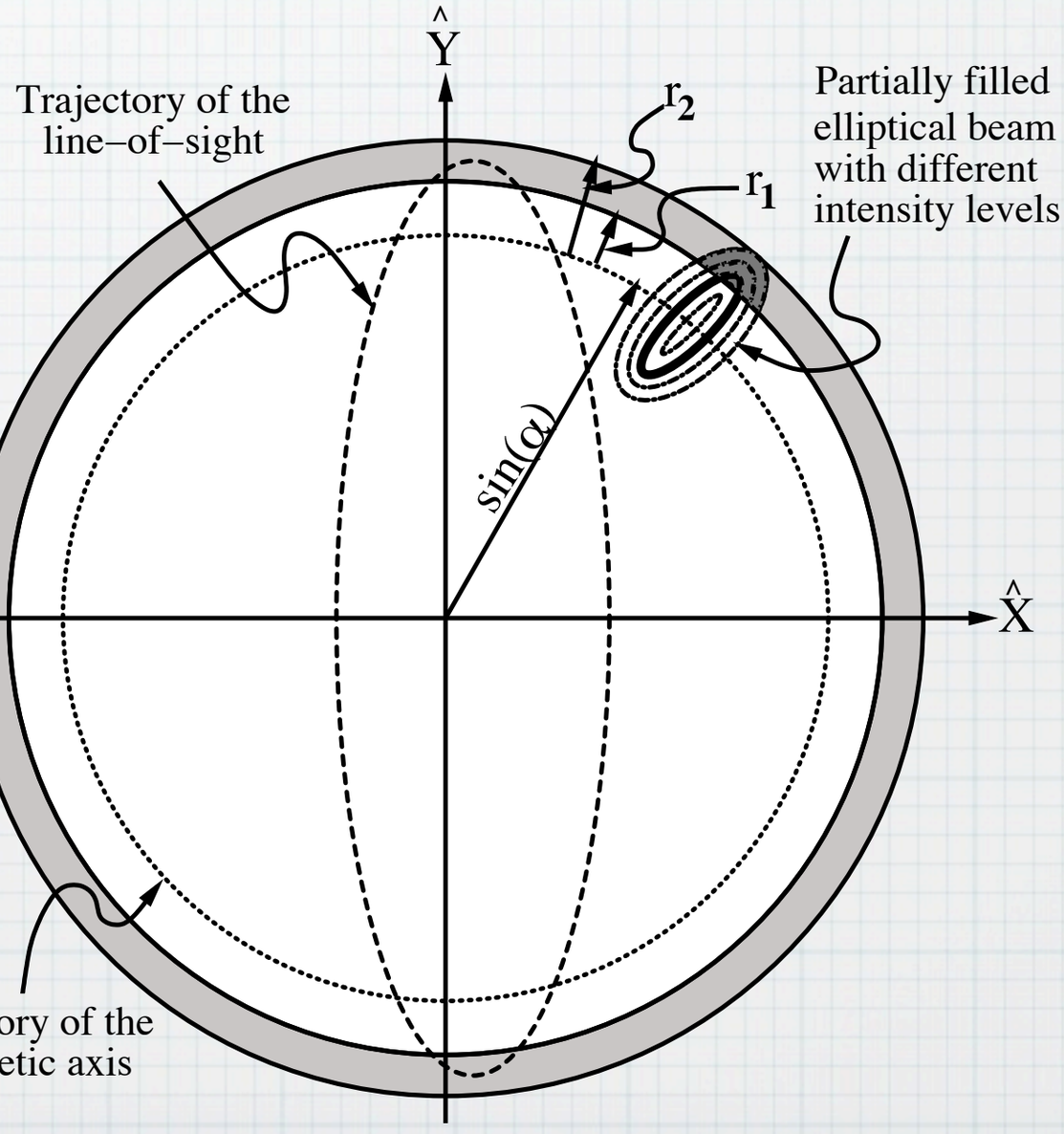

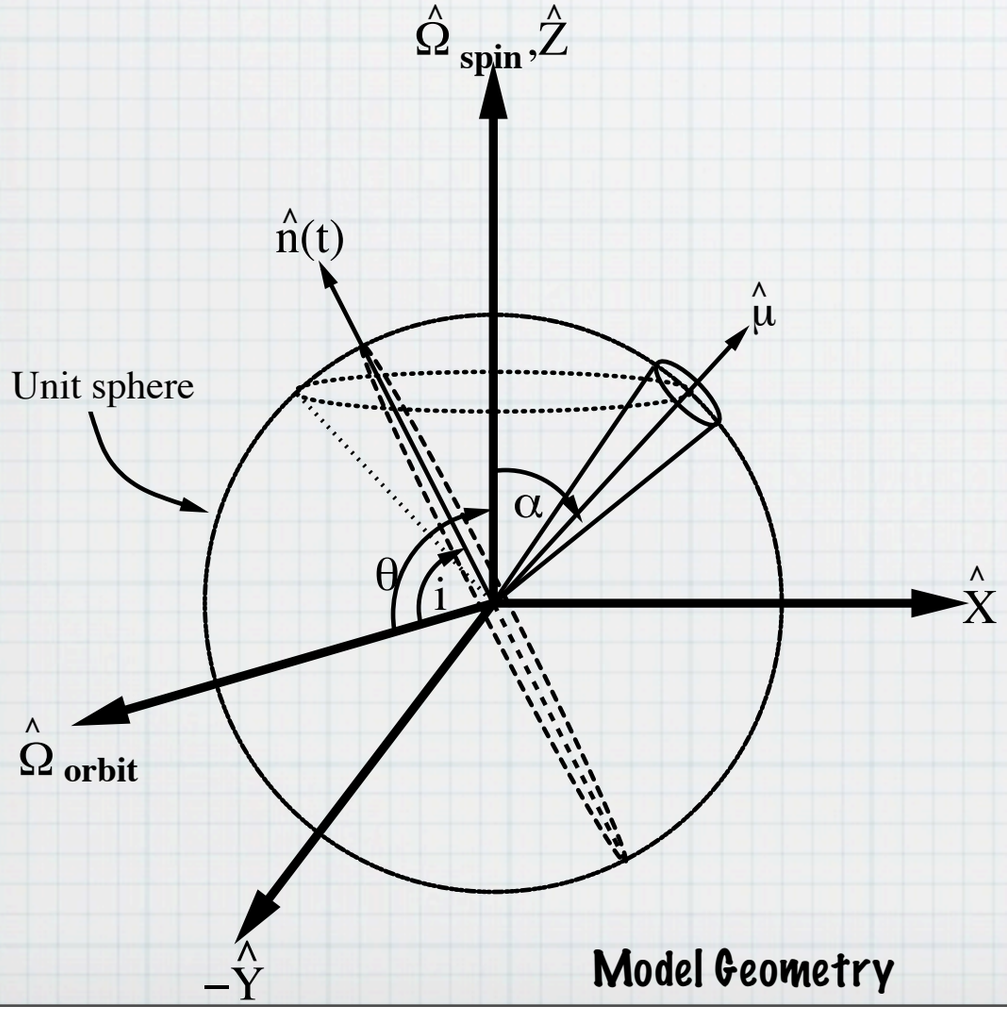

Model Geometry

Neutron Star Mass & Radius

The mass-radius relation of a neutron star is governed by the Tolman-Oppenheimer-Volkoff (TOV) equation

$$\frac{dP(r)}{dr} = -\frac{GM(r)\rho(r)}{r^2}\left[\frac{\left(1+\frac{P(r)}{\rho(r)c^2}\right)\left(1+\frac{4\pi r^3 P(r)}{M(r)c^2}\right)}{\left(1-\frac{2GM(r)}{rc^2}\right)}\right]$$

$$\frac{dM(r)}{dr} = 4\pi r^2 \rho(r)$$

$$P = P(\rho)$$ **Equation of State**

Neutron Star Mass & Radius

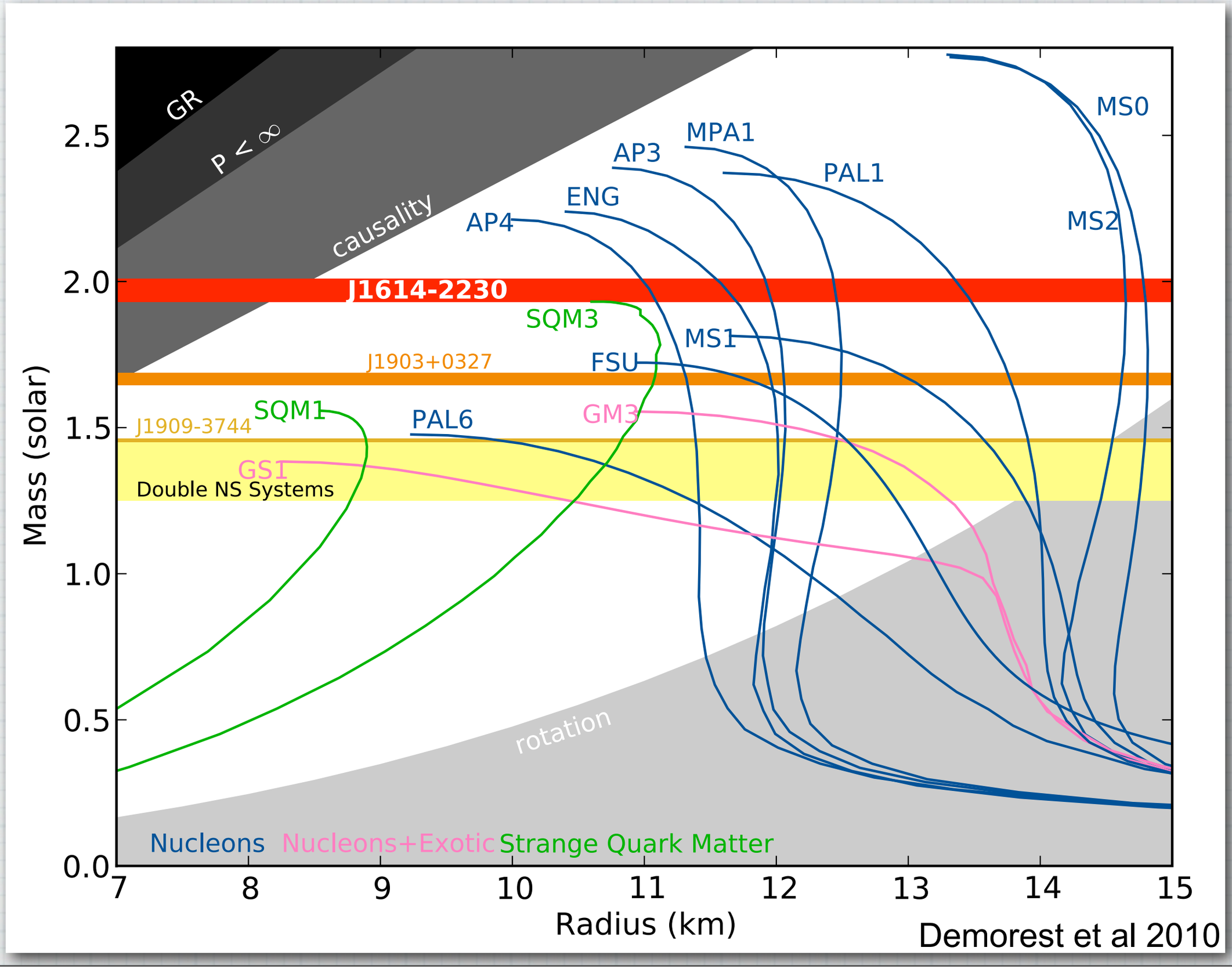

Rotation

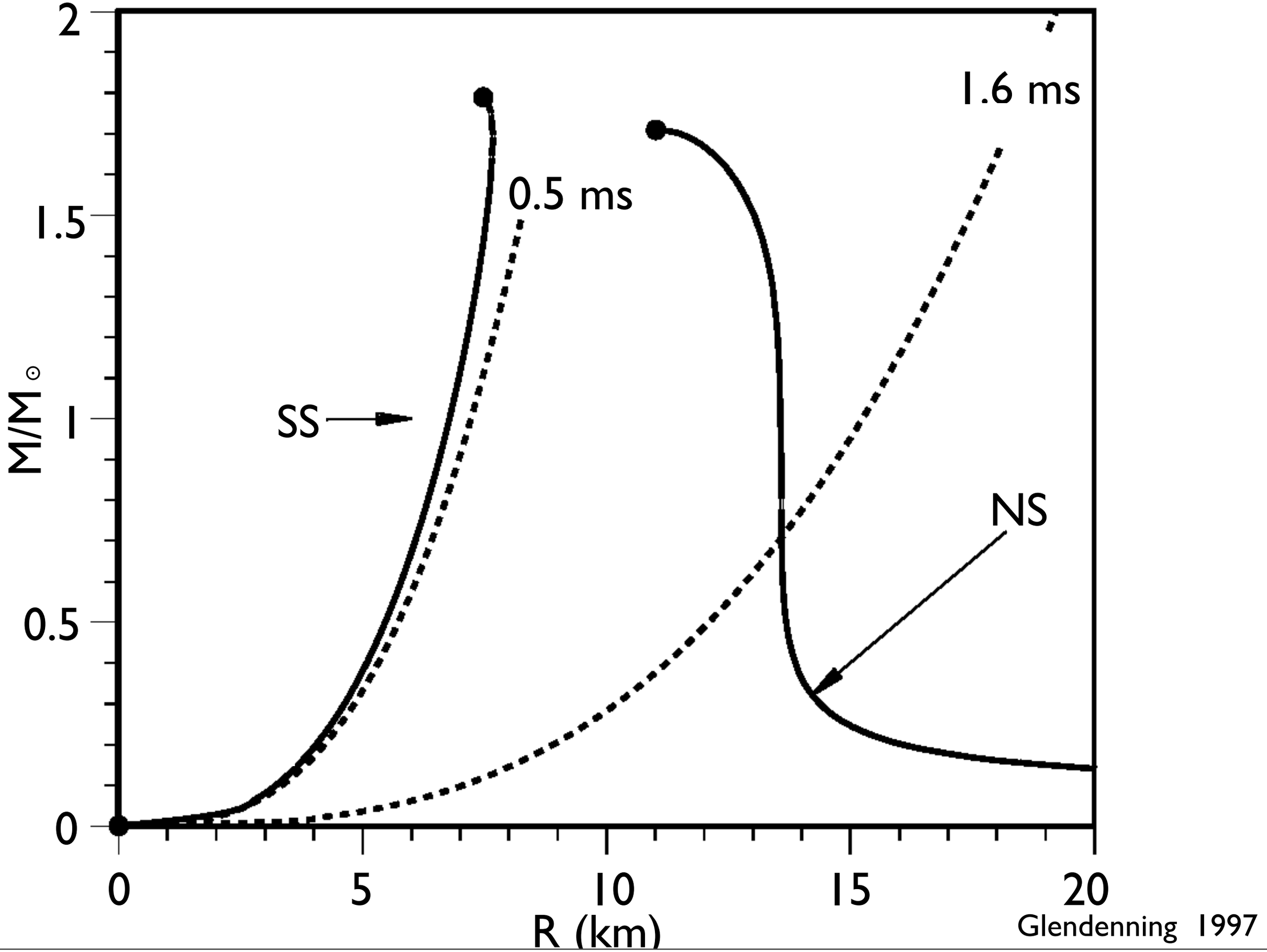

Neutron Star Mass & Rotation

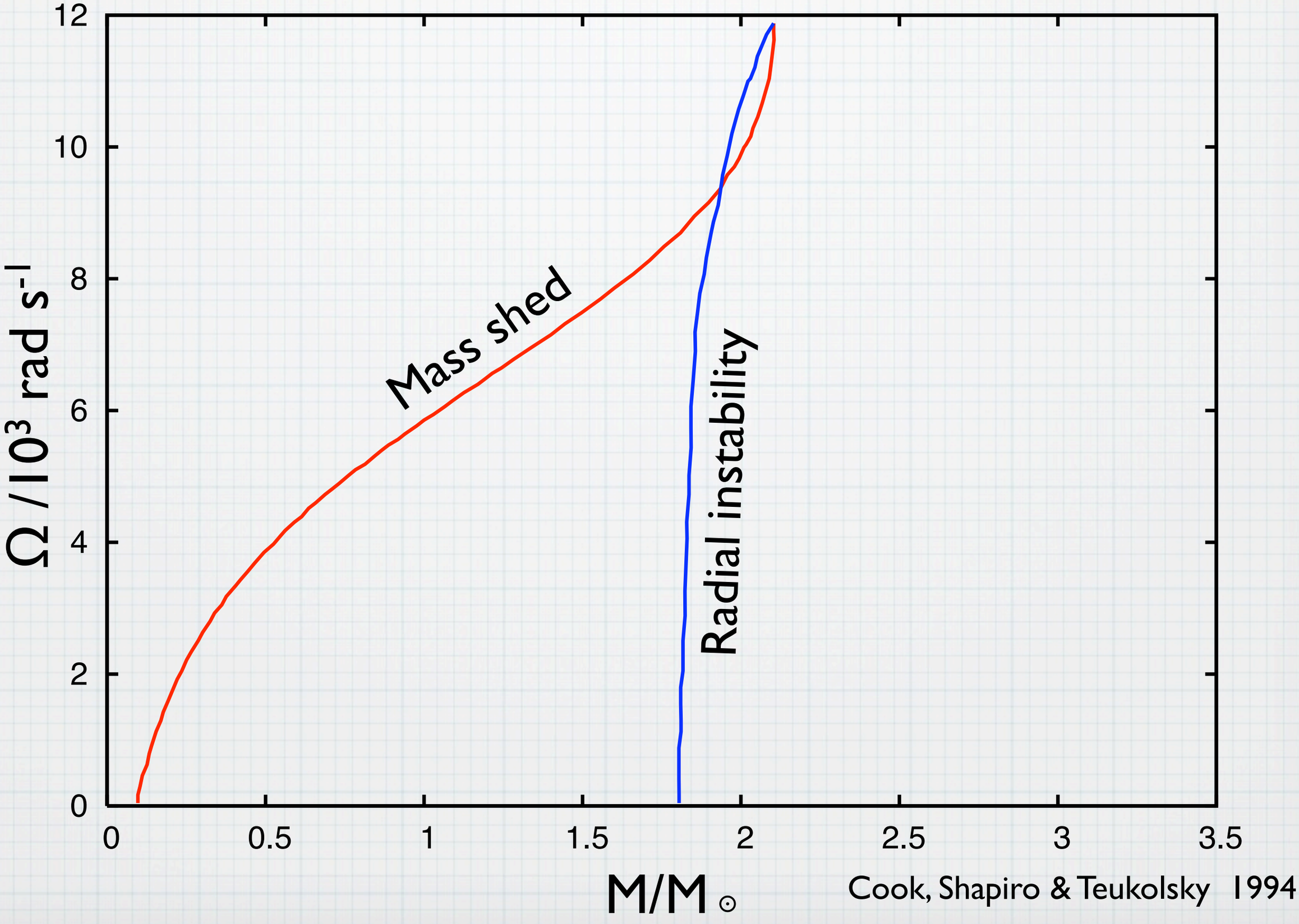

Neutron Star Mass & Rotation

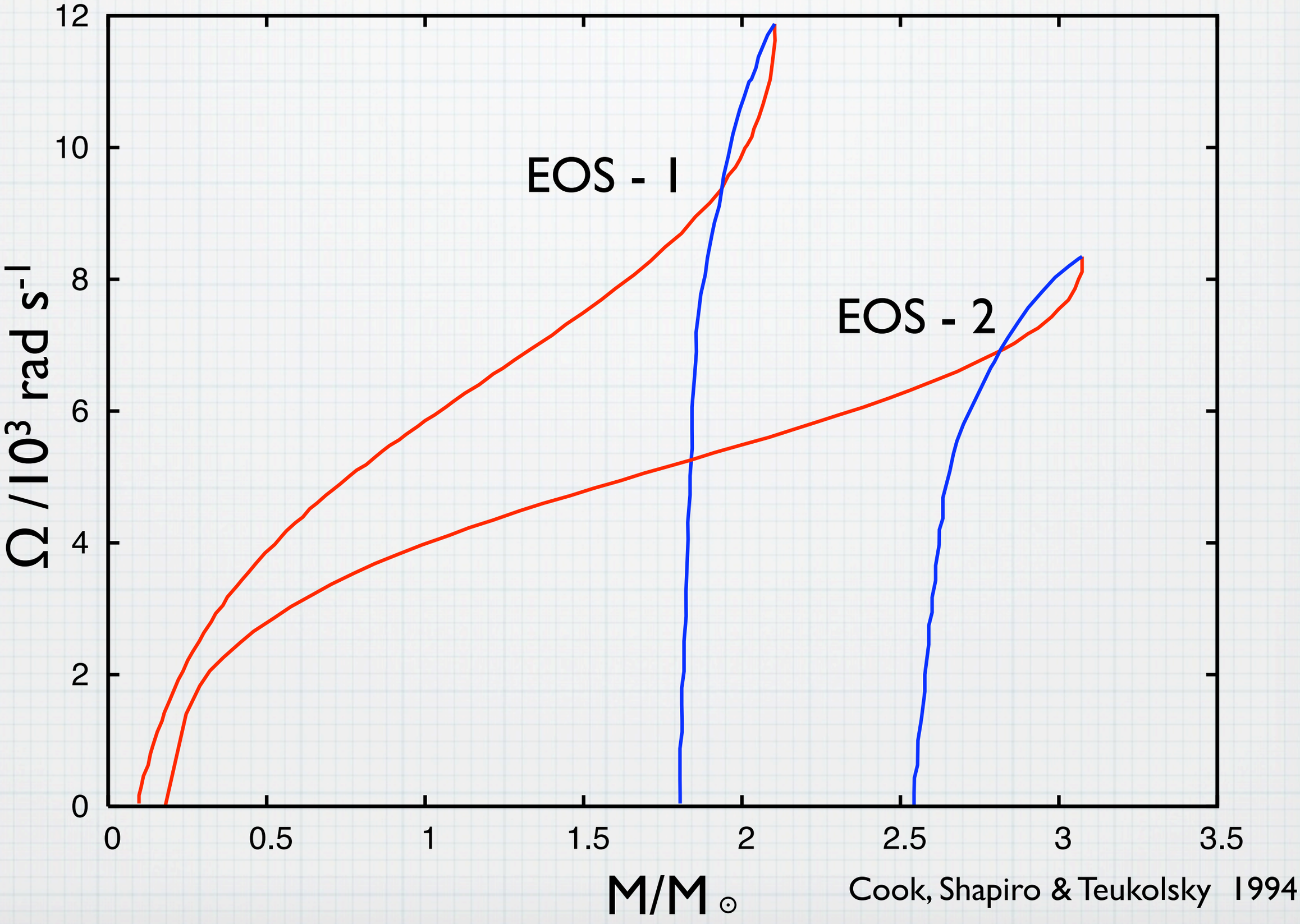

Spin distribution

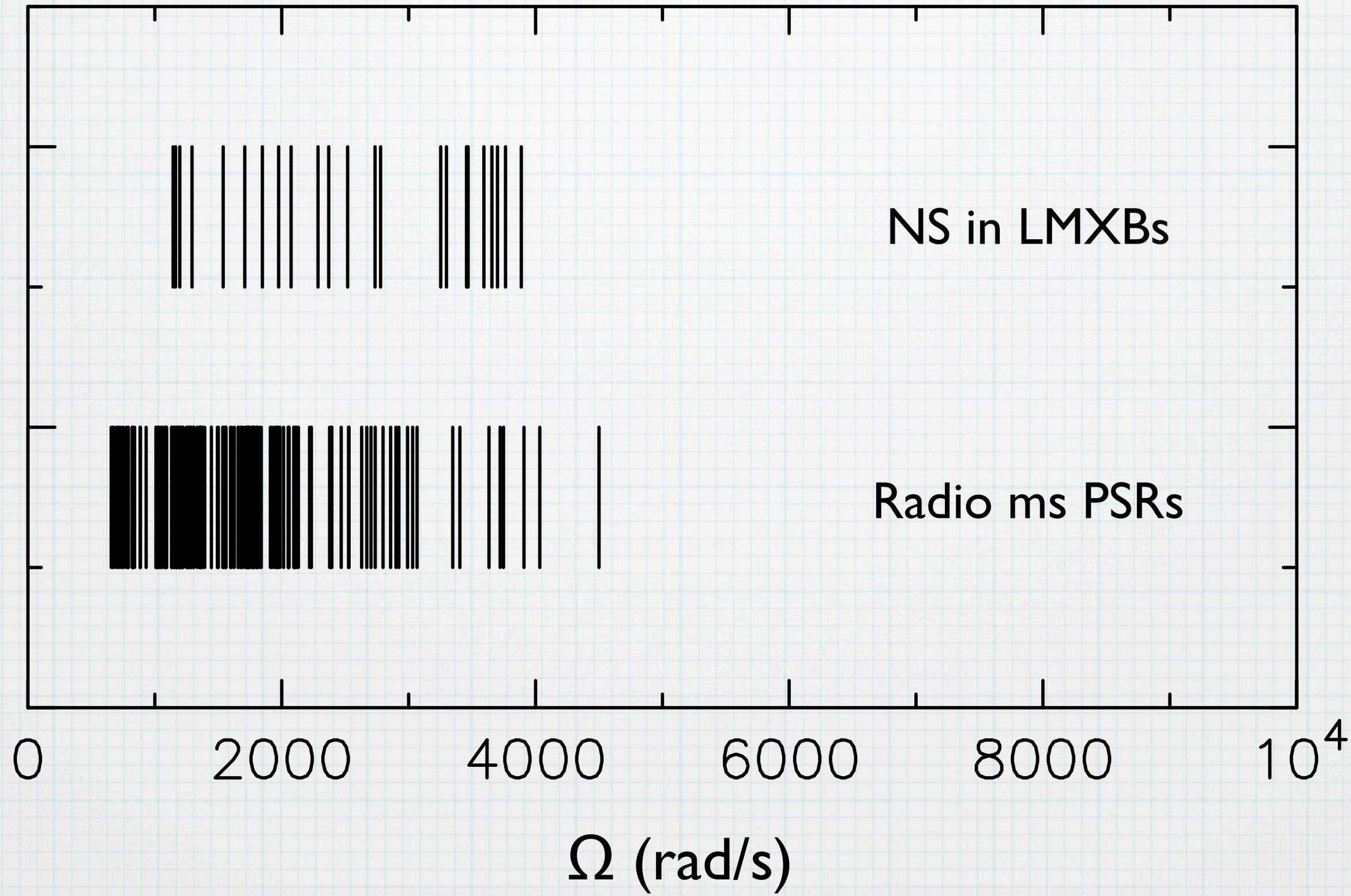

Neutron Star Mass & Rotation

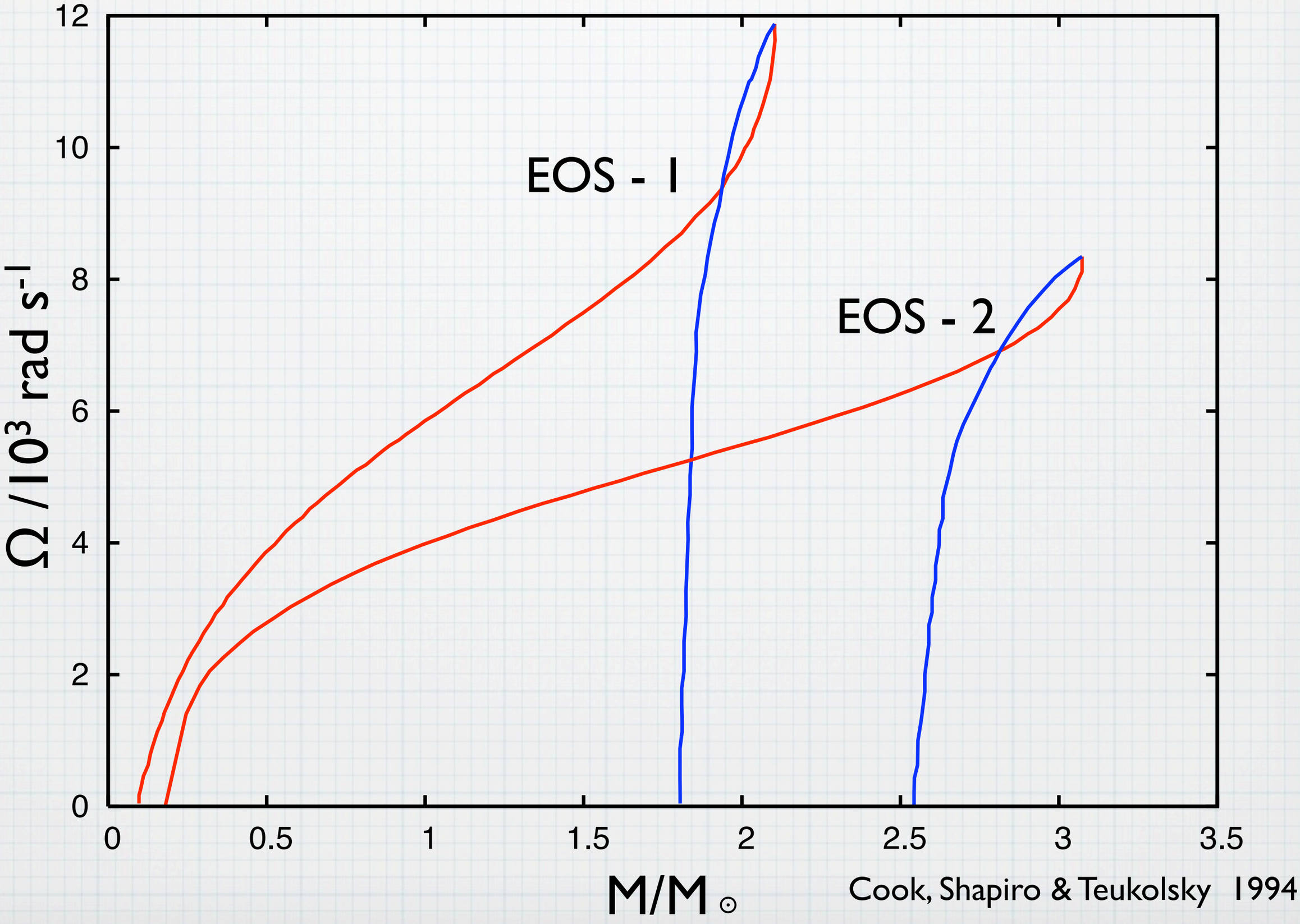

Neutron Star Mass & Rotation

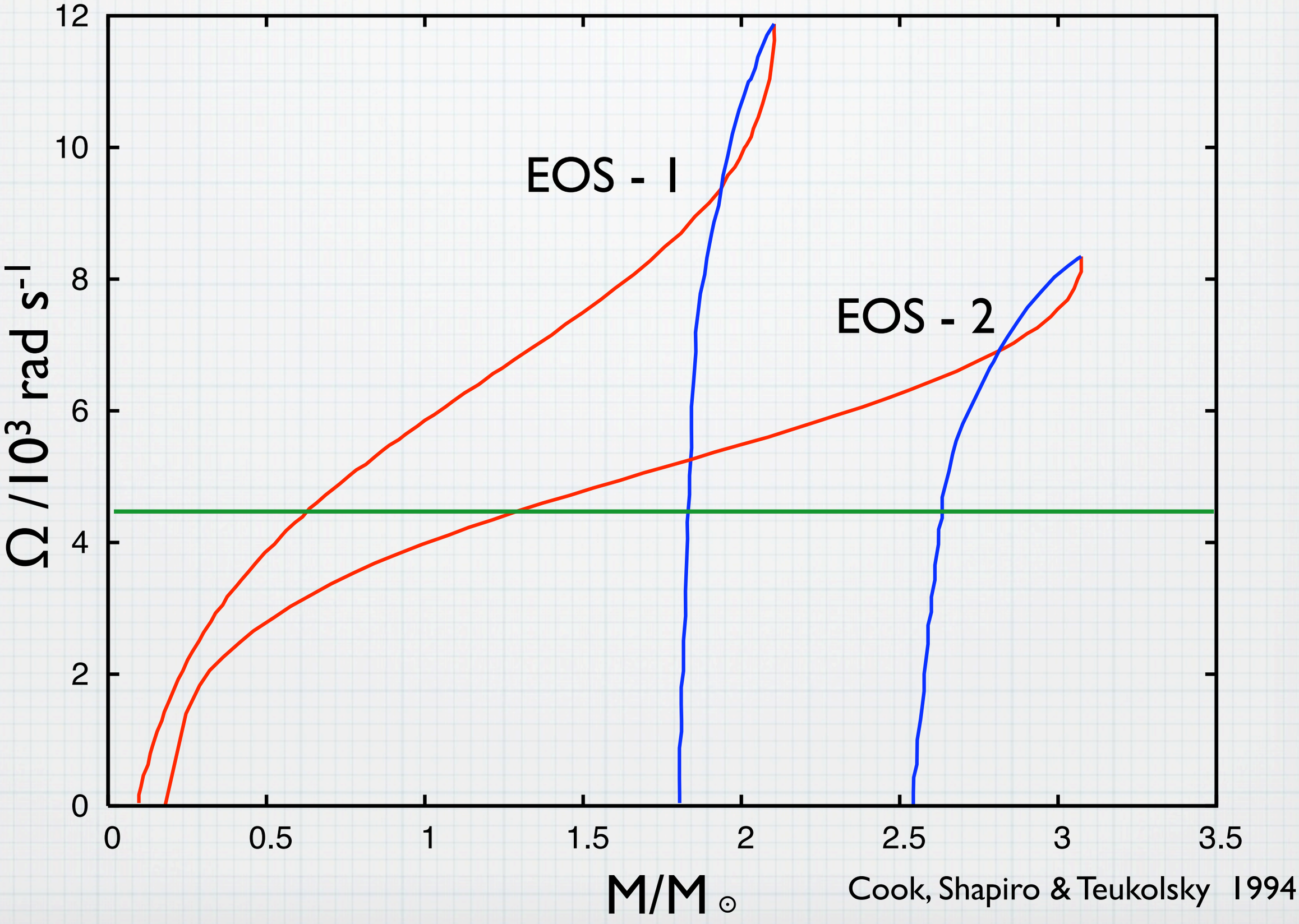

Neutron Star Mass & Rotation

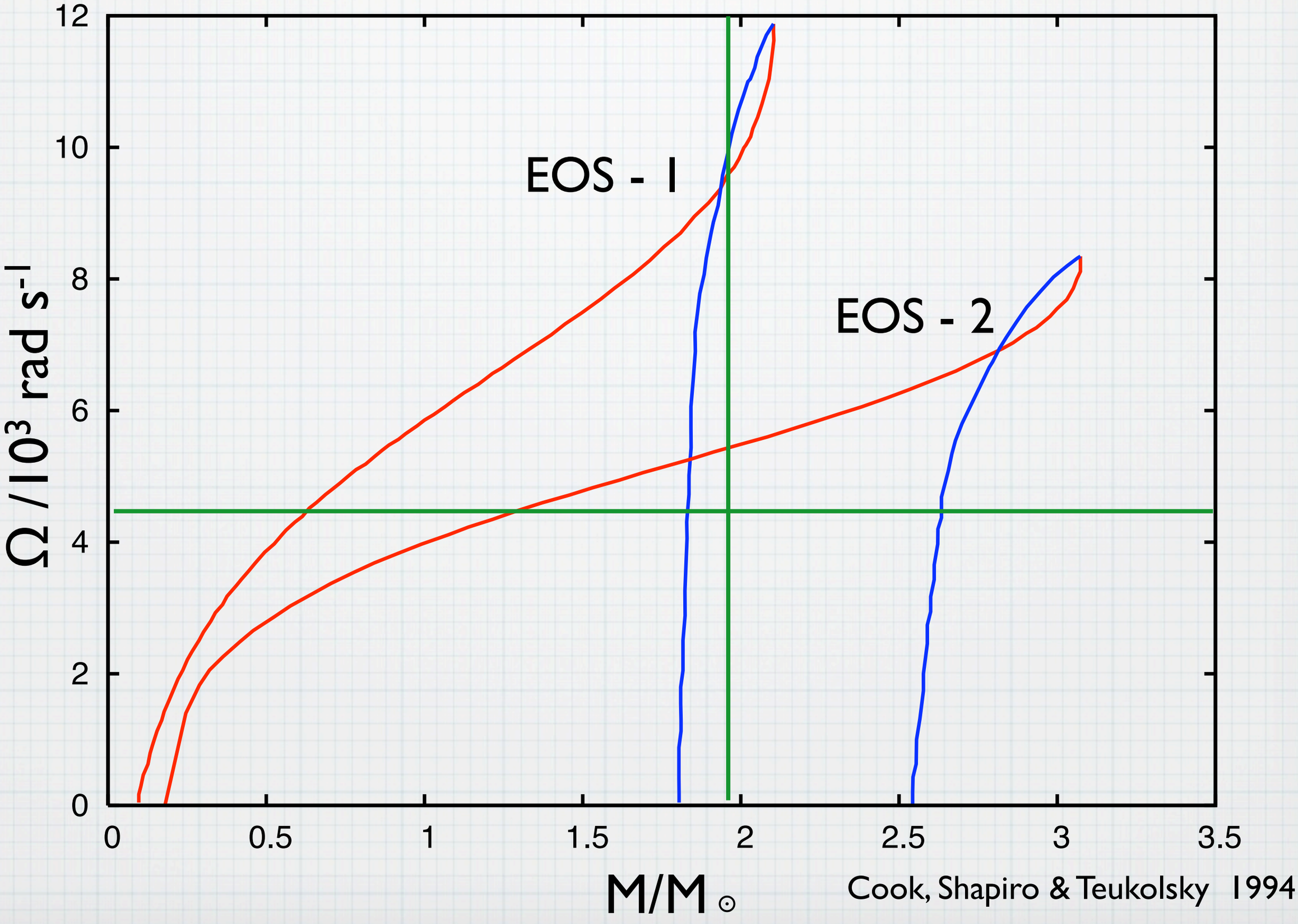

Neutron Star Mass & Rotation

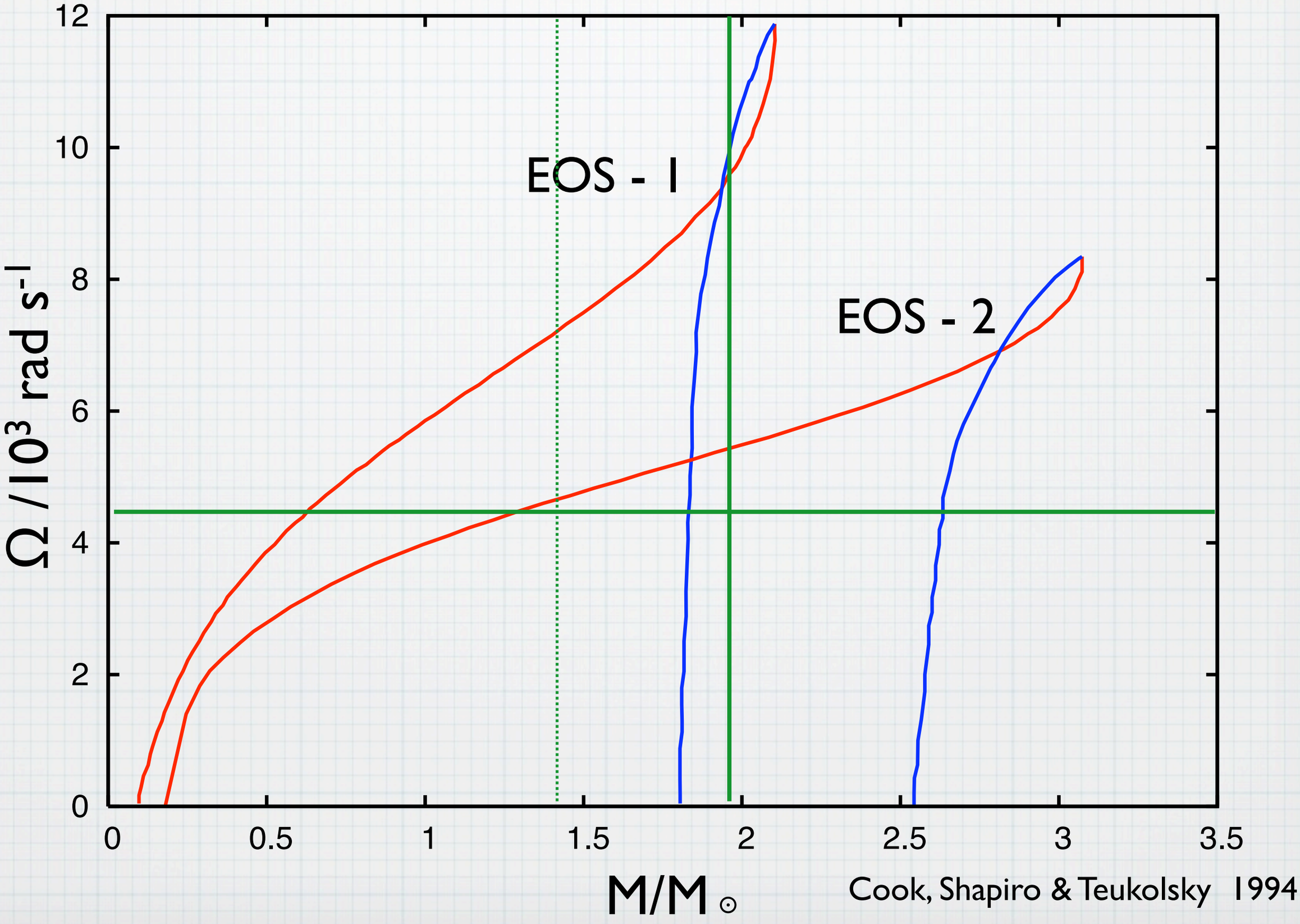

X-ray Bursts in accreting NS

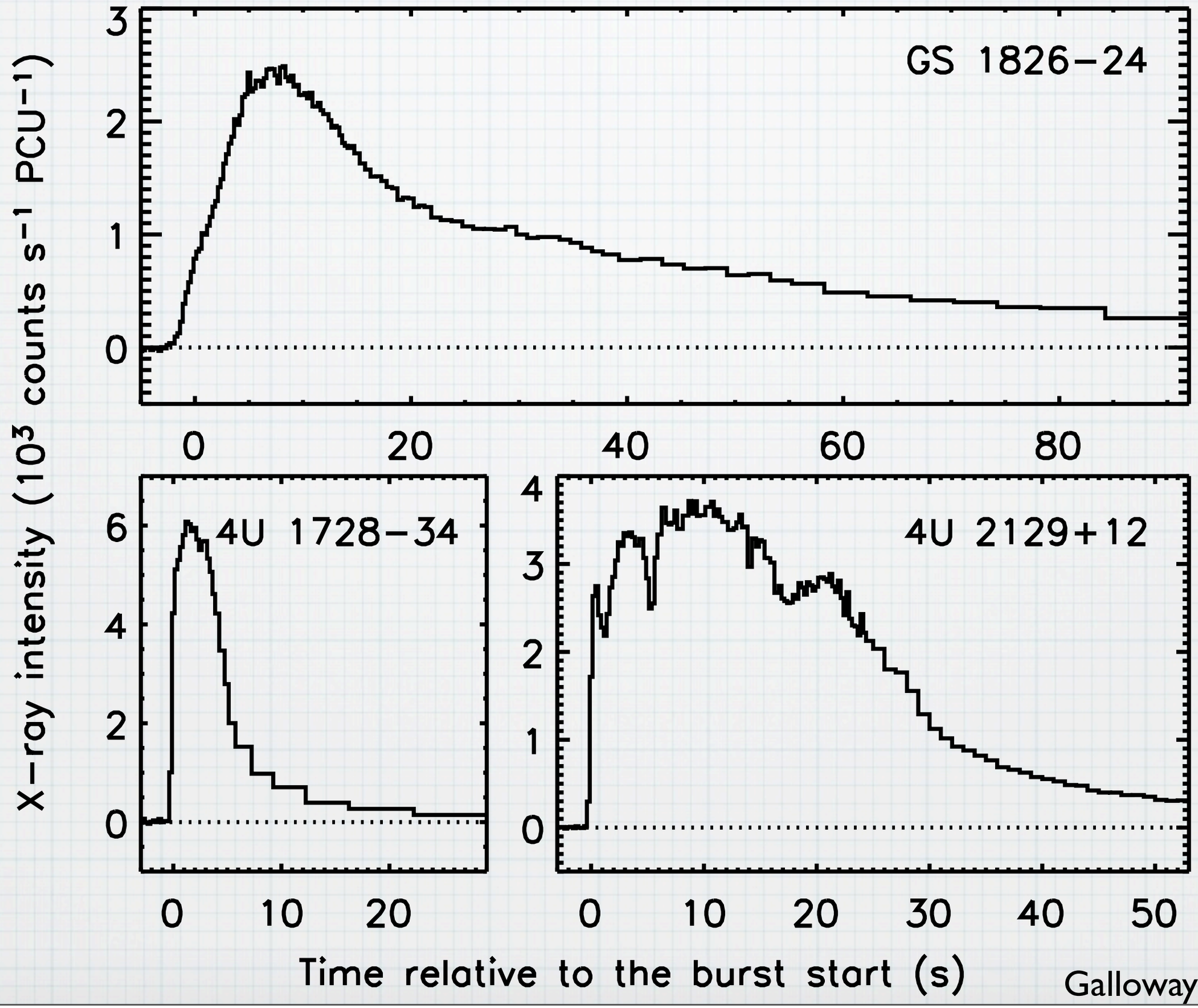

Galloway et al 2008

Burst Oscillations

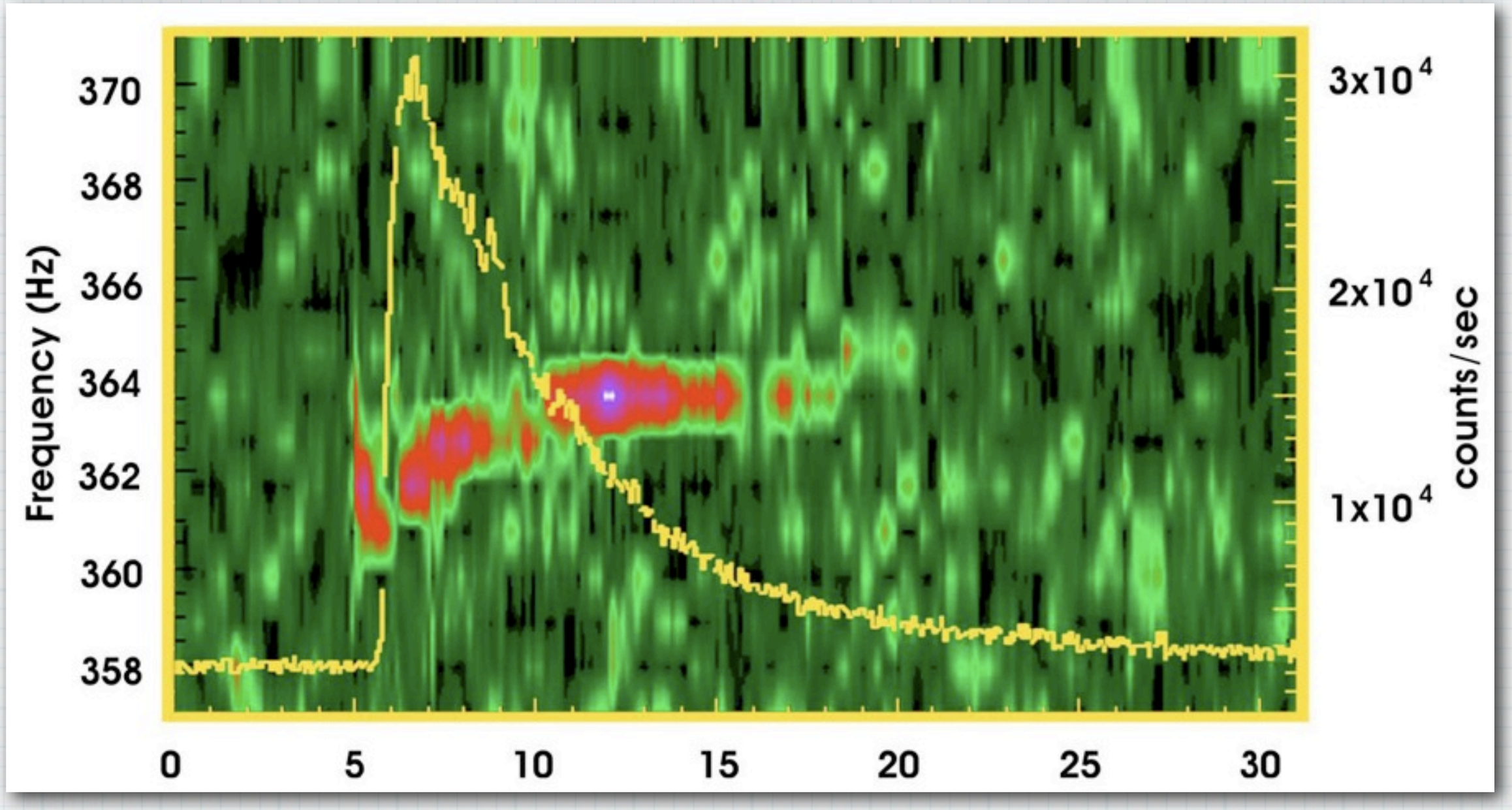

Strohmayer 1996

Burst Oscillations

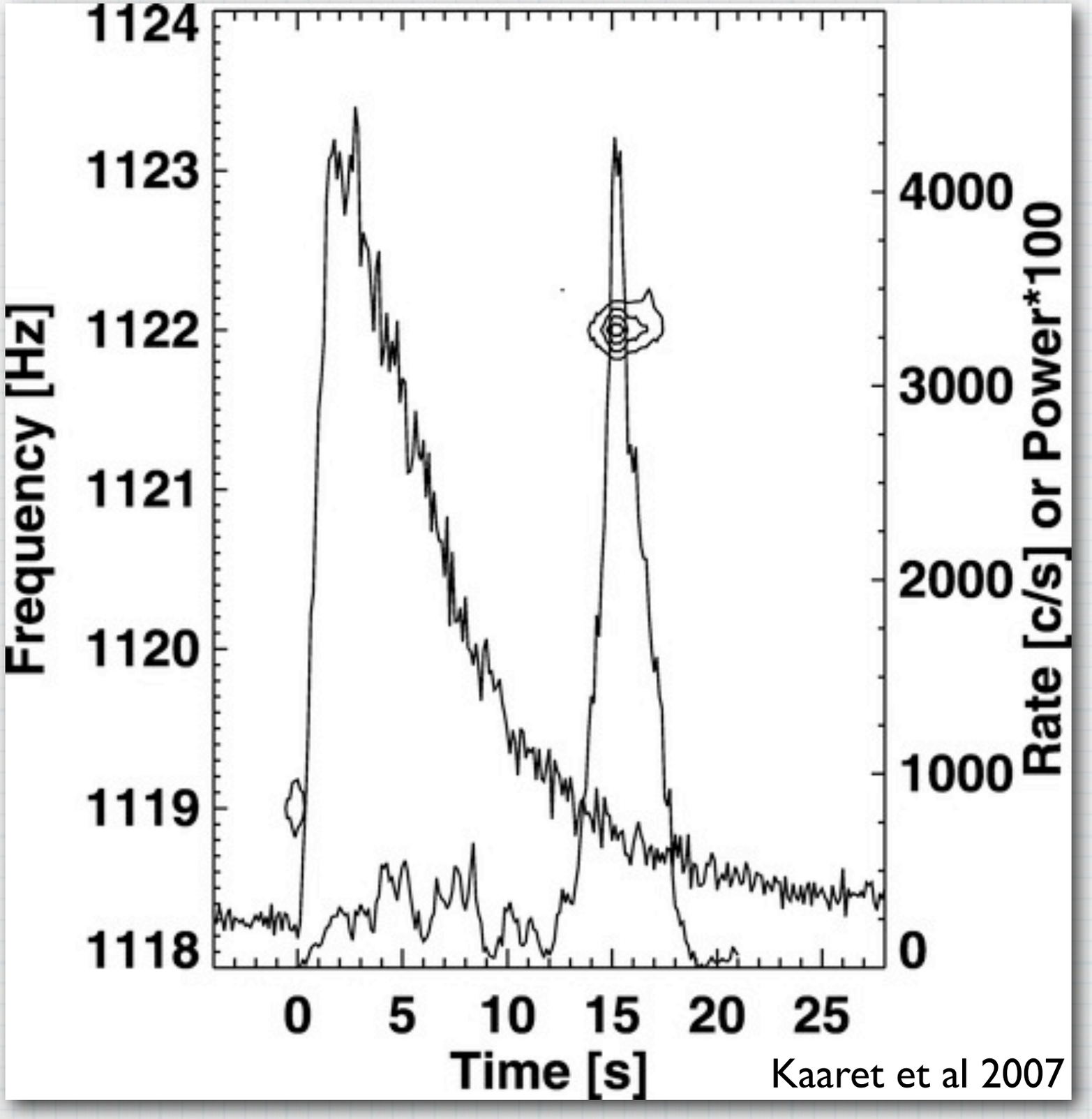

Neutron Star Mass & Rotation

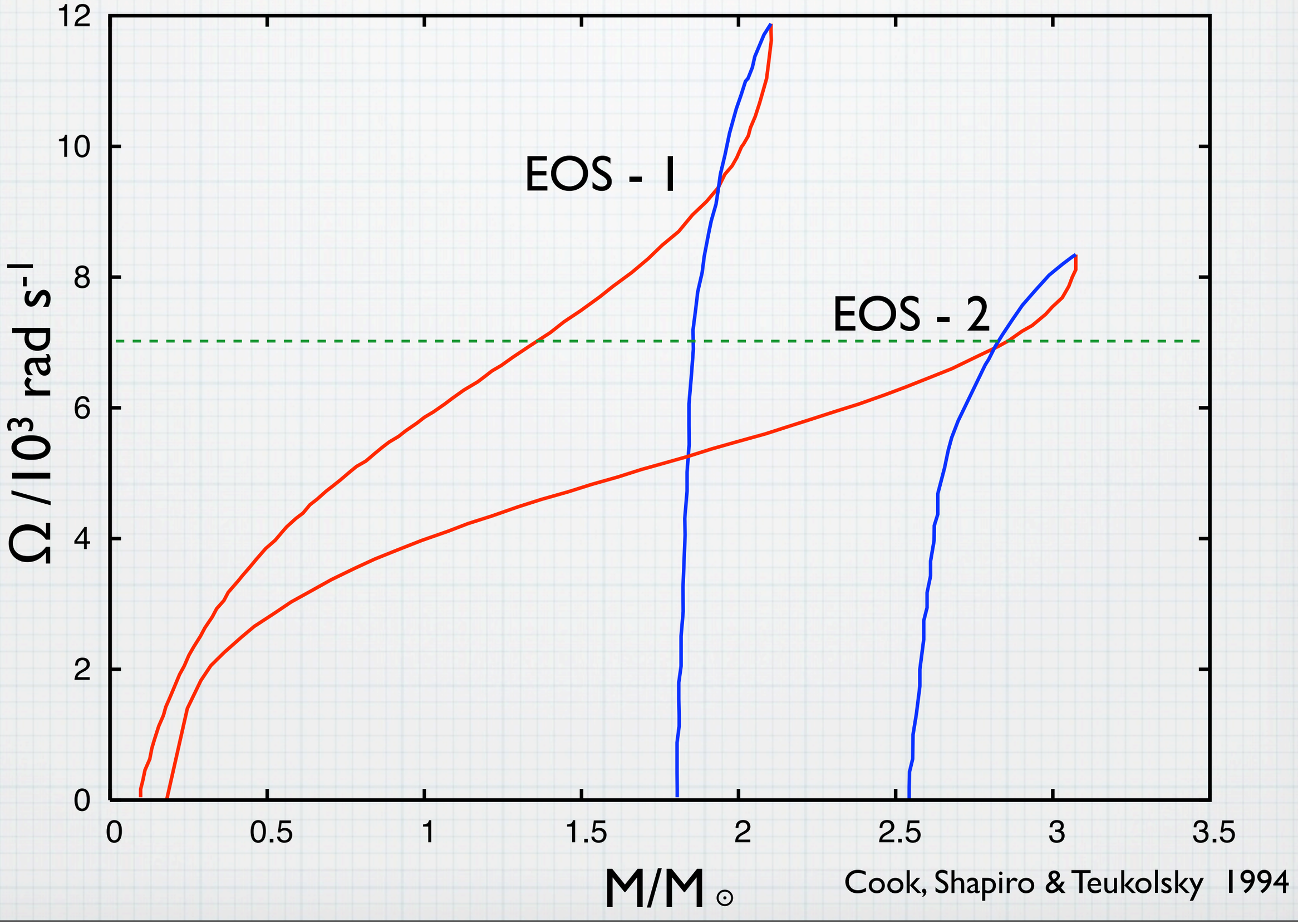

Neutron Star Mass & Rotation

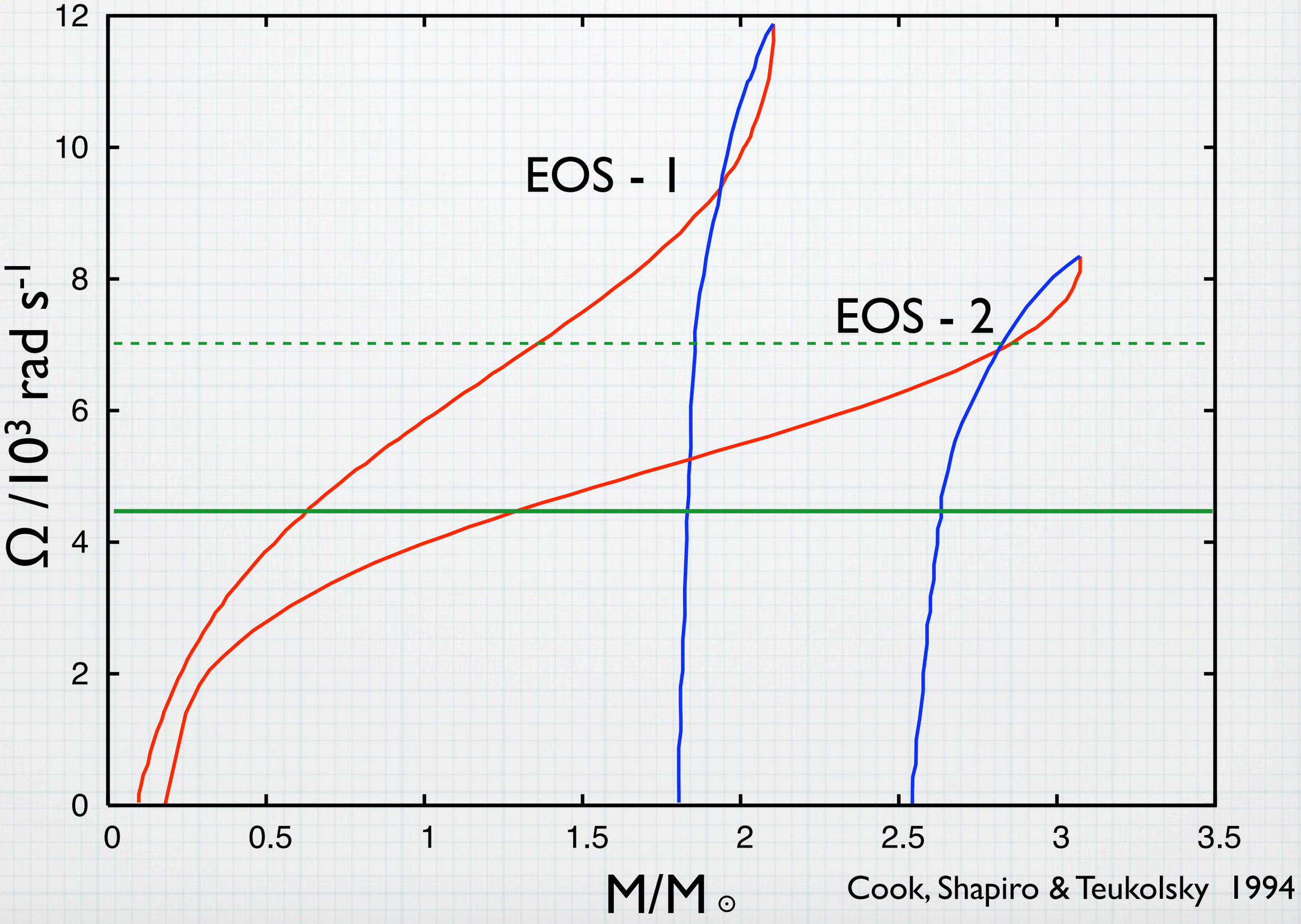

Neutron Star Mass & Rotation

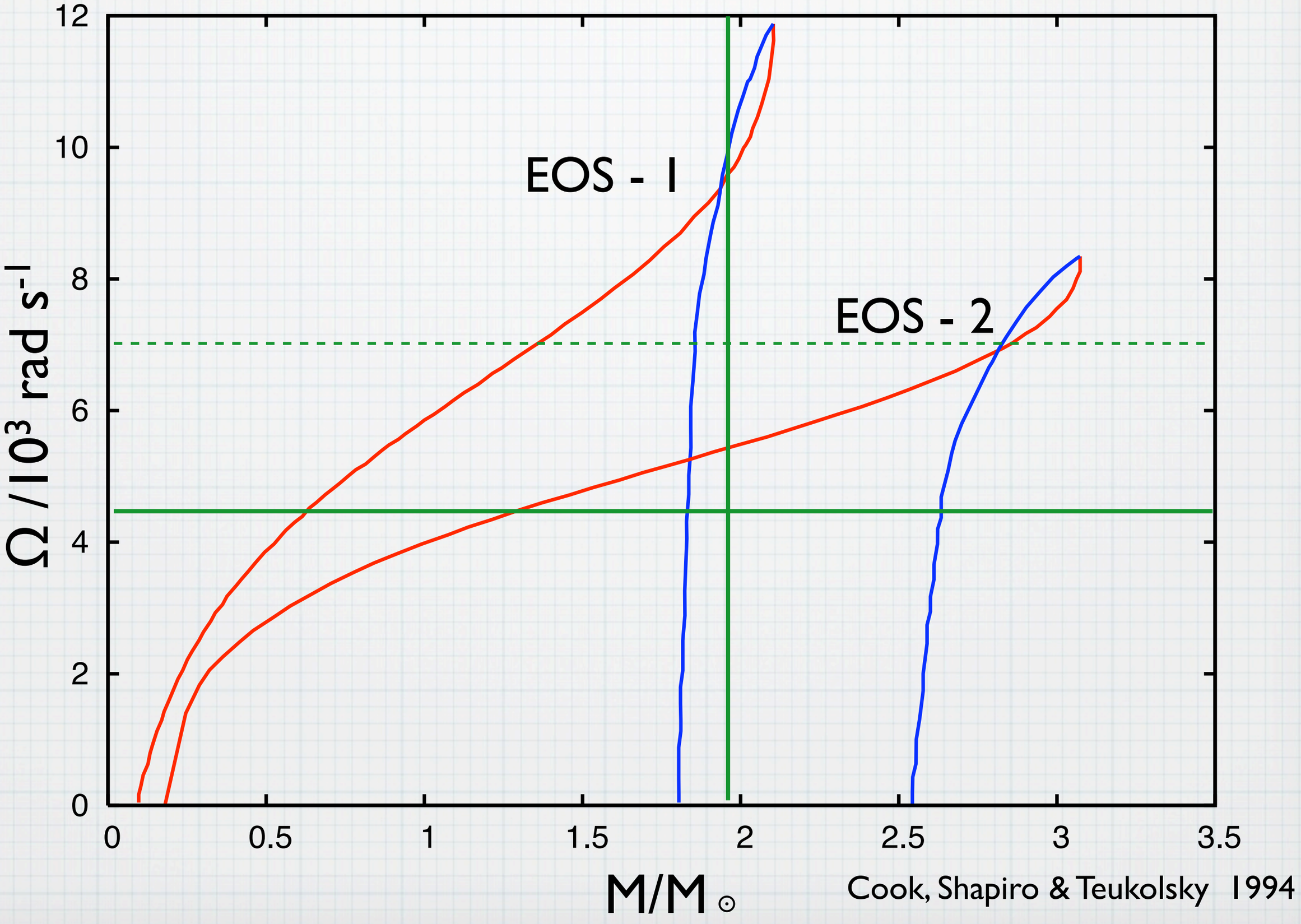

Neutron Star Mass & Rotation

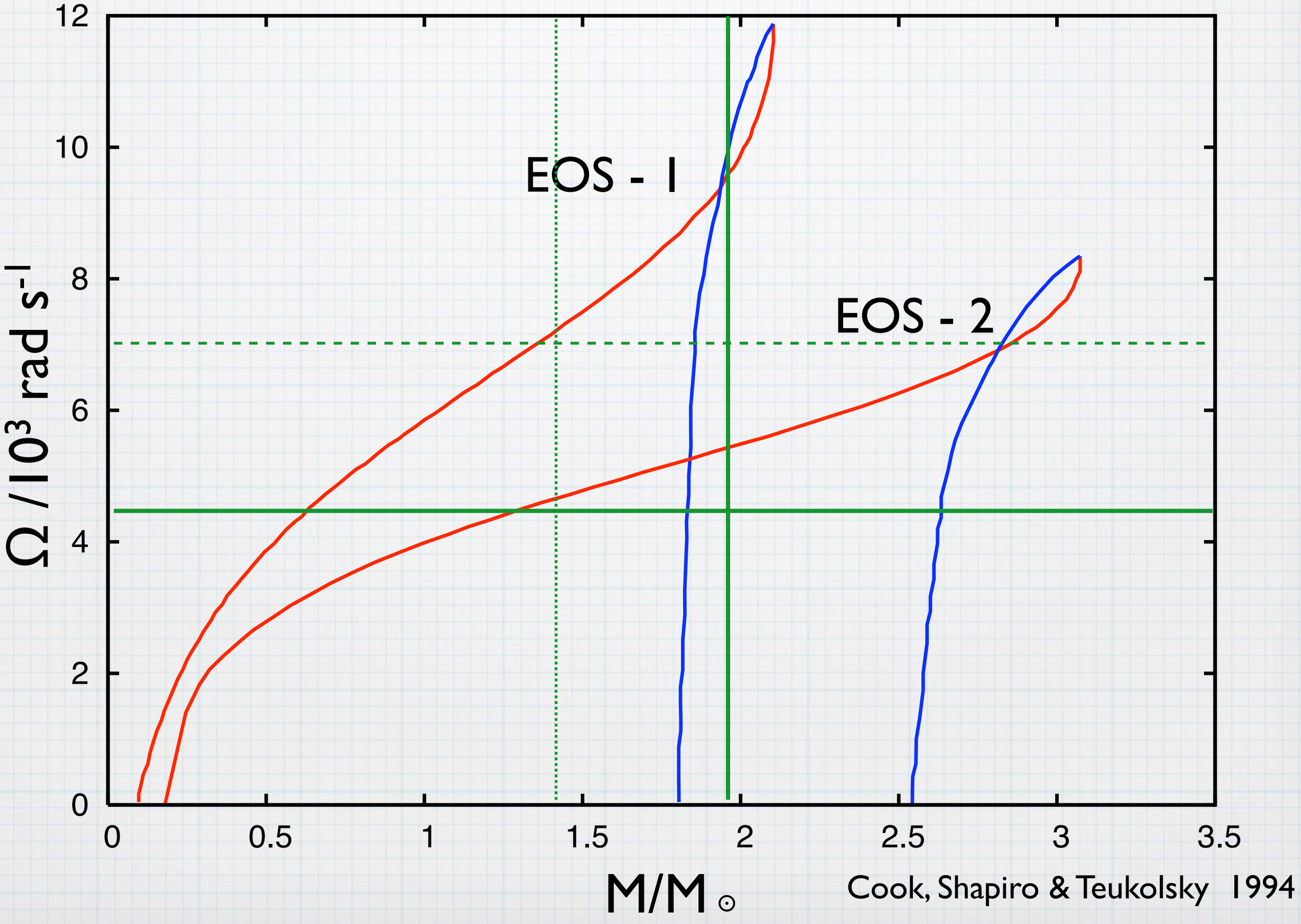

NS Radius from X-ray Bursts

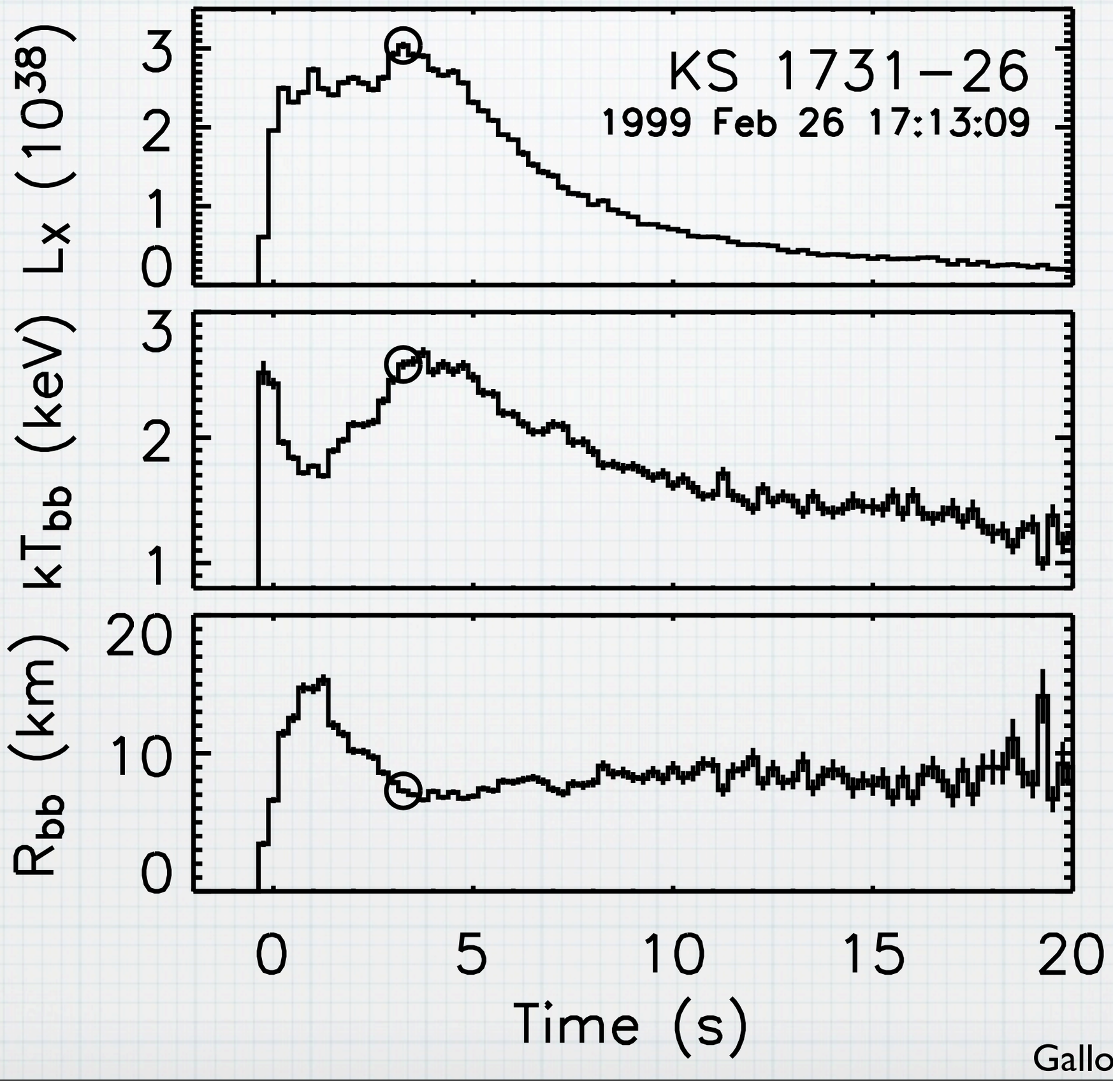

Galloway et al 2008

NS Radius from X-ray Bursts

NS Radius from X-ray Bursts

$$\frac{F_X}{\sigma T^4} = \frac{R^2}{d^2 f_c^4}\left(1 - \frac{2GM}{Rc^2}\right)^{-1}$$

NS Radius from X-ray Bursts

$$\frac{F_X}{\sigma T^4} = \frac{R^2}{d^2 f_c^4}\left(1 - \frac{2GM}{Rc^2}\right)^{-1}$$

$$F_{\rm Edd} = \frac{GMc}{d^2 \kappa_{\rm es}}\left(1 - \frac{2GM}{Rc^2}\right)^{1/2}$$

NS Radius from X-ray Bursts

$$\frac{F_X}{\sigma T^4} = \frac{R^2}{d^2 f_c^4}\left(1 - \frac{2GM}{Rc^2}\right)^{-1}$$

$$F_{\rm Edd} = \frac{GMc}{d^2 \kappa_{\rm es}}\left(1 - \frac{2GM}{Rc^2}\right)^{1/2}$$

$F_X, F_{\rm Edd}$ and $T(F_X)$ measurable from X-ray data

NS Radius from X-ray Bursts

$$\frac{F_X}{\sigma T^4} = \frac{R^2}{d^2 f_c^4}\left(1 - \frac{2GM}{Rc^2}\right)^{-1}$$

$$F_{\rm Edd} = \frac{GMc}{d^2 \kappa_{\rm es}}\left(1 - \frac{2GM}{Rc^2}\right)^{1/2}$$

$F_X, F_{\rm Edd}$ and $T(F_X)$ measurable from X-ray data

d estimate from independent source

NS Radius from X-ray Bursts

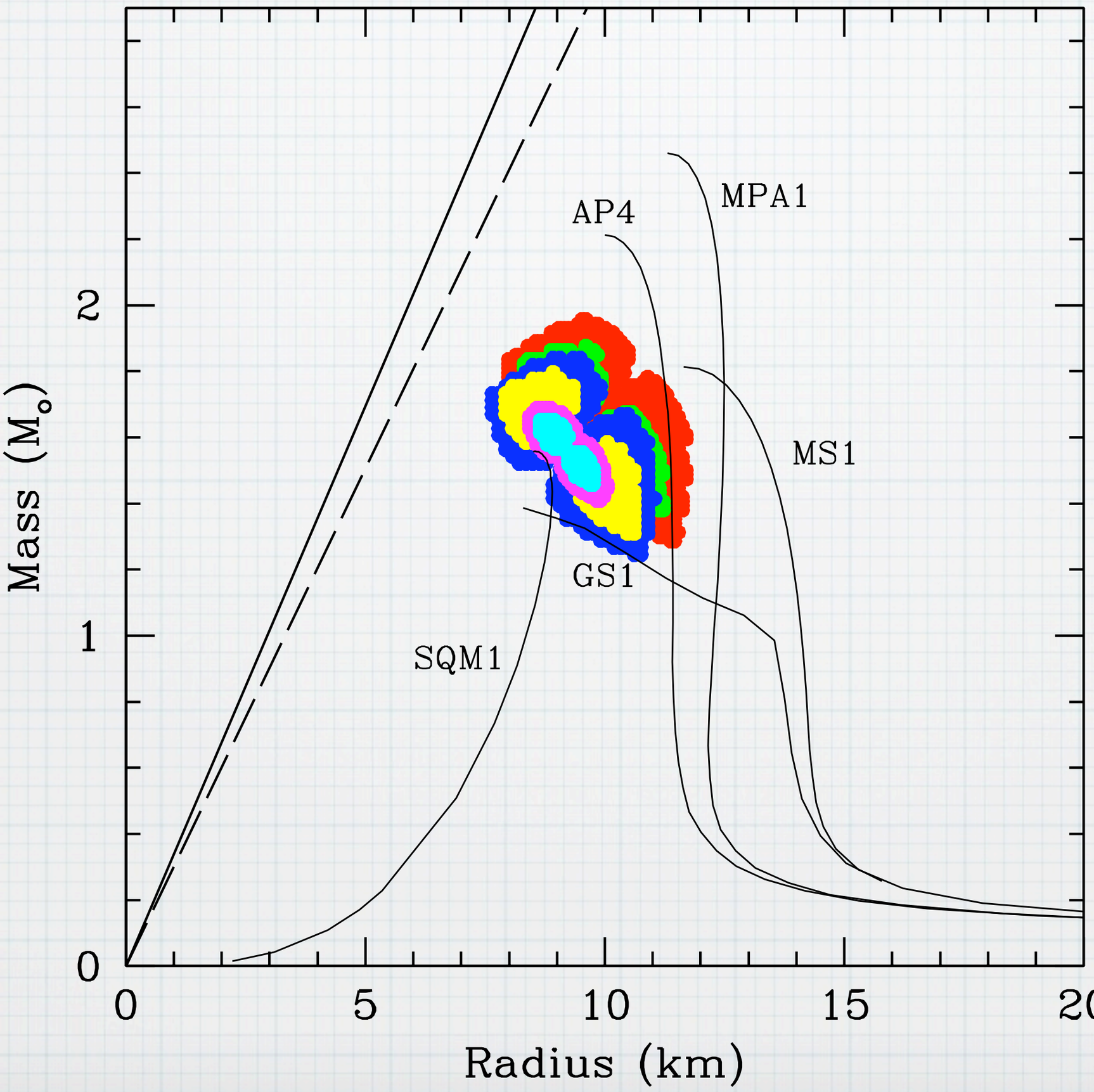

4U 1608-24
EXO 1745-248
4U 1820-30

Ozel et al 2010

Pulse profile

Pulse profile

Radio Pulsars : Sharp pulses, duty cycle ~ 5%, mod ~100%

Pulse profile

Radio Pulsars : Sharp pulses, duty cycle ~ 5%, mod ~100%

PSR B0833-45
13.7 GHz, EPN

Pulse profile

Radio Pulsars : Sharp pulses, duty cycle ~ 5%, mod ~100%

PSR B0833-45
13.7 GHz, EPN

Accr. X-ray PSRs : Wide, near-sinusoidal profile, mod < 20%

Pulse profile

Radio Pulsars : Sharp pulses, duty cycle ~ 5%, mod ~100%

PSR B0833-45
13.7 GHz, EPN

Accr. X-ray PSRs : Wide, near-sinusoidal profile, mod < 20%

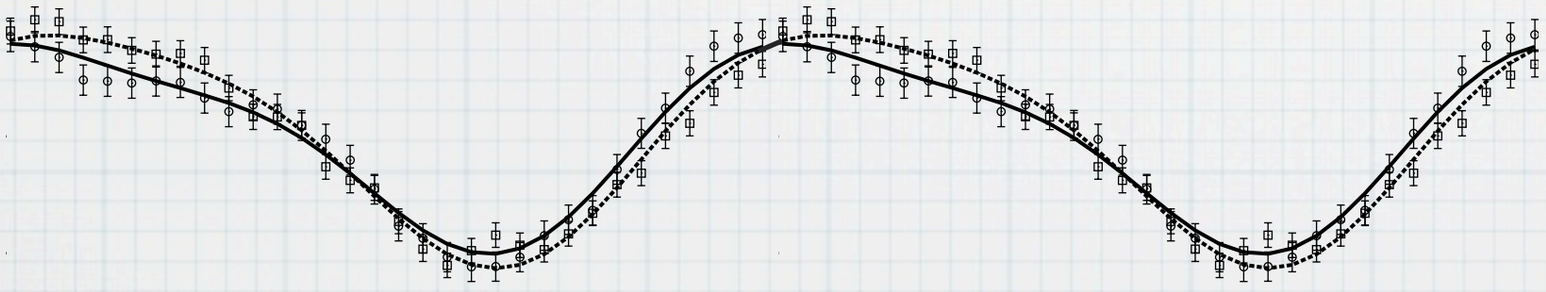

SAX J1808.4-3658
Morsink & Leahy 2011

Pulse profile

Radio Pulsars : Sharp pulses, duty cycle ~ 5%, mod ~100%

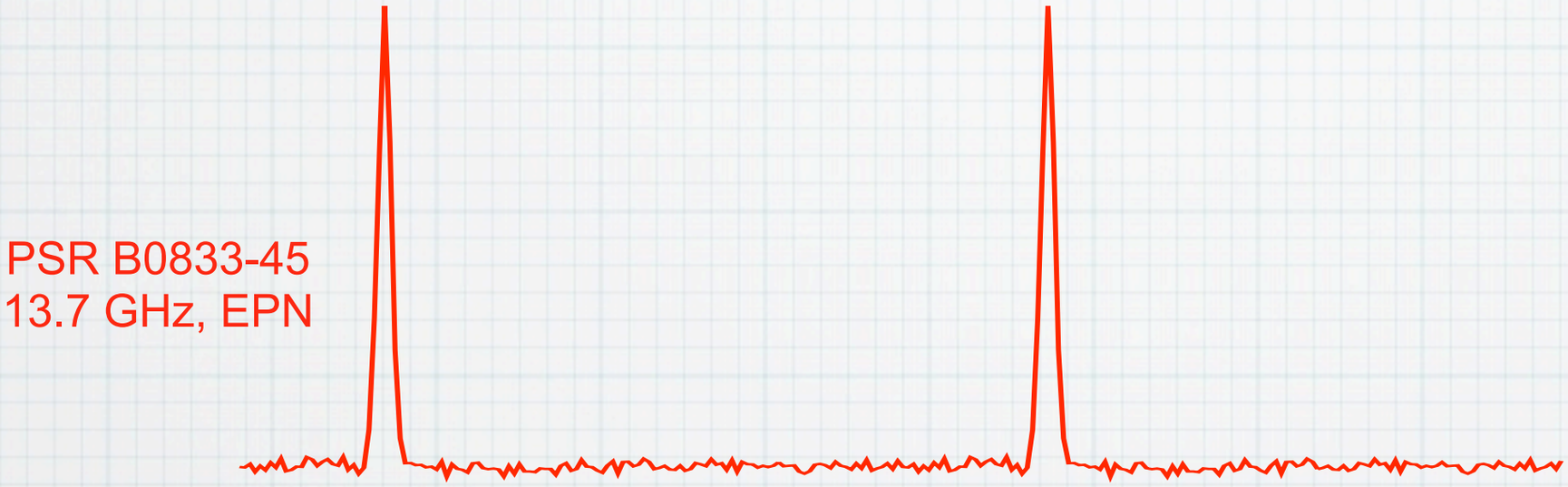

Accr. X-ray PSRs : Wide, near-sinusoidal profile, mod < 20%

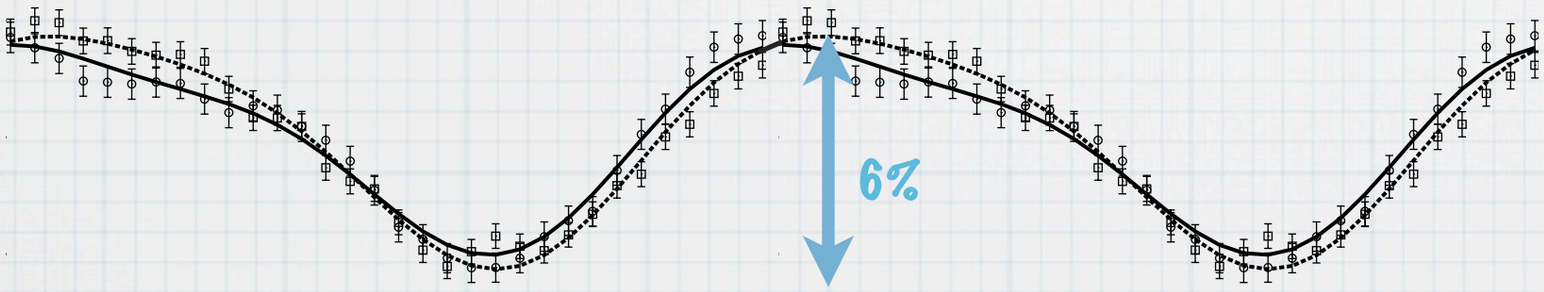

SAX J1808.4-3658
Morsink & Leahy 2011

Pulse profile

Radio Pulsars : Sharp pulses, duty cycle ~ 5%, mod ~100%

PSR B0833-45
13.7 GHz, EPN

Relativistically beamed emission occurring far from surface

Accr. X-ray PSRs : Wide, near-sinusoidal profile, mod < 20%

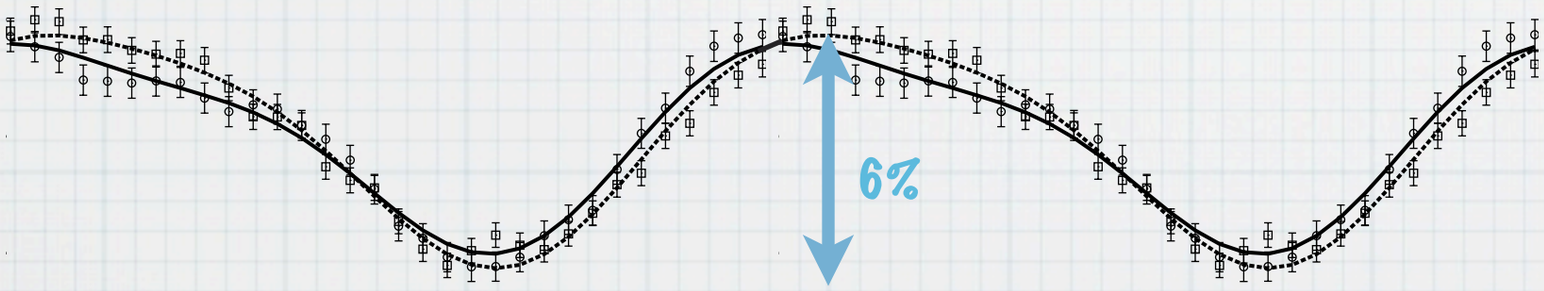

SAX J1808.4-3658
Morsink & Leahy 2011

Pulse profile

Radio Pulsars : Sharp pulses, duty cycle ~ 5%, mod ~100%

PSR B0833-45
13.7 GHz, EPN

Relativistically beamed emission occurring far from surface

Accr. X-ray PSRs : Wide, near-sinusoidal profile, mod < 20%

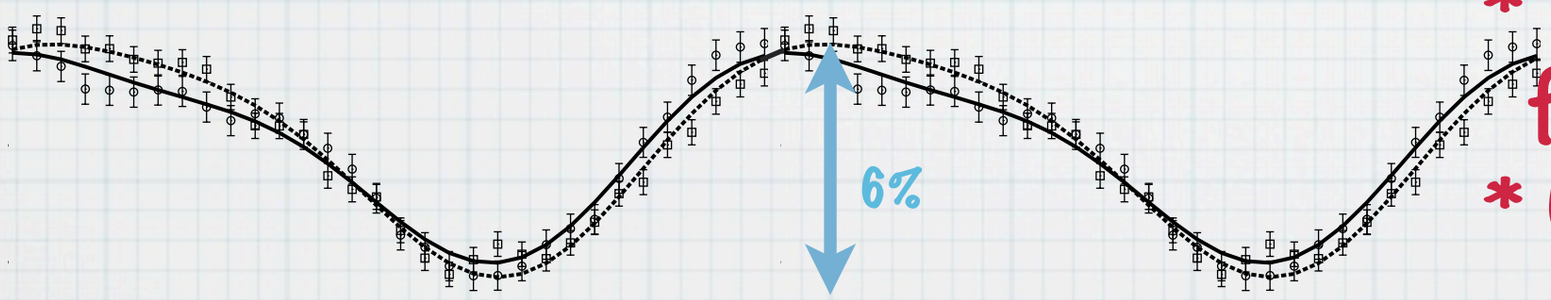

SAX J1808.4-3658
Morsink & Leahy 2011

* Near-isotropic emission from hot-spot on surface,
* Grav. light bending

Pulse profile

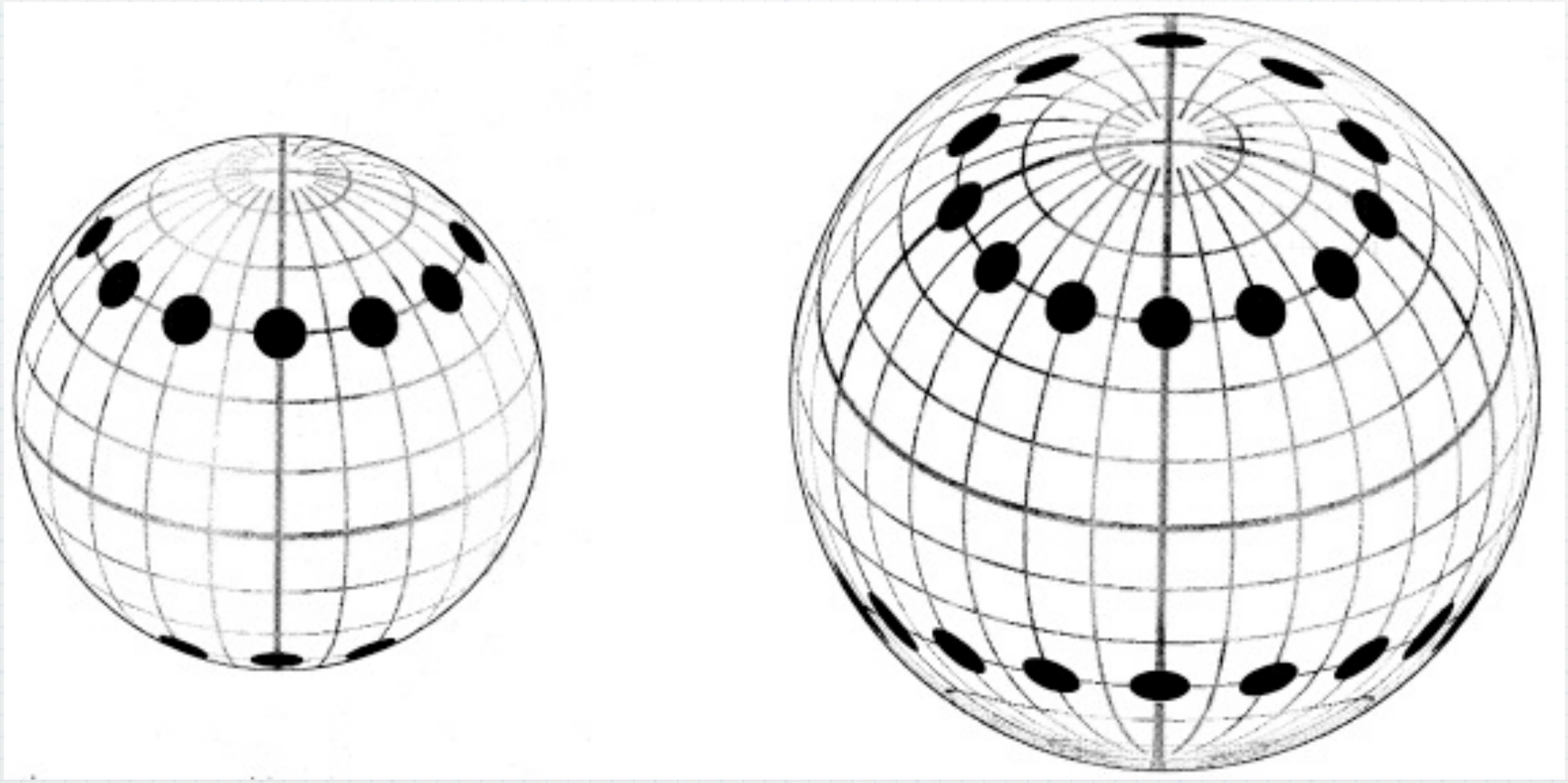

Effect of light bending

Pulse profile

of a small hotspot on a NS surface

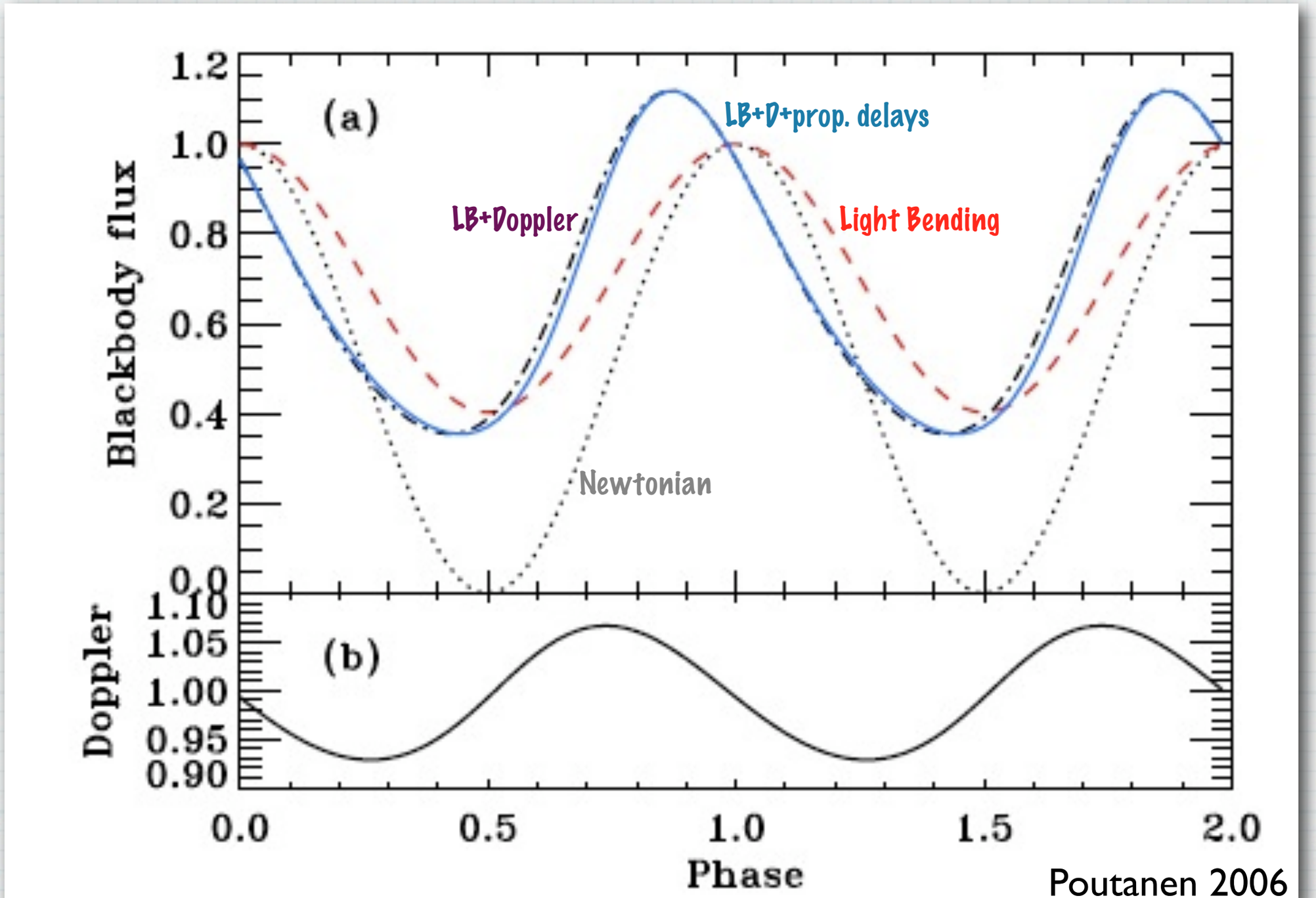

Poutanen 2006

Pulse profile

of SAX J1808.4-3658 with model fits

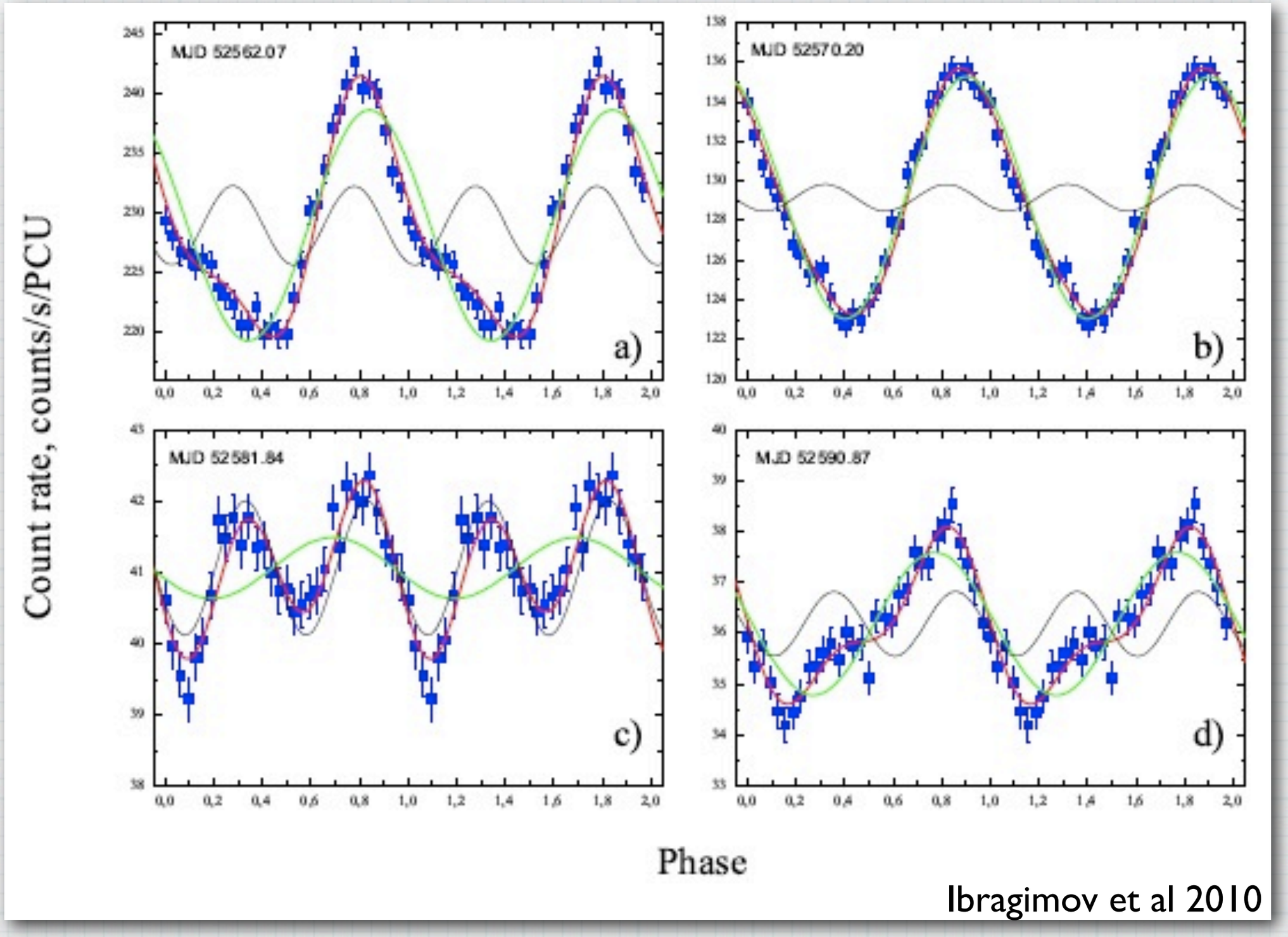

Ibragimov et al 2010

Burst oscillation profile

simulated variation of mean energy

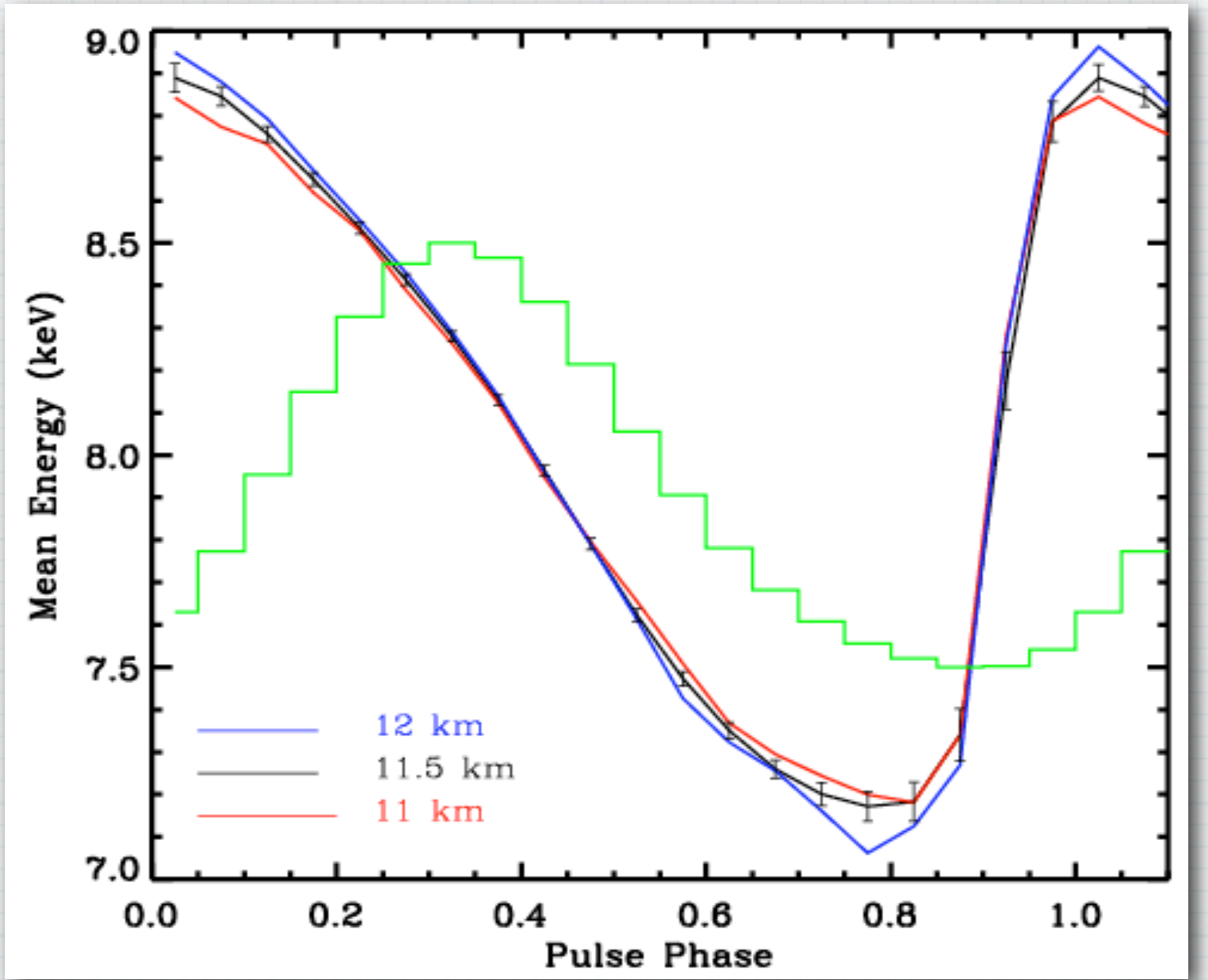

Arzoumanian 2010

Signatures in the accretion

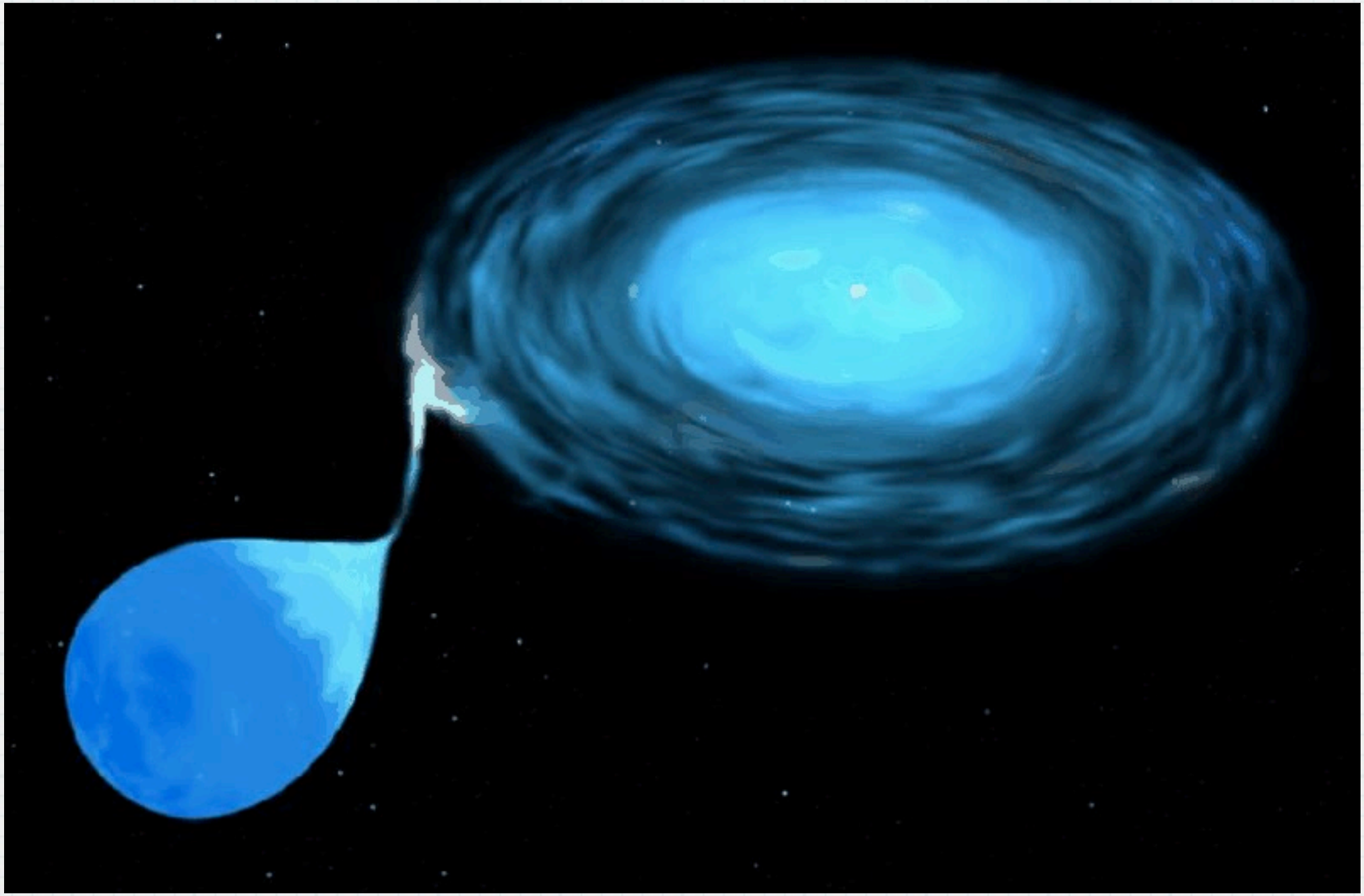

Signatures in the accretion

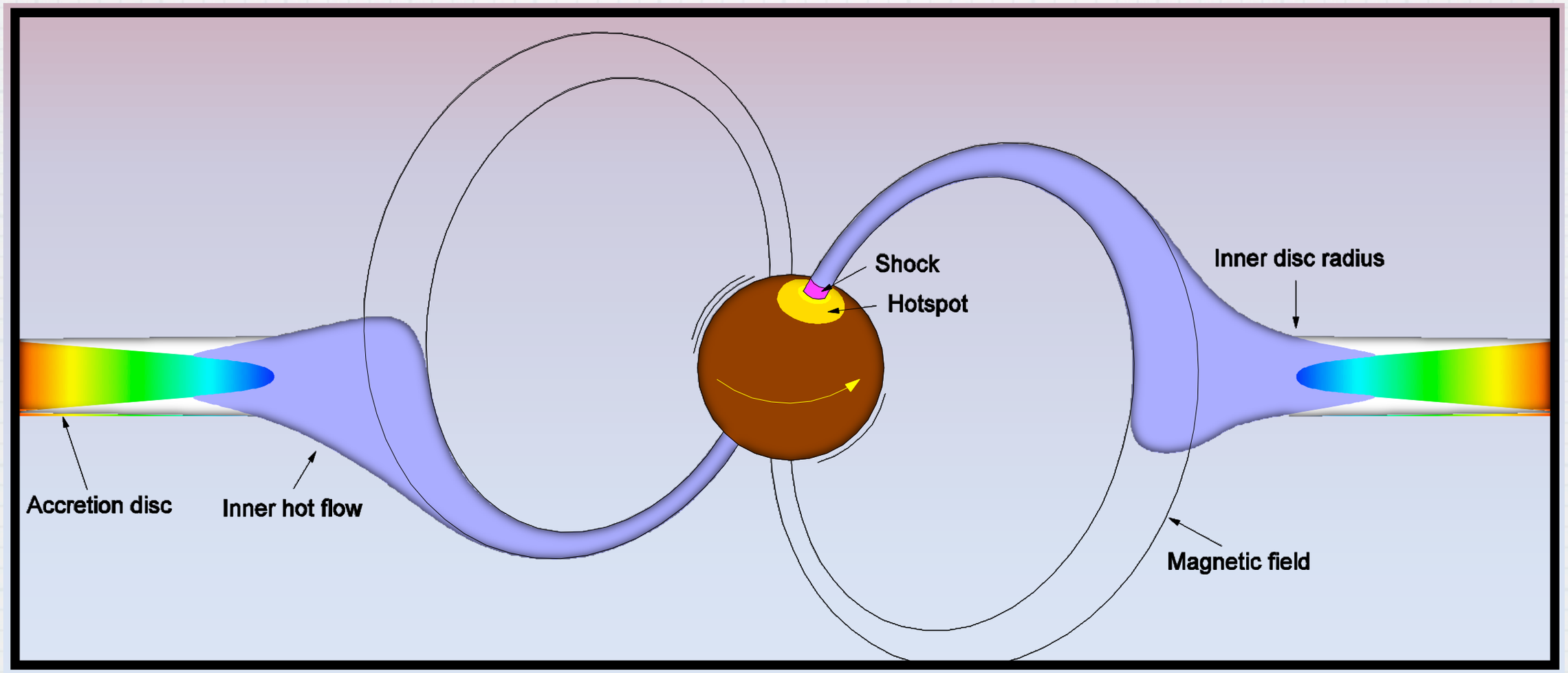

Flow channelled by magnetic field onto NS

HMXB: strong B, LMXB: weak B

Signatures in the accretion

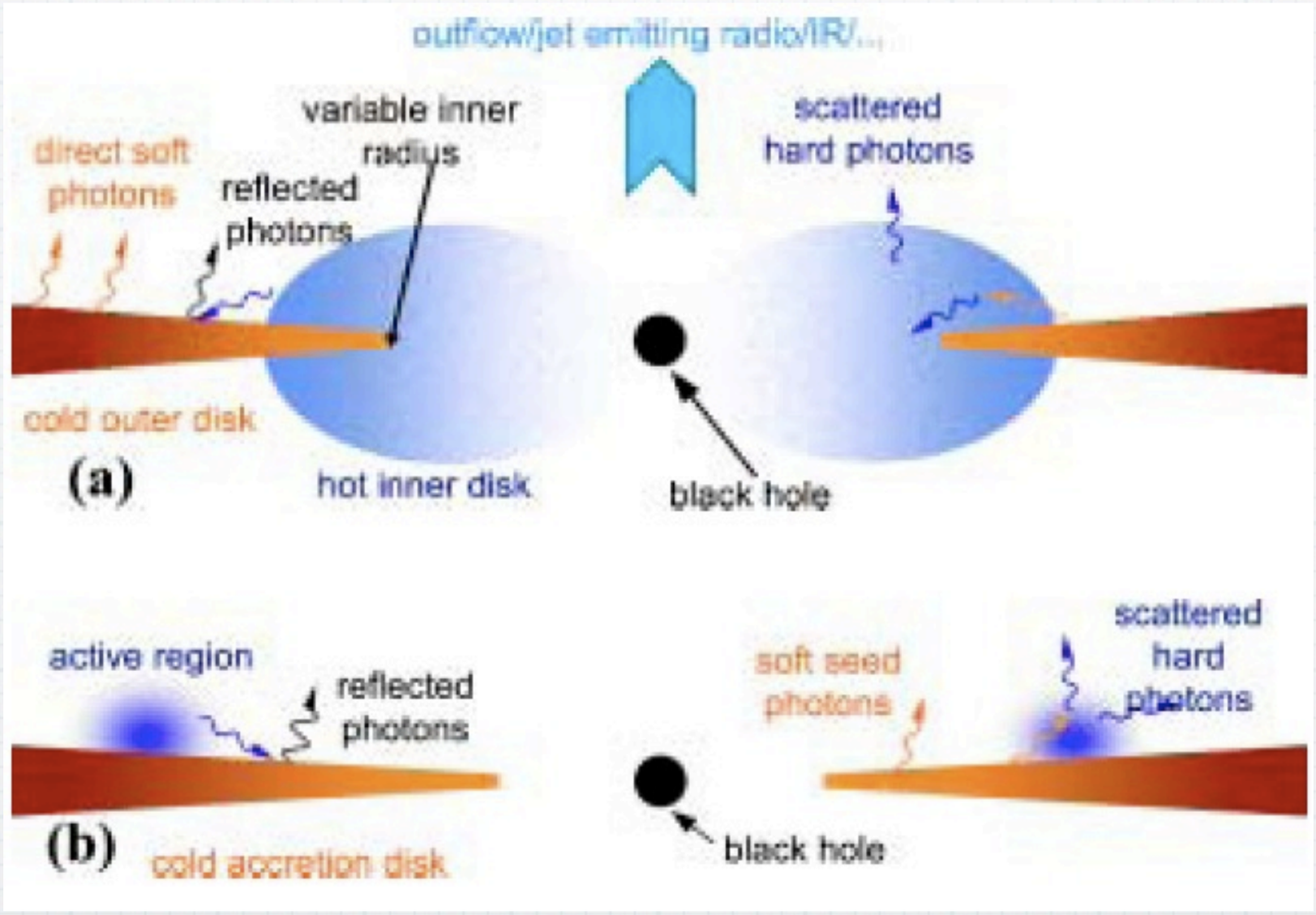

Accretion into a Black Hole

ISCO, Event Horizon

High Frequency Oscillations

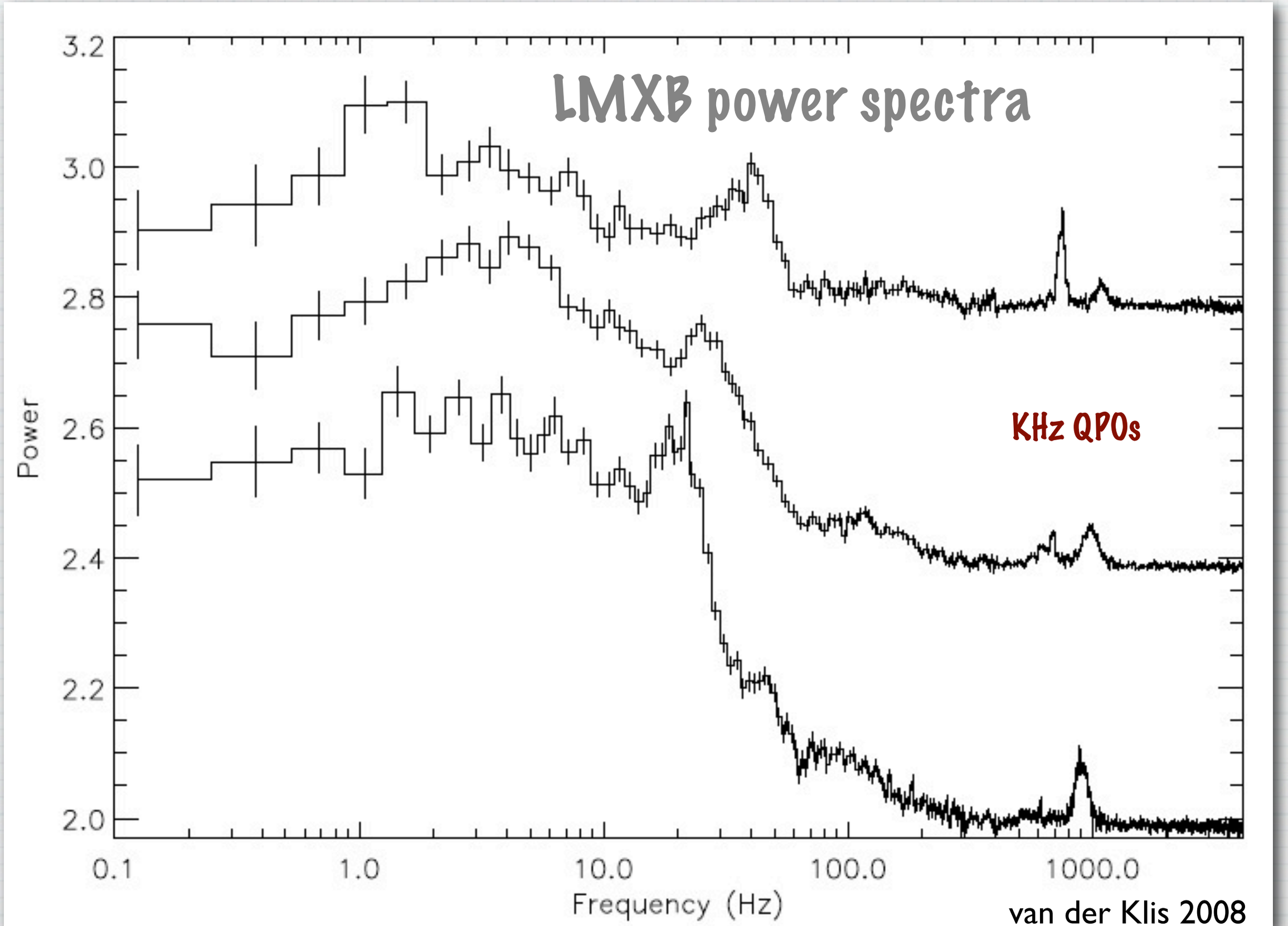

van der Klis 2008

KHz QPOs: Sco X-1

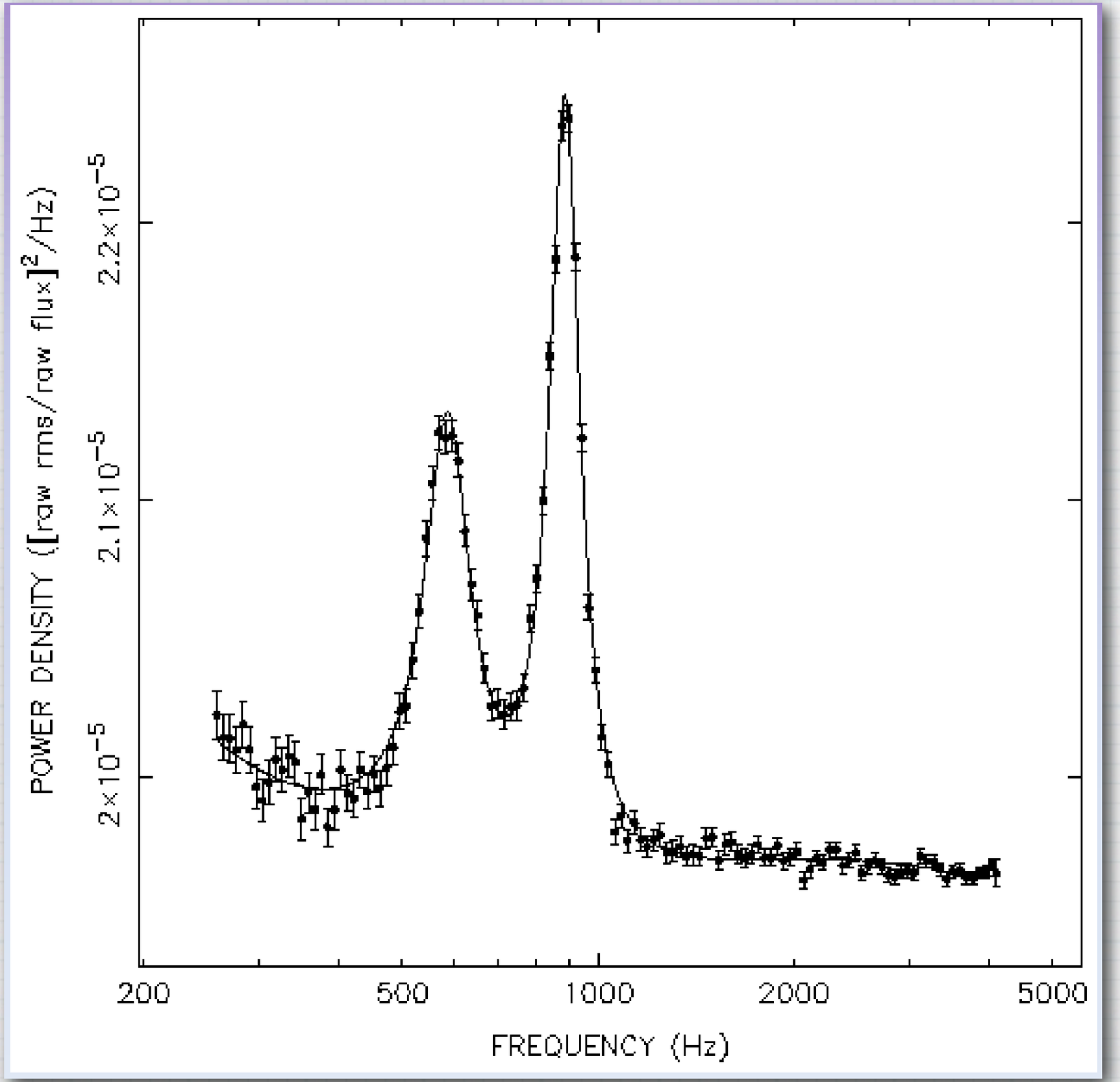

Black Hole twin QPOs

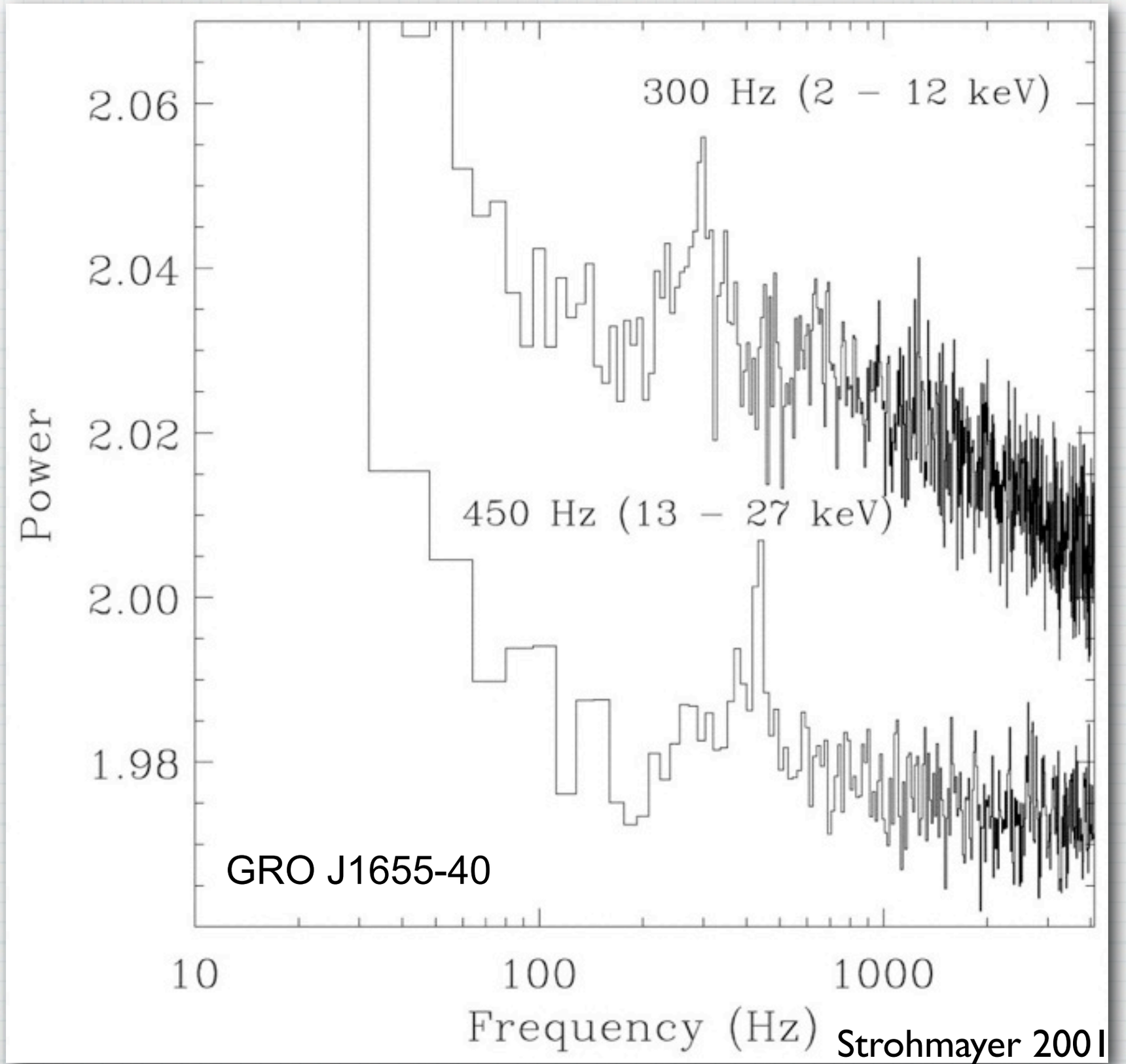

Strohmayer 2001

Beat Frequency Model

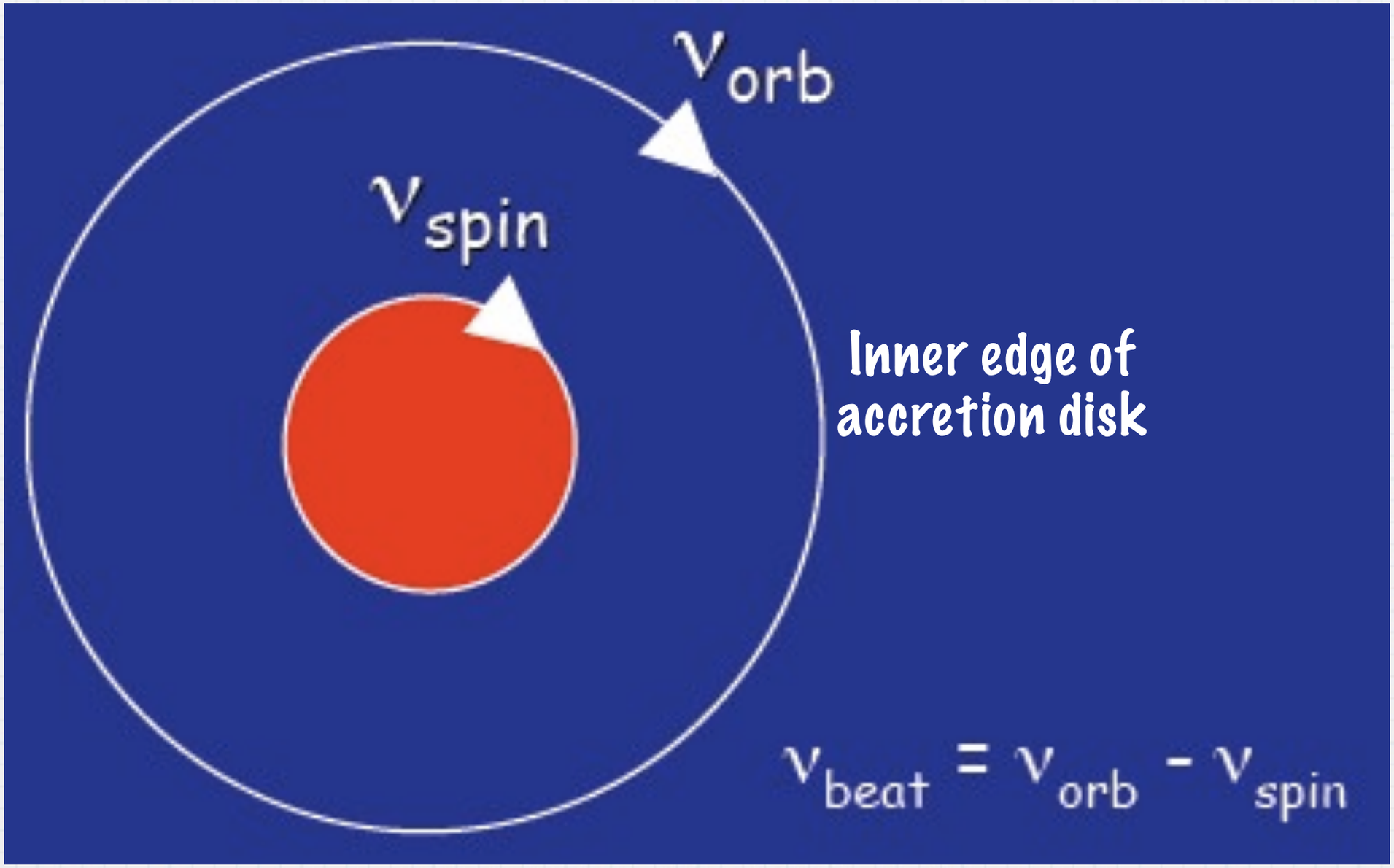

$\nu_{upper} = \nu_{orb}$

$\nu_{lower} = \nu_{beat}$

$\Delta\nu = \nu_{spin}$

Failure of beat freq model

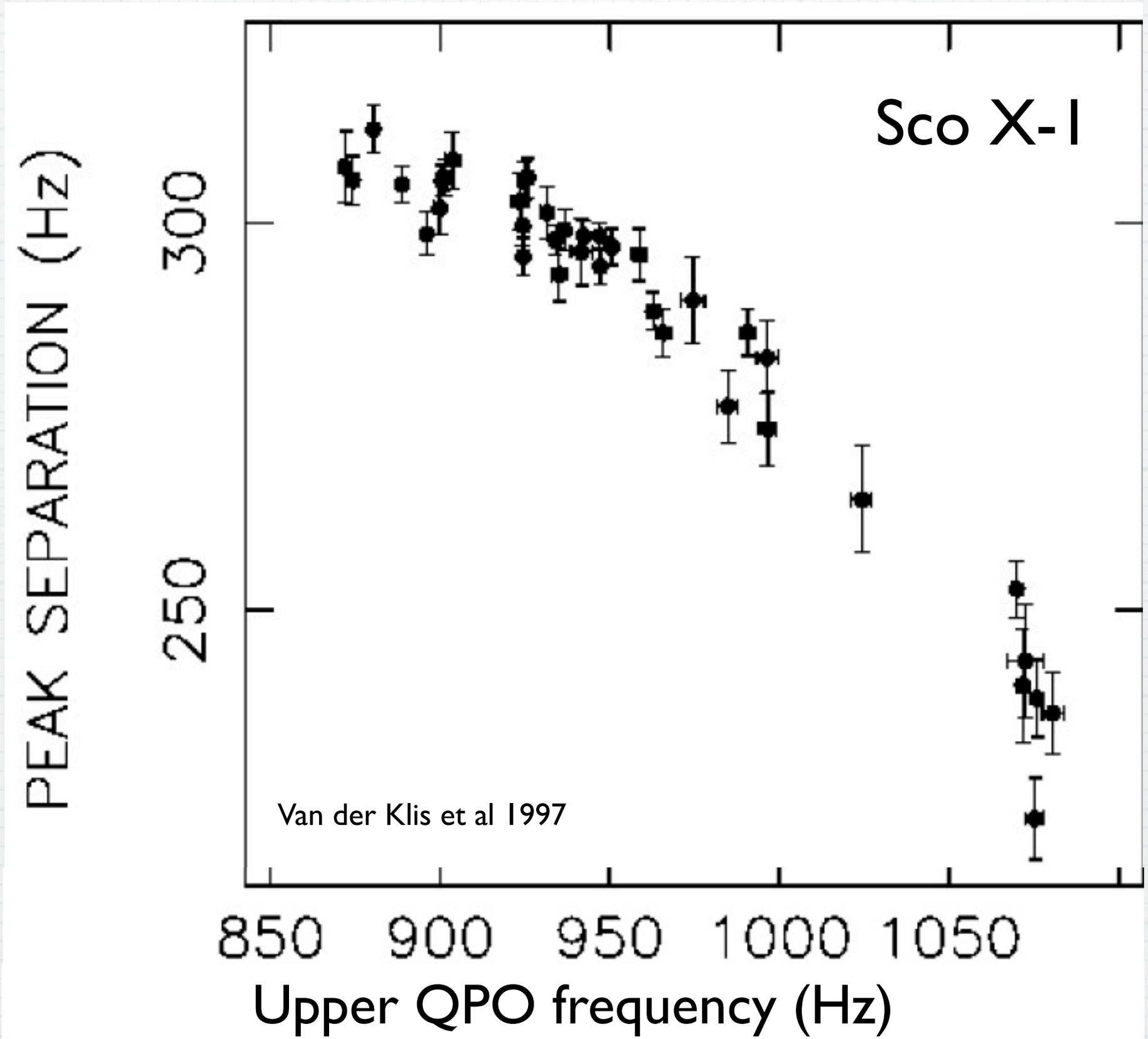

Relativistic Precession Model

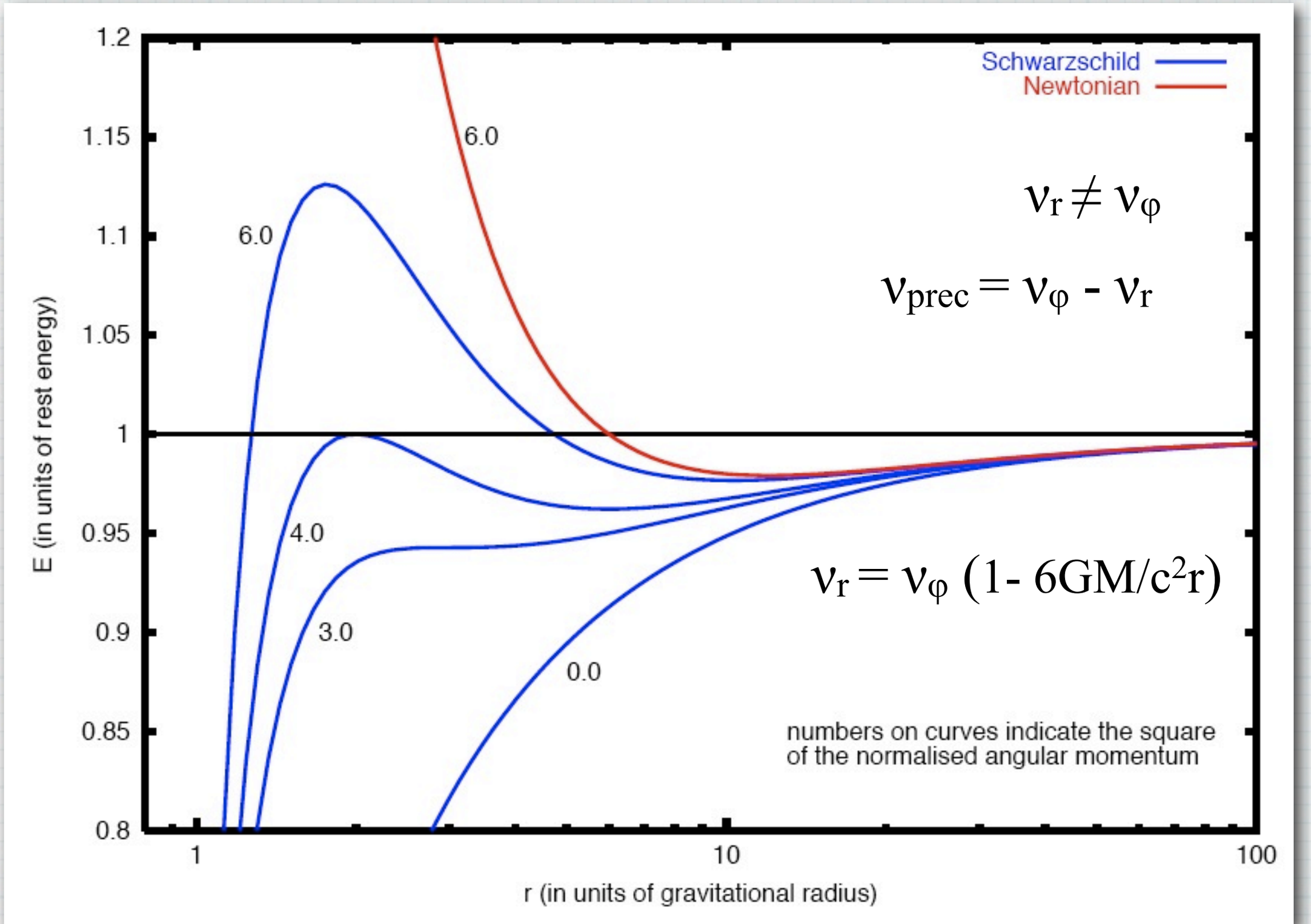

$\nu_{upper} = \nu_\phi$ $\nu_{lower} = \nu_{prec}$ $\Delta\nu = \nu_r$

Relativistic Precession Model

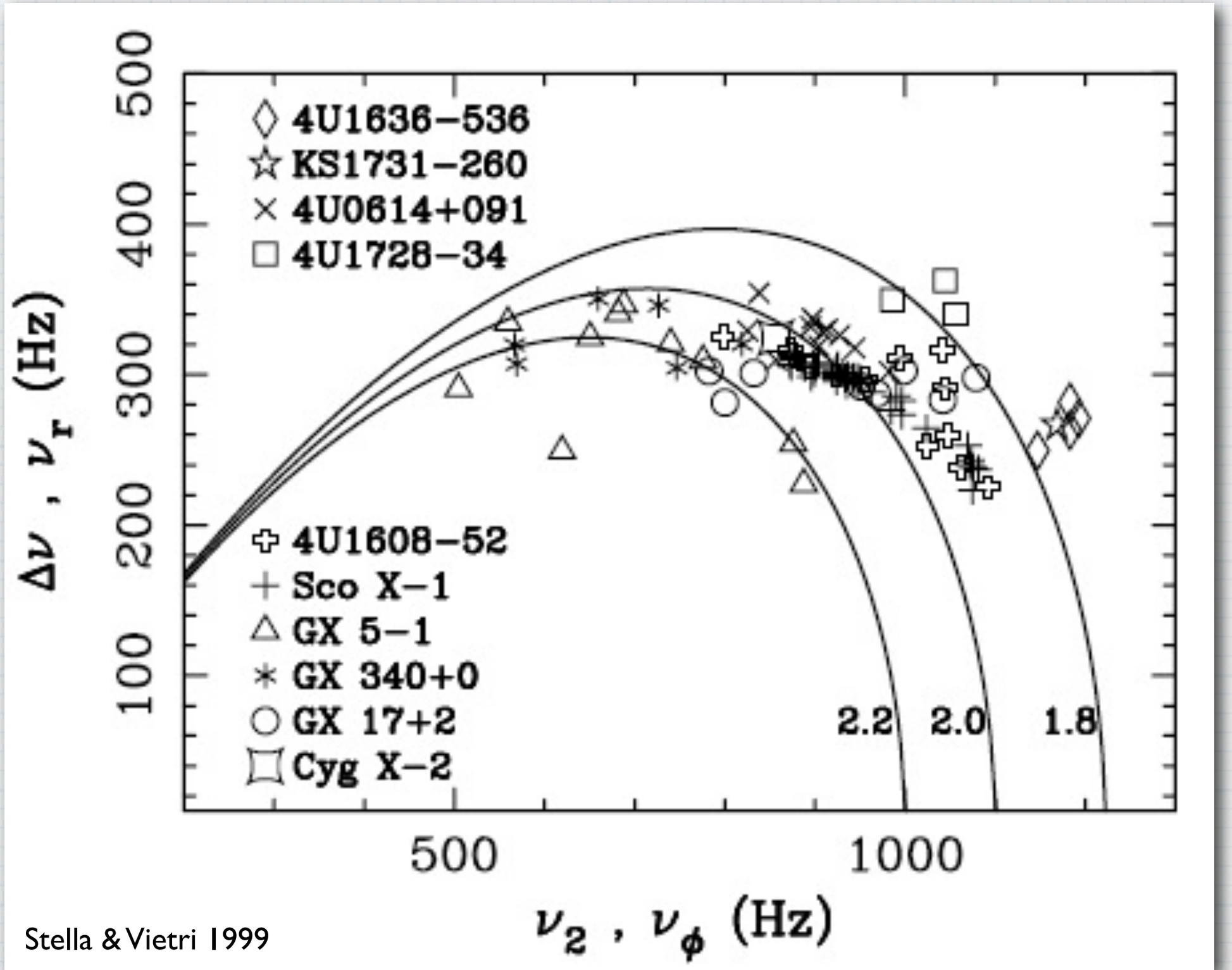

Stella & Vietri 1999

Atomic lines from NS surface?

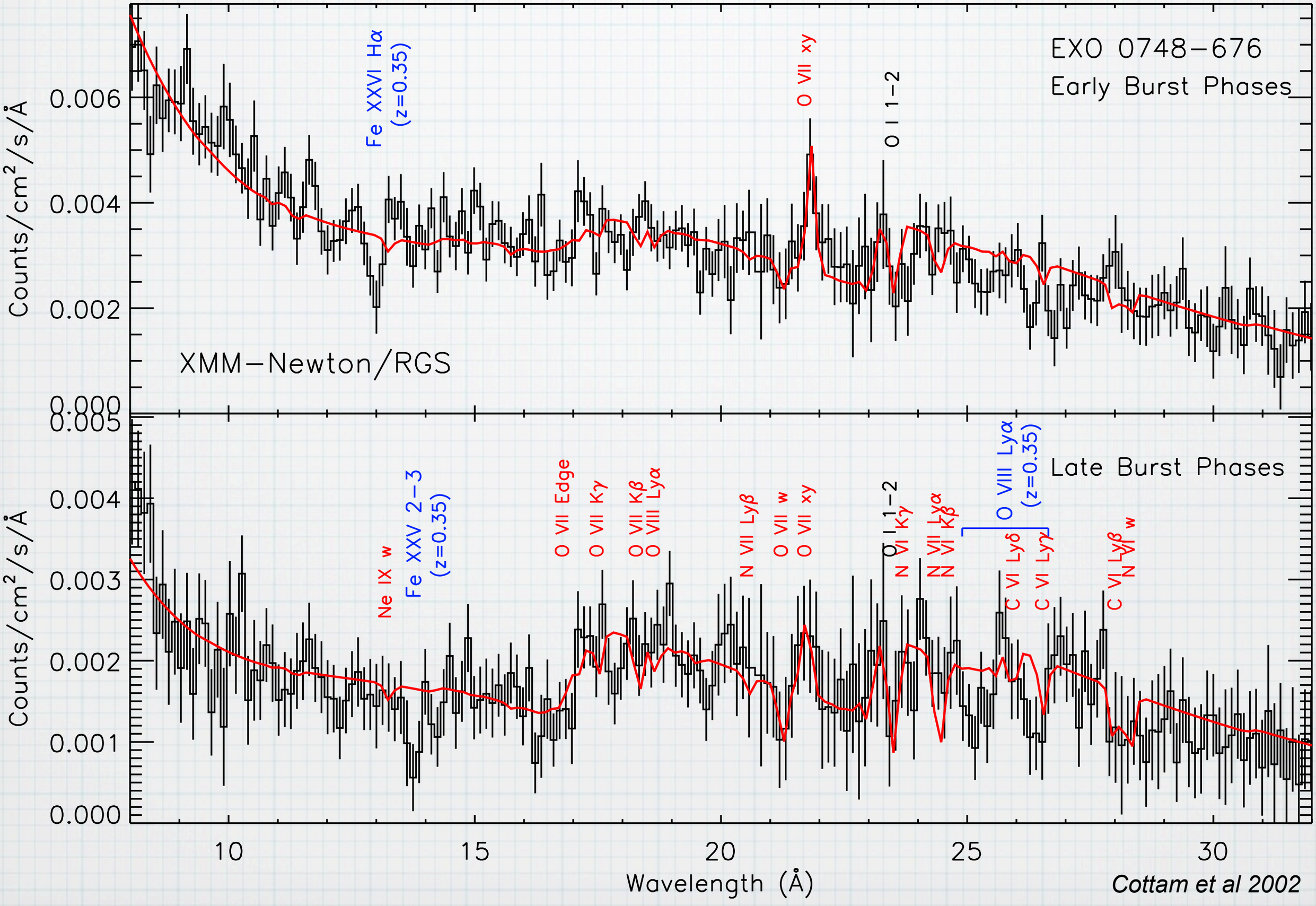

Relativistic Iron Lines

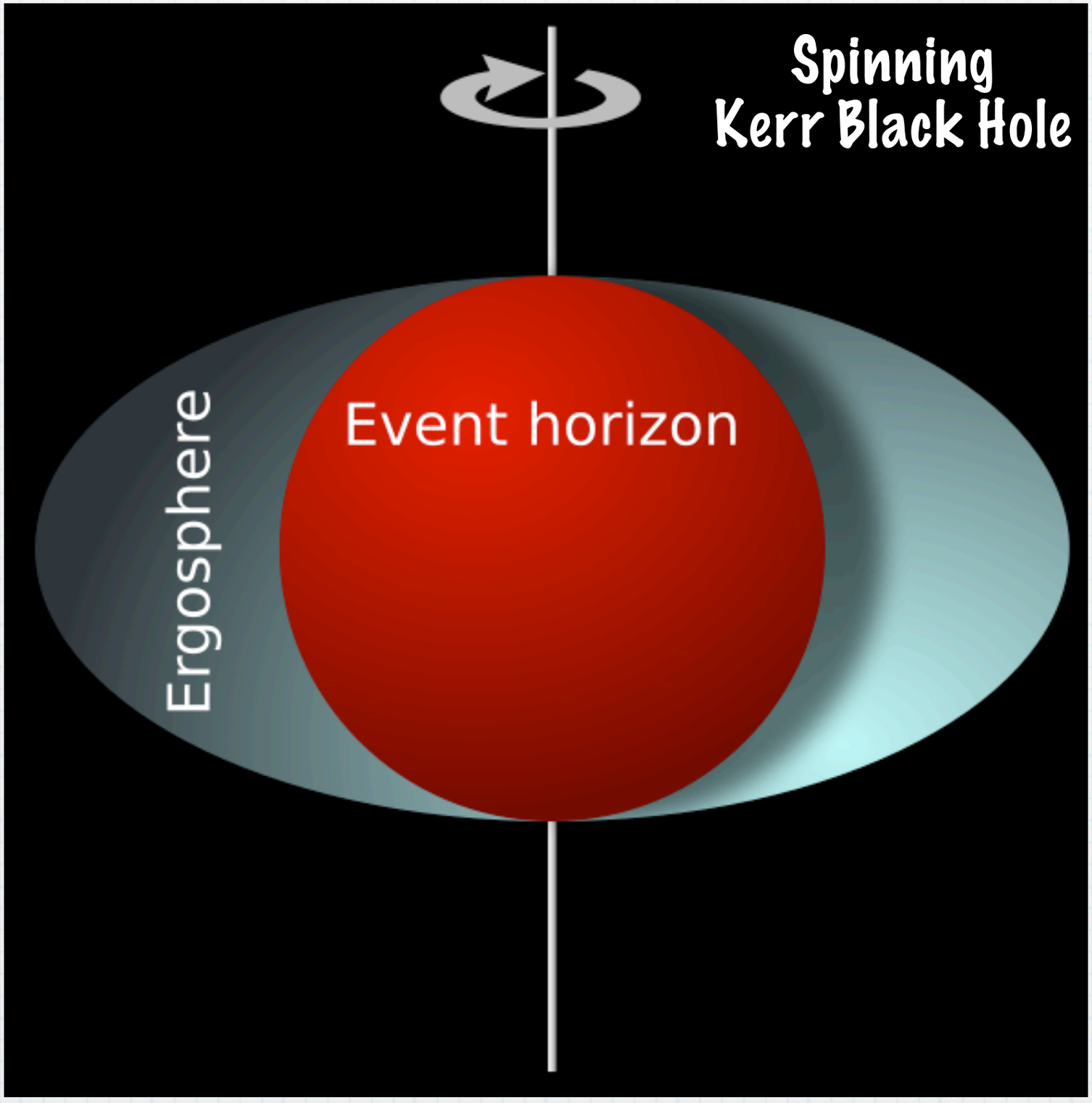

Wikipedia Commons

Relativistic Iron Lines

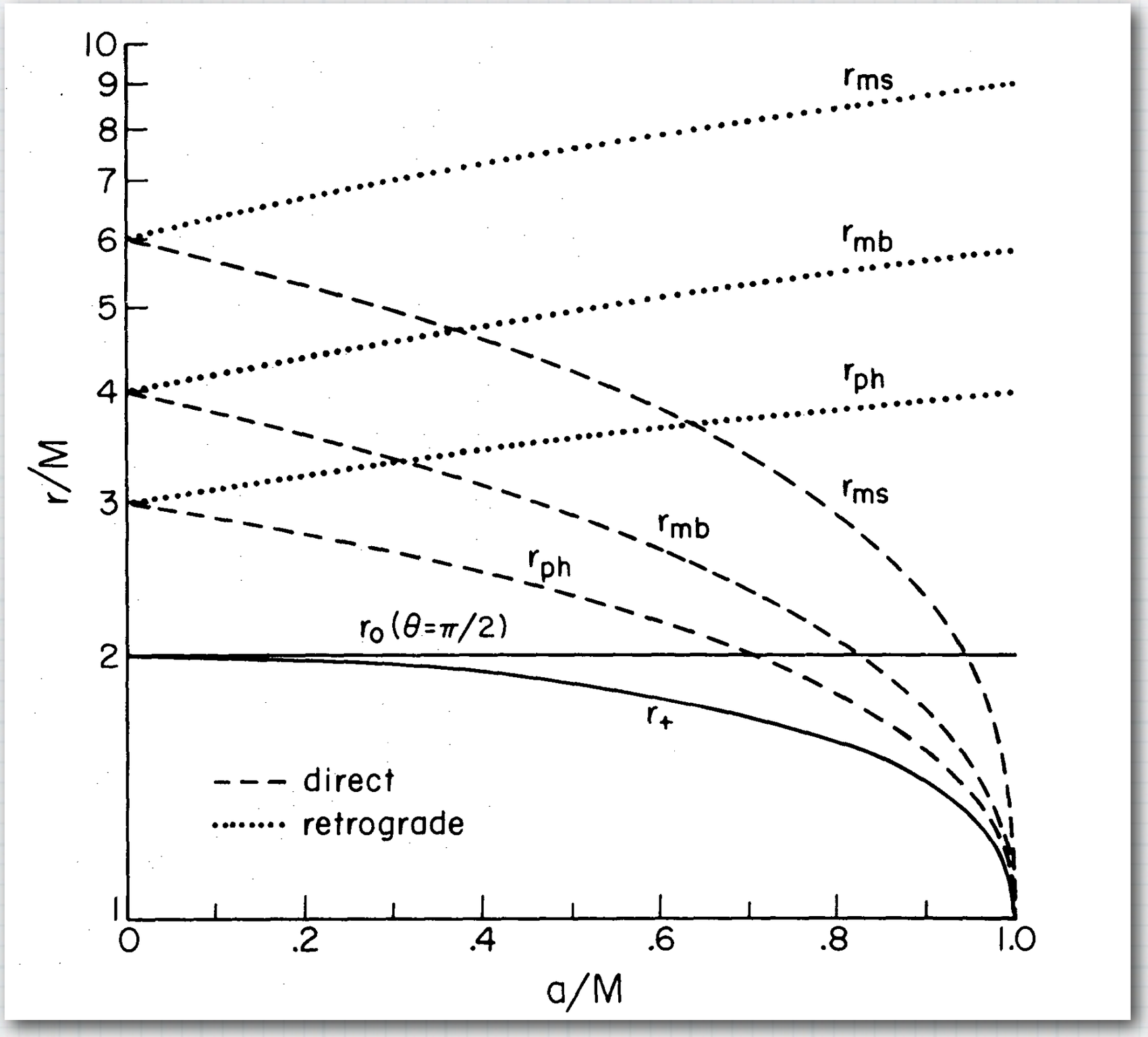

Relativistic Iron Lines

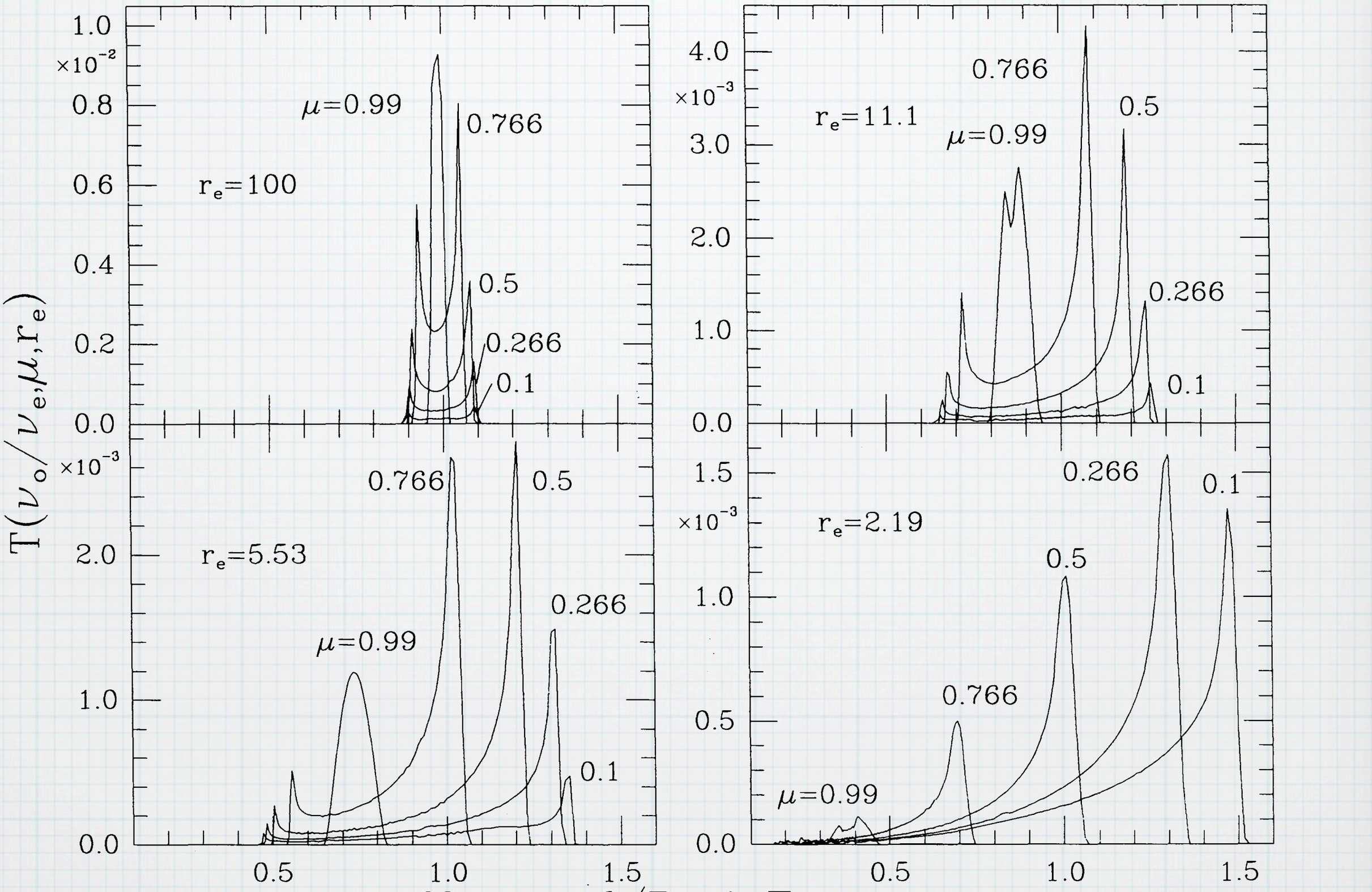

Laor 1991

Relativistic Iron Lines

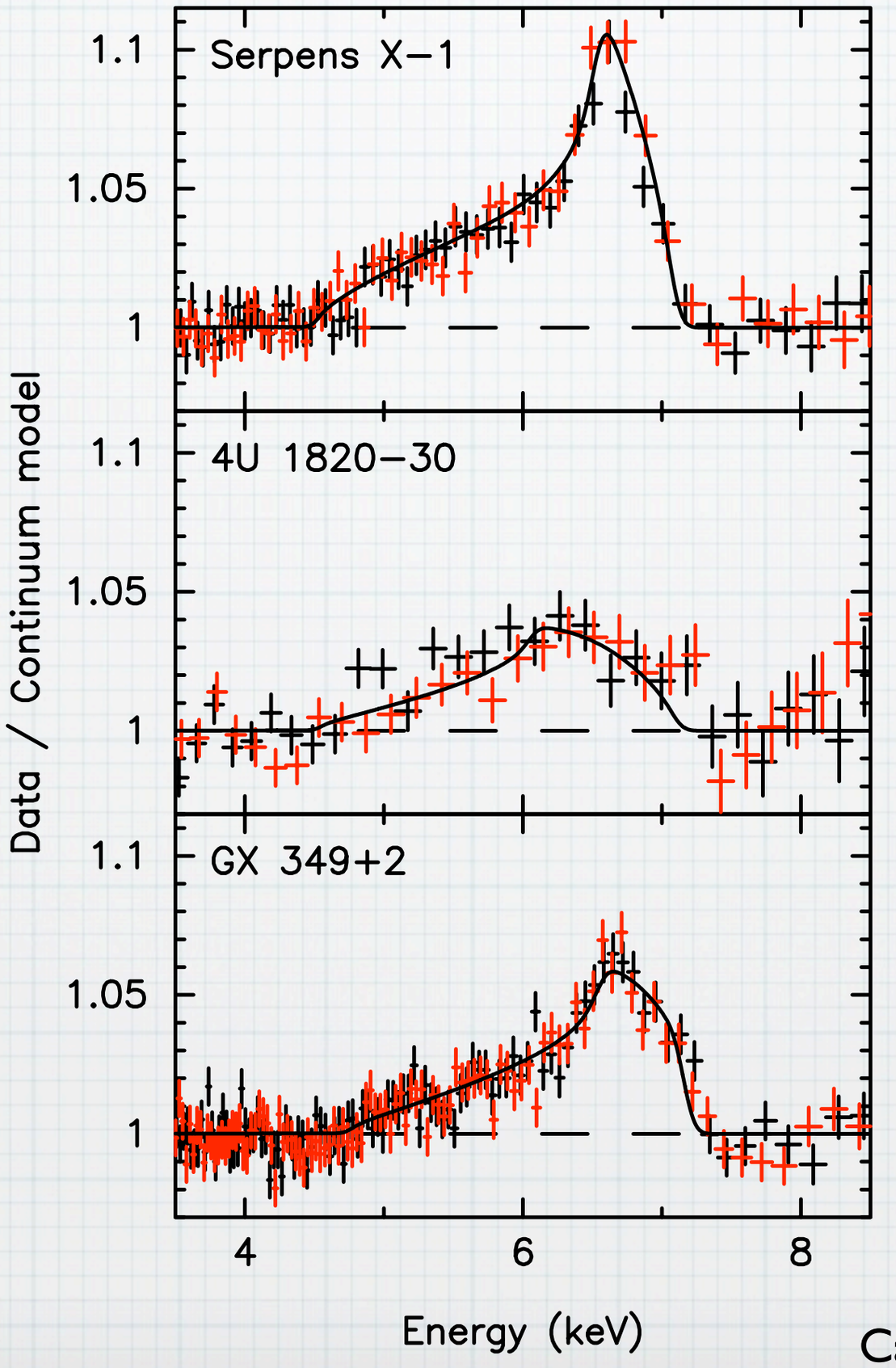

Suzaku spectra

Cackett et al 2008

Variability in BH source GRS 1915+105

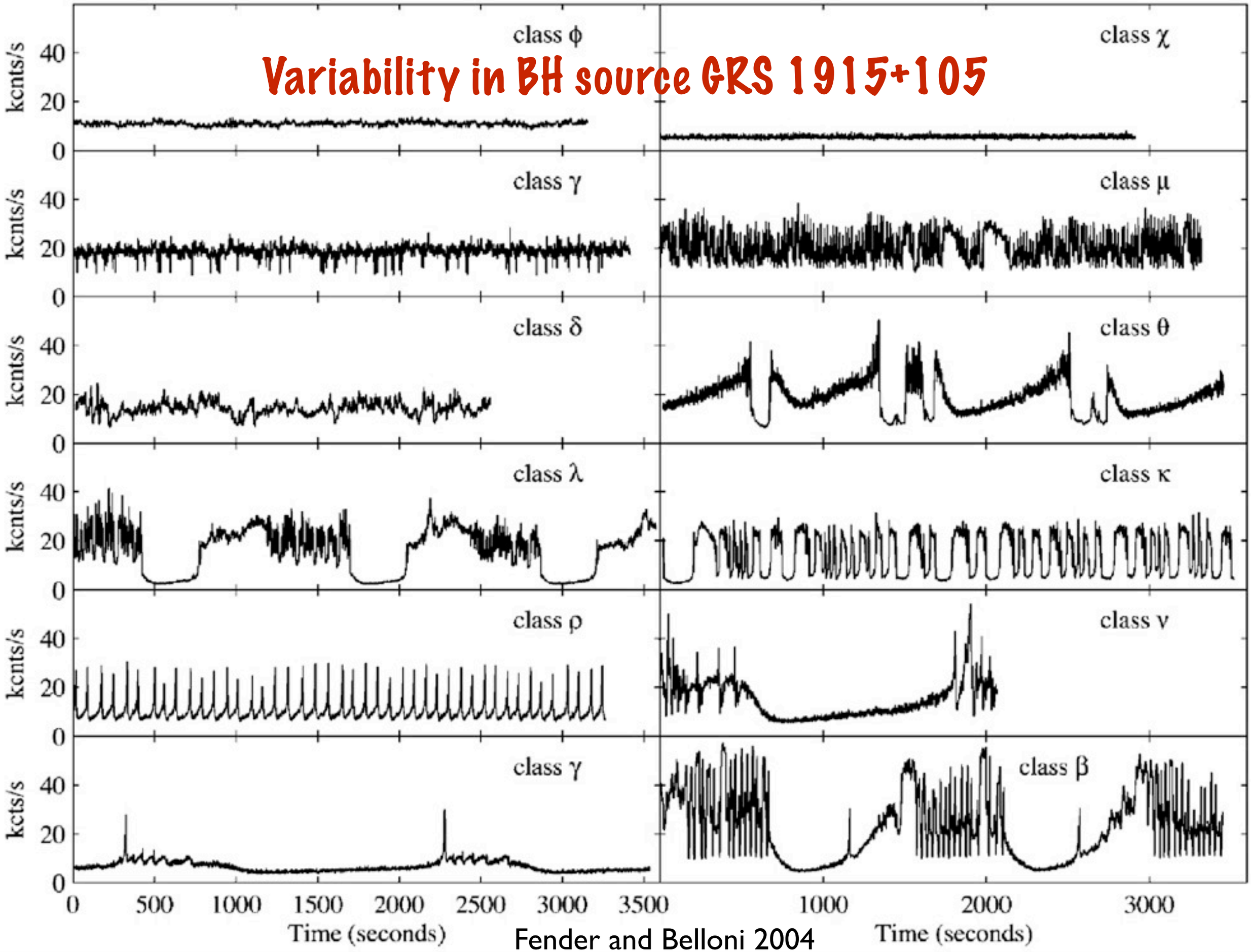

Fender and Belloni 2004

Variability in BH source GRS 1915+105

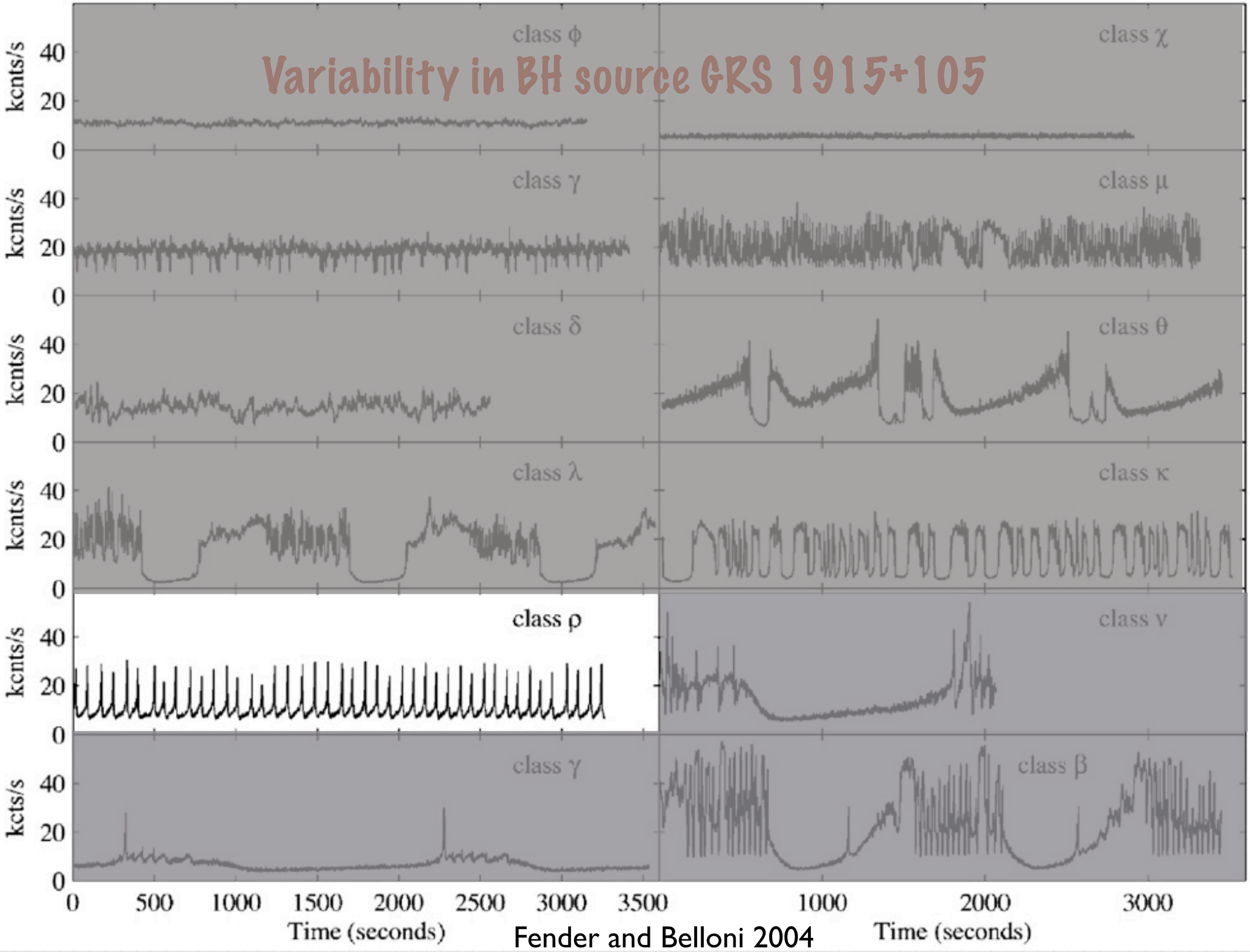

Fender and Belloni 2004

Bursts in BH source GRS 1915+105

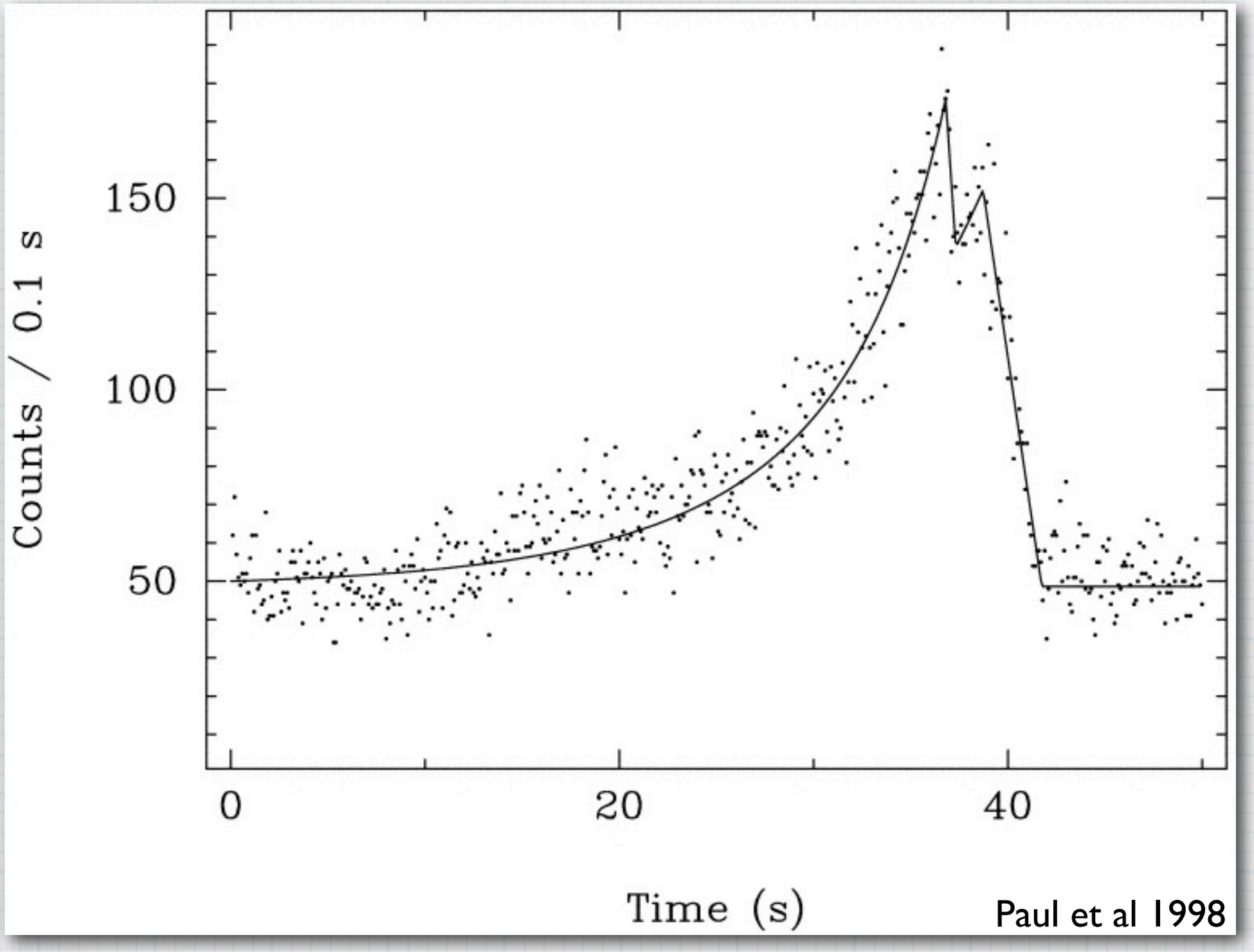

Paul et al 1998

Accreting Black Hole source GRS 1915

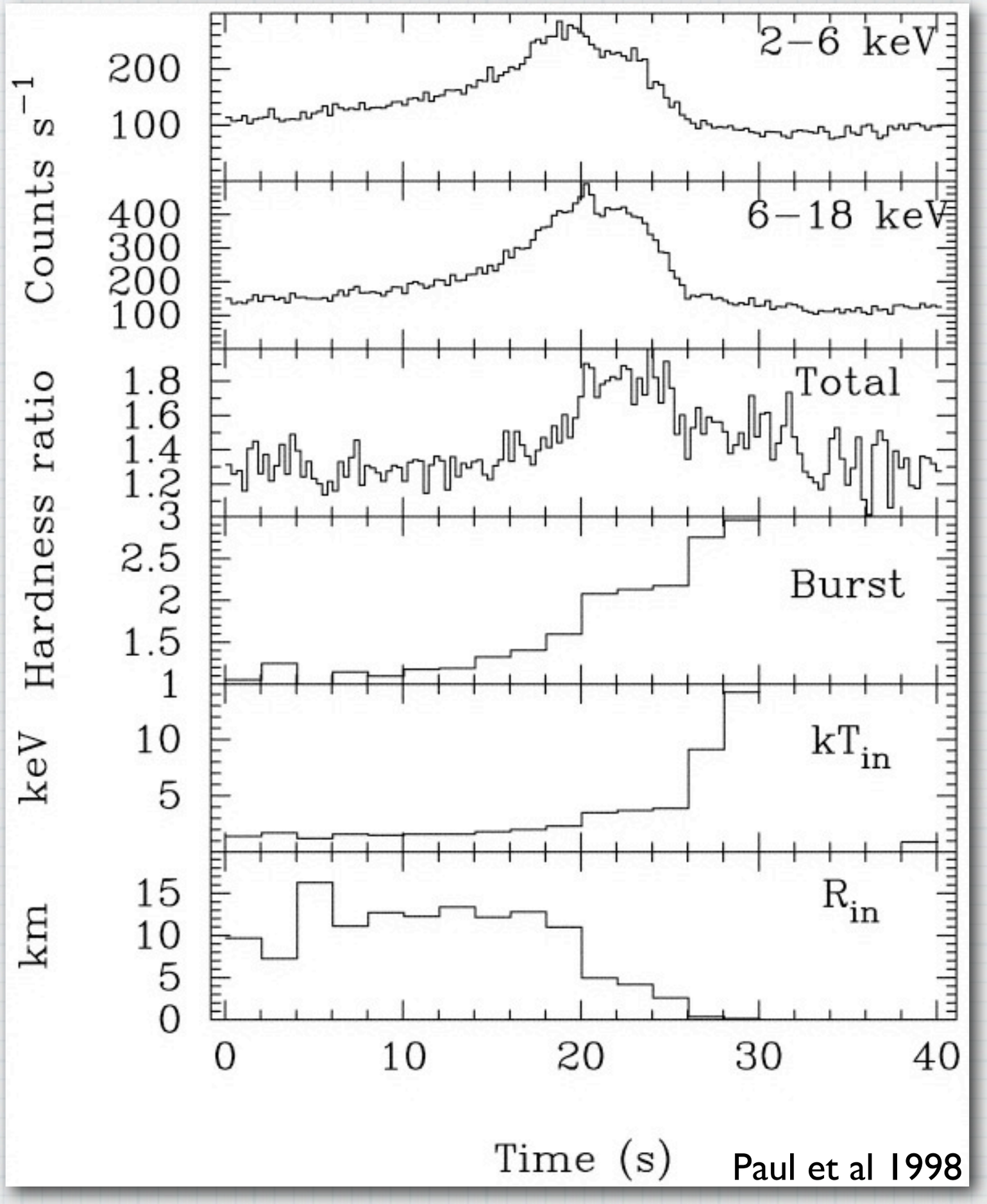

Paul et al 1998

Possible evidence of matter entering the BH horizon

Gravitational Waves

Gravitational Waves

Gravitational Wave observations, when successful, will open a new window on relativistic effects

Gravitational Waves

Gravitational Wave observations, when successful, will open a new window on relativistic effects

Compact Stars may generate gravitational waves by a variety of mechanisms:

Gravitational Waves

Gravitational Wave observations, when successful, will open a new window on relativistic effects

Compact Stars may generate gravitational waves by a variety of mechanisms:

- NS/BH/WD inspiral

Gravitational Waves

Gravitational Wave observations, when successful, will open a new window on relativistic effects

Compact Stars may generate gravitational waves by a variety of mechanisms:

- NS/BH/WD inspiral
- LMXBs at limiting spin-up: CFS/r-mode instabilities

Gravitational Waves

Gravitational Wave observations, when successful, will open a new window on relativistic effects

Compact Stars may generate gravitational waves by a variety of mechanisms:

- NS/BH/WD inspiral
- LMXBs at limiting spin-up: CFS/r-mode instabilities
- Accretion mound on strongly magnetized NS

Gravitational Waves

Gravitational Wave observations, when successful, will open a new window on relativistic effects

Compact Stars may generate gravitational waves by a variety of mechanisms:

- NS/BH/WD inspiral
- LMXBs at limiting spin-up: CFS/r-mode instabilities
- Accretion mound on strongly magnetized NS
- Low-mass binaries evolving via AML

Gravitational Waves

Gravitational Wave observations, when successful, will open a new window on relativistic effects

Compact Stars may generate gravitational waves by a variety of mechanisms:

- NS/BH/WD inspiral
- LMXBs at limiting spin-up: CFS/r-mode instabilities
- Accretion mound on strongly magnetized NS
- Low-mass binaries evolving via AML
- Isolated pulsars with residual quadrupole moment

Gravitational Waves

Gravitational Wave observations, when successful, will open a new window on relativistic effects

Compact Stars may generate gravitational waves by a variety of mechanisms:

- NS/BH/WD inspiral
- LMXBs at limiting spin-up: CFS/r-mode instabilities
- Accretion mound on strongly magnetized NS
- Low-mass binaries evolving via AML
- Isolated pulsars with residual quadrupole moment
- Collapse/explosion following compact star merger

Summary

Observations of Neutron Stars and Black Holes show several measurable signatures of strong field gravity:

* orbit precession & decay
* gravitational time delays
* geodetic precession
* gravitational redshift
* light bending
* relativistic line broadening..... etc.

Future instrumentation will continue to push the envelope.
LOFAR, MeerKAT, SKA, Astrosat, NuStar, NICER, LOFT, Athena.....

Gravity wave window will add a new dimension

Thank you

Alternative Gravity Theories

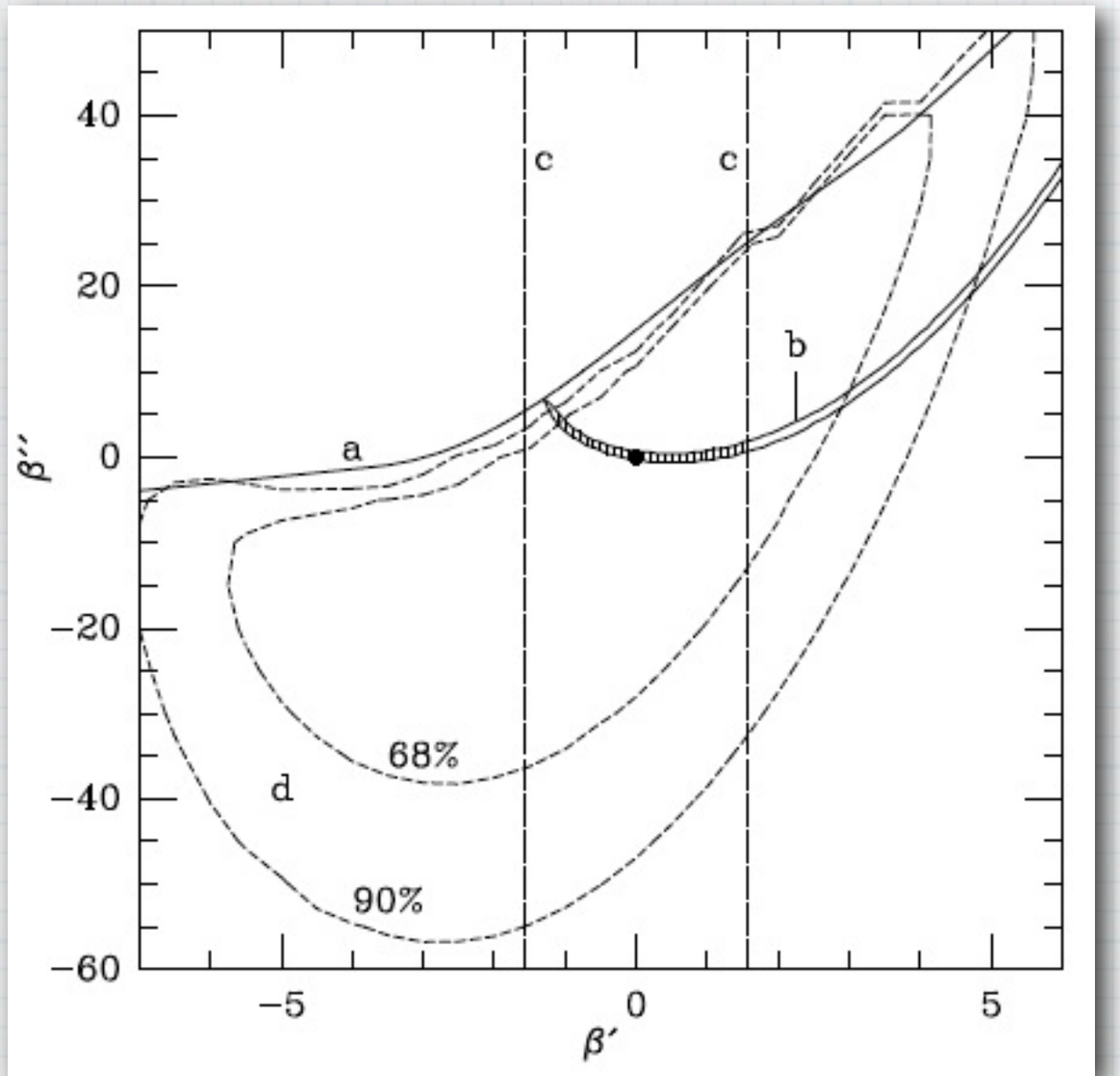

Taylor et al 1992

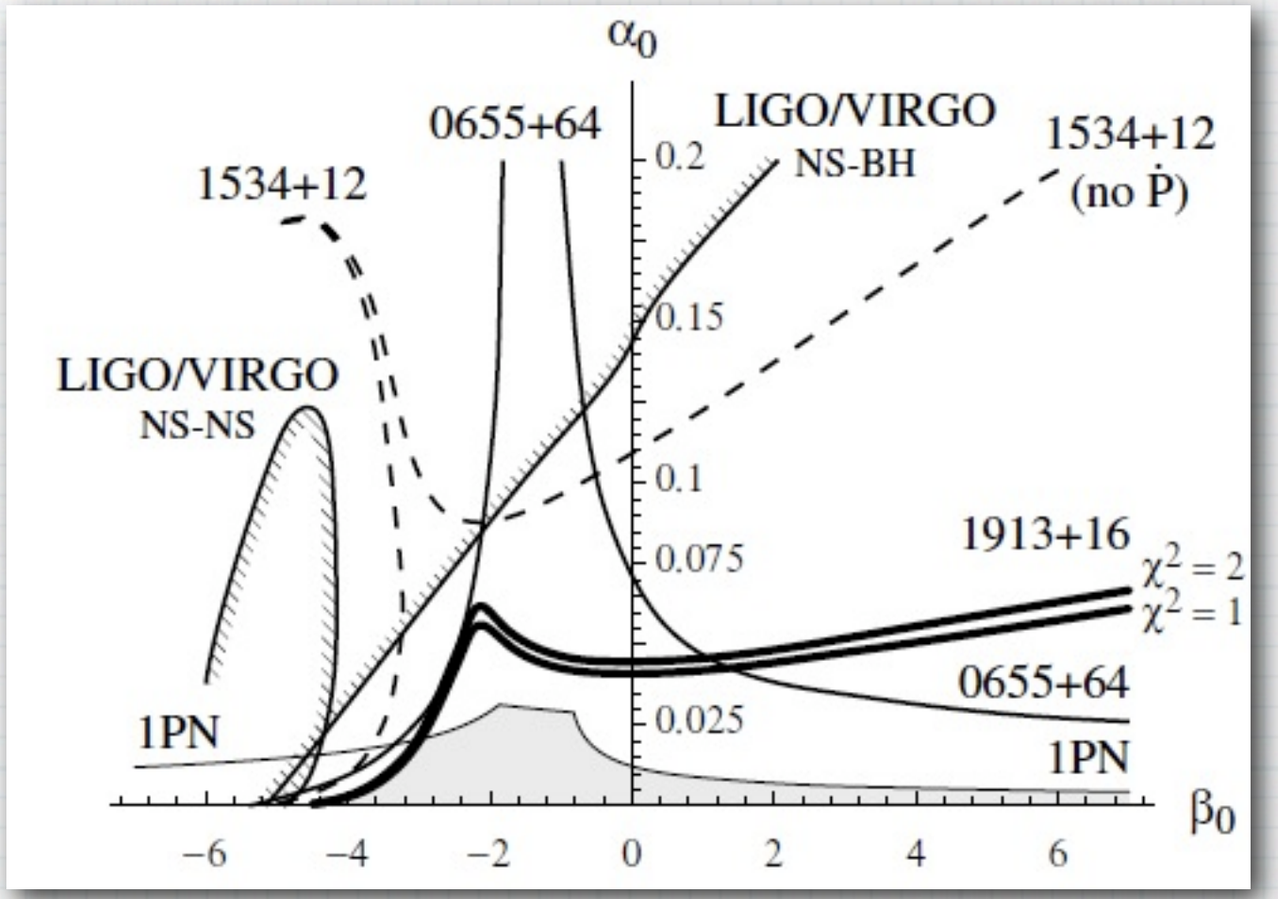

Damour & Esposito-Farese 1998

ASTROSAT